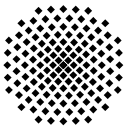

Institut für Theoretische Physik I
Universität Stuttgart
Pfaffenwaldring 57
70550 Stuttgart

On the Microscopic Limit for the Existence of Local Temperature

PhD. Thesis

Michael Hartmann

26th April 2005

Hauptberichter : Prof. Günter Mahler
Mitberichter : Prof. Ortwin Hess

Contents

1. Introduction

Thermodynamics describes the physical properties of systems composed of a large number of particles. In the beginning, it was a purely phenomenological science. Its basic notions, like pressure and temperature, where defined via the way they were measured and its only justification was the successful prediction of experimental results. Understanding of why the same notions were useful for the description of different types of matter and why the dynamics of different systems had some universal properties still did not exist.

The situation began to change with the works of Joule and in particular Boltzmann, who tried to establish a link between the theory describing the microscopic dynamics, the dynamics of single constituent particles and thermodynamics, which describes the collective dynamics of a macroscopic number of particles.

While the explanation of the irreversible collective dynamics, i.e. the second law, is still a subject of current debate [23, 5], the existence of thermodynamic notions can, for a large class of systems, be understood in a satisfactory manner. The key aspect here is the Thermodynamic Limit: Intensive thermodynamic quantities approach a limit value as the size of the system increases. If this limit exists, systems with a very large number of particles, of the same type have the same thermodynamic properties, irrespective of the microscopic state.

The existence of the Thermodynamic Limit justifies the usage of thermodynamic notions like temperature for very large systems. This immediately gives rise to the following question: How large do those systems need to be for a thermodynamical description to be successful?

This fundamental question remains unclarified until today. For a long time, the problem, besides being fundamental, may have been of purely academic interest, since thermodynamics was only used to describe macroscopic systems, where deviations form the Thermodynamic Limit may safely be neglected. With the advent of nanotechnology, the microscopic limit of the applicability of thermodynamics became relevant

for the interpretation of experiments and may in the near future even have technological importance.

In recent years, amazing progress in the synthesis and processing of materials with structures on nanometer length scales has been made [12, 75, 72, 67]. Experimental techniques have improved to such an extent that the measurement of thermodynamic quantities like temperature with a spatial resolution on the nanometer scale seems within reach [20, 60, 7]. To provide a basis for the interpretation of present day and future experiments in nanoscale physics and technology and to obtain a better understanding of the limits of thermodynamics, it is thus indispensable to clarify the applicability of thermodynamical concepts on small length scales starting from the most fundamental theory at hand, i. e. quantum mechanics. In this context, one question appears to be particularly important and interesting: Can temperature be meaningfully defined on nanometer length scales?

Why should we care about the non-existence of local temperature? There are at least three situations for which this possibility needs special attention: One obvious scenario refers to the limit of spatial resolution on which a temperature profile could be defined. However a spatially varying temperature calls for non-equilibrium - a complication which we will exclude here. A second application deals with partitions on the nanoscale: If a modular system in thermal equilibrium is partitioned into two pieces, say, the two pieces need no longer be in a canonical state, let alone have the same local temperature. Finally, local physical properties may show different behavior depending on whether the local state is thermal or not.

The existence of thermodynamical quantities, i. e. the existence of the Thermodynamic Limit strongly depends on the correlations between the considered parts of a system. With increasing diameter, the volume of a region in space grows faster than its surface. Thus effective interactions between two regions, provided they are short ranged, become less relevant as the sizes of the regions increase. This scaling behavior is used to show that correlations between a region and its environment become negligible in the limit of infinite region size and that therefore the Thermodynamic Limit exists [18, 63, 50].

To explore the minimal region size needed for the application of thermodynamical concepts, situations far away from the Thermodynamic Limit should be analyzed. On the other hand, effective correlations be-

tween the considered parts need to be small enough [66, 30].

The scaling of interactions between parts of a system compared to the energy contained in the parts themselves thus sets a minimal length scale on which correlations are still small enough to permit the definition of local temperatures. It is our aim to study this connection quantitatively.

This thesis is organized as follows: As a motivation, we first describe an experiment, where the question of the existence of local temperatures arises (chapter 2). In this context, the definition of local temperature and the definition of its existence are of particular relevance. They are discussed in chapter 3. In chapter 4, we then outline our approach to determine whether those local temperatures exist. It is based on a central limit theorem for quantum systems, which is discussed in chapter 5. Chapter 6 contains some applications of this theorem different from the one in the main text. The purpose of this treatment is twofold. We rederive known properties of quantum many particle systems and thus confirm the validity of the theorem. On the other hand, the theorem can be used to calculate properties of quantum many particle systems for cases, where no other analytical results are available. Since numerical analysis of such systems is very demanding due to the enormous dimension of the Hilbert space, these applications might prove to be very useful. In the following chapter, 7, we present the general theoretical approach which derives two conditions on the effective group interactions and the global temperature. These two conditions are the main result of this thesis. In the following two chapters, we apply them to two concrete models and derive estimates for the minimal subgroup size: Ising spin chains, where the elementary subsystems (spins) have finite dimension, are discussed in chapter 8, and a harmonic chain, where the elementary subsystems (harmonic oscillators) have infinite dimension, in chapter 9. Since harmonic lattice models have been successfully applied to describe thermal properties of insulating solids, we deduce minimal lengths for the existence of local temperatures in those materials in chapter 10. A discussion of the results on length scales and their possible flaws is given in chapter 11. In the following, chapter 12, we discuss possible consequences of the breakdown of the concept of temperature on small scales, that can be observed in experiments. In the conclusions section 13, we sum up the results, discuss the conclusions and give a short outlook on interesting questions and open topics.

2. Motivation: A Thermal Nanoscale Experiment

In recent years, there has been substantial progress in the fabrication and operating of material with structure on nanoscopic scales and nanoscale devices. In this context, several experiments, that study thermal properties, have been done. We describe here, as an example, one experiment that nicely shows where the existence or non-existence of local temperature becomes relevant.

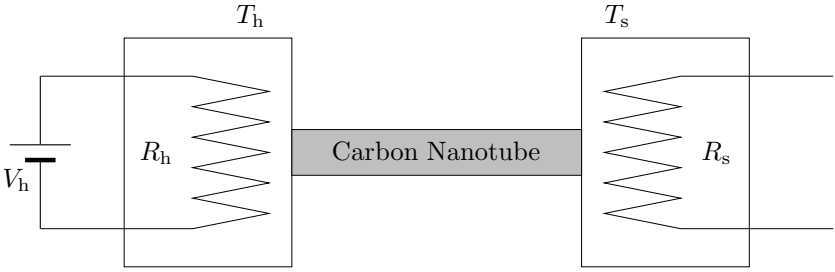

Figure 2.1.: Setup of the experiment. Two, otherwise thermally well isolated islands are connected by a carbon nanotube. The left island is heated by an electric current running through the coil with resistance R_h and thus maintained at the temperature T_h. The temperature of the right island is measured via the temperature dependent resistance R_s.

The experiment, we describe [44], studies the heat conduction across a carbon nanotube. A sketch of the setup is given in figure 2.1. Two, otherwise thermally well isolated islands are connected through a carbon nanotube of a few μm length. One island is heated by an electric current that runs through a coil with the resistance R_h. This island is thus at a "hot" temperature T_h. Heat can flow across the nanotube to the

other island, which is at a lower temperature T_s. This temperature in turn is measured by another coil, the resistance of which R_s, depends on temperature. Figure 2.2 shows a picture of this setup.

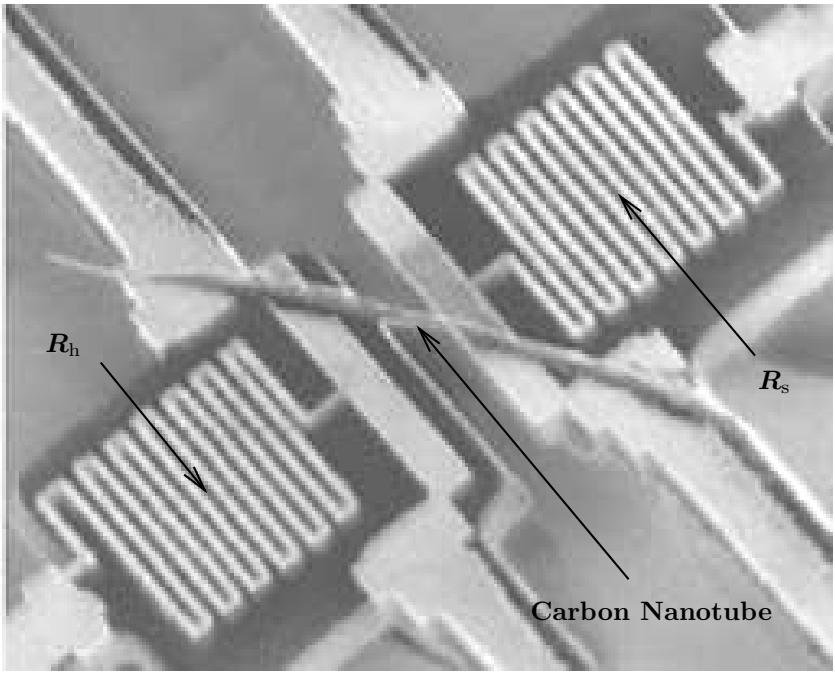

Figure 2.2.: Picture of the setup. The heated island is in the lower left corner and the island where the temperature is measured in the higher right corner. Both are connected by a single carbon nanotube.

At what point is the existence or non-existence of local temperatures of relevance for the interpretation of this experiment? We know that there is an electric current in the coil of the heated island. This current constantly delivers thermal energy to the island. This energy is transported across the nanotube to the other island, where we observe, that the temperature T_s rises. We thus know, that the nanotube connects a hot spot T_h to a cold spot T_s. This directly gives rise to the following questions:

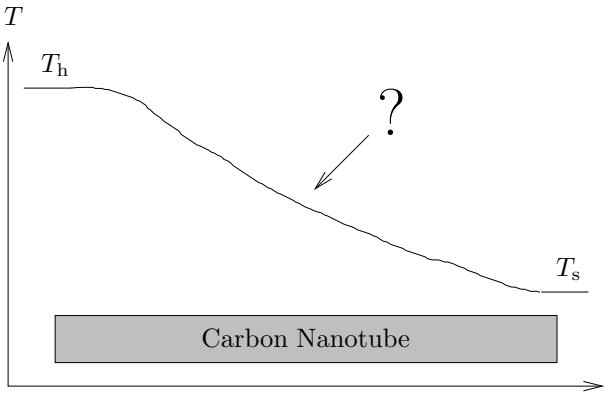

Figure 2.3.: The question, whether a temperature profile exists for the nanotube in the present setup, is not clarified.

How hot is the nanotube in between? Can we meaningfully talk at all about temperature for parts of the nanotube?[1] The answer to these two questions would clarify whether and in what sense a temperature profile (see figure 2.3) could exist for the present setup.

While a temperature profile can obviously be defined and measured in a macroscopic version of the present experiment, say two buckets of water at different temperatures and connected via an iron bar, its existence, possible resolution and measurability are completely unclear for the nanoscopic version.

It is the purpose of this thesis to clarify the existence of local temperatures on small scales from a theoretical point of view.

[1] The answer of our approach to this question for the case, in which the entire tube is in thermal equilibrium, is given in chapter 10.

3. What is Temperature?

Temperature is one of the central quantities in Thermodynamics and Statistical Mechanics. There exist two standard ways to define it:

3.1. Definition in Thermodynamics

The thermodynamical definition is purely empirical. Thermodynamics itself is an empirical theory on systems whose macroscopic physics can be sufficiently characterized by a set of a few variables like volume, energy and the number of particles for example, the values of this variables are called a macro state [3]. A system is said to be in equilibrium if its macro state is stationary for given constraints. As a consequence of this definition, a equilibrium state depends on the applied constraints, e.g. whether the volume or the energy is kept constant etc. An important, special case of constraints, is a bipartite (or multipartite) system with a fixed total energy, where the parts may exchange energy among themselves. The parts are then said to be in thermal equilibrium. In Thermodynamics, temperature is defined by the following property:

Definition: *Two systems that can exchange energy and are in thermal equilibrium, have the same temperature.*

To fix a temperature scale, a reference system is needed. The simplest choice for this reference system is the ideal gas , where temperature may be defined by

$$T \equiv \frac{p\,V}{n\,k_\mathrm{B}}\,. \tag{3.1}$$

Here, p is the pressure of the gas, V its volume, n the number of its particles and k_B Boltzmann's constant.

Of course the above definition only is unambiguous if the states of thermal equilibrium form a one-dimensional manifold [3]. Only then, one quantity is sufficient for their characterization. This quantity is the temperature T.

3.2. Definition in Statistical Mechanics

In Statistical Mechanics, temperature is defined via the derivative of the entropy S with respect to the internal energy $\overline{E}$. In Quantum Mechanics the entropy can be defined according to von Neumann as

$$S \equiv -k_{\mathrm{B}} \operatorname{Tr} \hat{\rho} \ln \hat{\rho} \,, \tag{3.2}$$

it is a measure of the amount of possible pure states, the system could be in. With this definition, entropy always exists, but shows its standard properties, e.g. extensivity, only in the Thermodynamic Limit [63].

In Statistical Mechanics, an equilibrium state is defined to be the state with the maximal entropy, that is the state with the maximal amount of possible pure states. This definition is motivated by the fact that, for statistical reasons, physical systems tend to evolve into a state with a large number of microscopic realizations, i.e. a state with large entropy. Hence the maximum entropy state is stationary.

For systems that interact with their surrounding, such that they can exchange energy with it but have a fixed expectation value for the energy, the equilibrium state is a so called canonical state, described by a density matrix of the form

$$\hat{\rho} = \frac{\exp(-\beta \hat{H})}{Z} \,, \tag{3.3}$$

where the partition sum Z normalizes $\hat{\rho}$ such that $\operatorname{Tr} \hat{\rho} = 1$.

In Quantum Mechanics the internal energy is given by the expectation value of the energy,

$$\overline{E} \equiv \operatorname{Tr} \hat{\rho} \hat{H} \,, \tag{3.4}$$

where the Hamiltonian is the energy operator of the isolated system at hand. It does not contain any interactions of the system with its environment. The internal energy is therefore a property of the system

itself, it only depends on the state of the system and not on the state of the environment.

Temperature is then defined by

$$\frac{1}{T} \equiv \frac{\partial S}{\partial \overline{E}}\,, \tag{3.5}$$

which in turn exists as long as the entropy S is a function of the internal energy $\overline{E}$. However, the notion of temperature, as defined in equation (3.5), just like entropy shows its characteristic thermodynamical properties (see above) only for equilibrium states [3, 63, 70].

3.3. Local Temperature

Local temperature is, by definition, the temperature of a part of a larger system. Hence, this subsystem is not isolated but can exchange energy with its surrounding. On the other hand we limit our considerations to cases without particle exchange. We thus adopt the following convention:

Definition: *Local temperature exists if the considered part of the system is in a canonical state.*

Besides the arguments of statistical mechanics, described above, there are further practical reasons for this definition: The canonical distribution is an exponentially decaying function of energy characterized by one single parameter. This implies that there is a one to one mapping between temperature and the expectation values of observables, by which temperature is usually measured. Temperature measurements via different observables thus yield the same result, contrary to distributions with several parameters.

We think that this is a basic property of systems that can be characterized by thermodynamic description. The temperature, if it exists, describes a system in a sufficiently complete way, such that several properties of it can be predicted if one only knows its temperature.[1].

[1] Scenarios, in which local temperatures cease to exist and the consequences of this breakdown are discussed in chapter 12

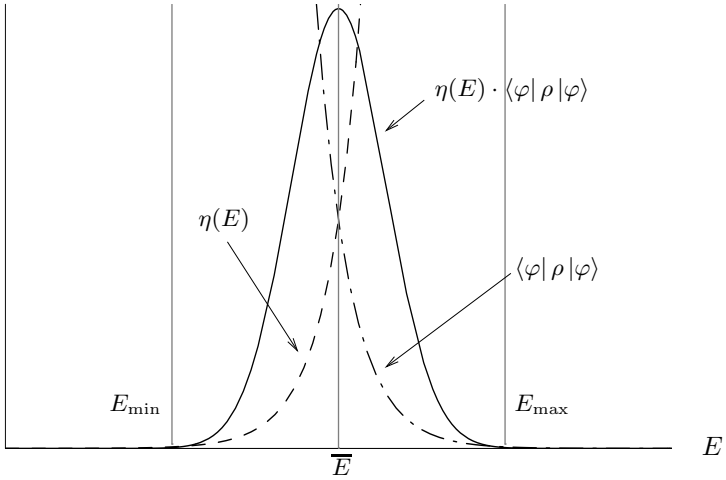

Figure 3.1.: The product of the density of states $\eta(E)$ times the occupation probabilities $\langle\varphi|\,\rho\,|\varphi\rangle$ forms a strongly pronounced peak at $E = \overline{E}$.

Why does the distribution need to be exponentially decaying? In large systems with a modular structure, the density of states is a strongly growing function of energy [70]. The product of the density of states times an exponentially decaying distribution of occupation probabilities thus forms a strongly pronounced peak at the internal energy $\overline{E}$, see figure 3.1

If the distribution were not exponentially decaying, the product of the density of states times the distribution would not have a pronounced peak and thus physical quantities like energy would not have "sharp" values.

4. Outline of the Approach

After having introduced and discussed our conception, when temperature is defined to exist locally, we now turn to outline our approach.

Since we define temperature to exist locally, i. e. for a given part of the system we consider, if the respective part is in a thermal equilibrium state, we define it to exist on a certain length scale, if all possible partitions of the corresponding size are simultaneously in an equilibrium state.

The requirement for the local equilibrium states in the parts to exist at the same time needs some further discussion: For a given temperature profile, it should not make a difference whether the profile is scanned by one single thermometer, which is moved in small steps across the sample, or whether the profile is measured by several thermometers simultaneously, which are located at small distances to each other.

For systems which are globally in a non-equilibrium state it is very difficult to decide under what conditions equilibrium states show up locally [47] and only very few exact results are known [57]. Nonetheless, whenever local equilibrium exists, the macroscopic temperature gradient is small ($\delta T/T \ll 1$). Here, we restrict ourselves to systems which are in a global equilibrium state (3.3) [1]. In these situations, subunits of the total system are in an equilibrium state whenever their effective interaction is weak enough and correlations between them are small so that the global thermal state approximately factorizes into a product of local thermal states.

Whenever the macroscopic temperature gradient is small ($\delta T/T \ll 1$), we expect our results to be applicable even for situations with only local equilibrium but non-equilibrium on the global scale.

To explore how local temperature can exist, that is how small the respective part may be, we will look at parts of different sizes. The idea

[1] One can imagine that the system has been brought into thermal contact with an even larger bath and has, in this way, relaxed into its thermal state. However, the way the system has reached its state is not relevant for our considerations.

behind this approach is the following:

We consider systems that are composed of elementary subsystems with short range interaction, for simplicity say nearest neighbor interaction. If then n adjoining subsystems form a part, the energy of the part is n times the average energy per subsystem and is thus expected to grow as the size of the part, n. Since the subsystems only interact with their nearest neighbors, two adjacent parts interact via the two subsystems at the respective boundaries, only. As a consequence, the effective coupling between two parts is independent of the part size n and thus becomes less relevant compared to the energy contained in the parts as their size increases. This reasoning also lies at the heart of the known proofs of the Thermodynamic Limit [63, 50].

We therefore consider homogeneous systems with nearest neighbor interactions which we divide into identical parts. The Hamiltonian of the system, thus reads

$$H = \sum_{\mu} \left(H_{\mu}^{(0)} + I_{\mu,\mu+1} \right) , \tag{4.1}$$

where the $H_{\mu}^{(0)}$ are the Hamiltonians of the isolated parts and the $I_{\mu,\mu+1}$ the interactions between the parts.

To test whether a part $H_{\mu_0}^{(0)}$ is in a thermal state, we have to calculate its reduced density matrix by tracing out the rest of the system. This trace can only be performed in a basis formed by products of the eigenstates of the $H_{\mu}^{(0)}$,

$$H_{\mu}^{(0)} \left| a_{\mu} \right\rangle = E_{\mu} \left| a_{\mu} \right\rangle \qquad \text{with} \qquad \left| a \right\rangle = \prod_{\mu} \otimes \left| a_{\mu} \right\rangle . \tag{4.2}$$

We thus have to write the global equilibrium state (3.3) in the basis formed by the states $|a\rangle$. Denoting the eigenstates and eigenenergies of the global Hamiltonian with Greek indices, $|\varphi\rangle$, $|\psi\rangle$ and E_{φ}, E_{ψ}, the global equilibrium state $\hat{\rho}$ reads

$$\left\langle \varphi \right| \hat{\rho} \left| \psi \right\rangle = \frac{\mathrm{e}^{-\beta E_{\varphi}}}{Z} \, \delta_{\varphi\psi} \tag{4.3}$$

in the global eigenbasis and the diagonal elements in the product basis

are

$$\langle a|\,\hat{\rho}\,|a\rangle = \int_{E_0}^{E_1} w_a(E)\,\frac{\mathrm{e}^{-\beta E}}{Z}\,dE\,, \tag{4.4}$$

where $\sum_\varphi$ has been replaced by an integral over the energy and

$$w_a(E) = \frac{1}{\Delta E} \sum_{\{|\varphi\rangle : E \le E_\varphi < E+\Delta E\}} |\langle a|\varphi\rangle|^2\,. \tag{4.5}$$

Here the sum runs over all states $|\varphi\rangle$ with energy eigenvalues E_φ in the respective energy range and ΔE is small [2].

We consider it sufficient to determine when the diagonal elements (4.4) are distributed as in an equilibrium state, since this guarantees that every temperature measurement via observables that commute with the $H_\mu^{(0)}$ yields the same result as for equilibrium states.

Fig. 4.1 shows the canonical distribution $\mathrm{e}^{-\beta E_\varphi}$ and two representatives of the distributions $w_a(E)$ for two different product states $|a\rangle$ and $|a'\rangle$. We have to analyze when the integral over the product $\mathrm{e}^{-\beta E} \times w_a(E)$ is again of the form $\mathrm{e}^{-\beta E_a}$, i.e. is again exponentially decaying in the energy E_a.

As is obvious from fig. 4.1, the steepness of the left flank (towards low energies) of the distributions $w_a(E)$ plays a crucial role. The less steep the flank is, the more large values of $\mathrm{e}^{-\beta E}$ enter into the integral, causing its value to become larger. The left flanks thus have to vary in a suitable way from one distribution $w_a(E)$ to another one $(w_{a'}(E))$ such that the values of the corresponding integrals have a ratio given by the Boltzmann factor of a canonical distribution.

A second obstacle is the energy of the ground state E_0. The energy of every stable system has to be bounded from below. Thus there is a minimal energy E_0. The distributions $w_a(E)$ of course vanish at E_0. Nevertheless, the product of $\mathrm{e}^{-\beta E}$ times $w_a(E)$ can have a finite value at E_0. This affects the balance between terms with $\mathrm{e}^{-\beta E} < \mathrm{e}^{-\beta E_a}$ and terms with $\mathrm{e}^{-\beta E} > \mathrm{e}^{-\beta E_a}$ that enter the integral. Thus for low E_a, the lower limit E_0 has an influence on the values of the integral (4.4).

[2] The way, $w_a(E)$ is written here, is of course not mathematically precise. A rigorous definition of $w_a(E)$ and the proof of its existence are given in chapter 5

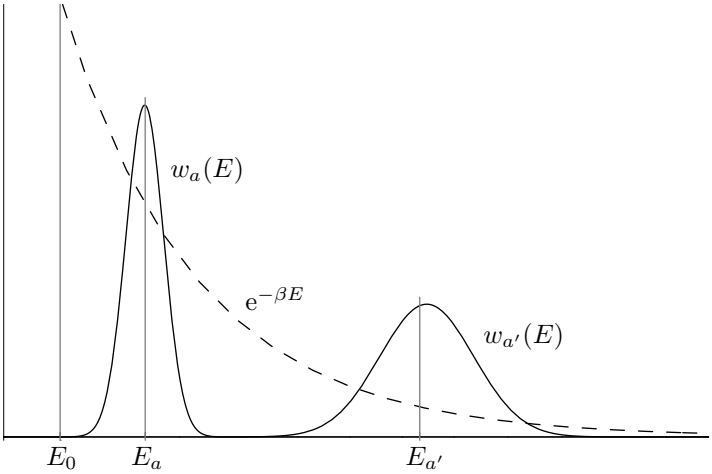

Figure 4.1.: The canonical distribution $\mathrm{e}^{-\beta E_\varphi}$ and two representatives of the distributions $w_a(E)$ for two different product states $|a\rangle$ and $|a'\rangle$.

To check whether the diagonal elements (4.4) are indeed canonically distributed, we thus need to know the distributions $w_a(E)$. In the following chapter, we will prove, that they converge to Gaussian normal distributions in the limit of infinitely many parts. As a consequence of this result, the requirement, that the diagonal elements (4.4) should be canonically distributed, poses two conditions on the expectation value and the variance of the Gaussian distribution $w_a(E)$ and on the global temperature $T = \beta^{-1}$. These two conditions are associated one to one with the two obstacles described above.

For the existence of local temperature, we only require that the diagonal elements (4.4) are canonically distributed in an appropriate energy range. As described in the previous chapter, the density of states $\eta(E)$ is, for large modular systems, an exponentially growing function of energy and its product with the exponentially decaying canonical distribution $\langle\varphi|\,\rho\,|\varphi\rangle$ forms a strongly pronounced peak at the expectation value of the global energy $\overline{E}$, see figure 3.1.

If the diagonal elements (4.4) are canonically distributed in an energy

range, that is centered at this peak and is large enough to entirely cover it, all observables with non-vanishing matrix elements in that range show the same behavior as for a canonical distribution. Observables which are not of that kind are in general not of interest. If one considers for example 1 kg of iron at 300 Kelvin with an average energy of roughly 130 kJ, one is usually not interested in processes, that take place at energies of 0.1 kJ or 10^5 kJ.

In the following chapters, we present the details of the approach sketched here.

5. Quantum Central Limit Theorem

The approach, we use to explore on what length scales temperatures can exist locally, is based on a central limit theorem for quantum many body systems with nearest neighbor interaction.

Since physical systems, composed of interacting identical (or similar) subsystems appear in many branches of physics and are standard in condensed matter physics [52, 68, 51], we dedicate an entire chapter to this theorem.

In its classical form, the central limit theorem states that the distribution of the sum of n independent, identically distributed random variables converges to a Gaussian normal distribution in the limit of large n. The theorem presented here, is not a statement about random variables, but about the distribution of the eigenvalues of an operator in a pure state, that is not its eigenstate.

The connection of this result to probability theory is entirely due to the Copenhagen Interpretation of Quantum Theory. If an observable $\mathcal{O}$ of a quantum system is measured and the system is not in an eigenstate of $\mathcal{O}$, say $|a\rangle$, the possible outcomes of the measurement are the eigenvalues O_φ of $\mathcal{O}$ and the probabilities of their occurrences are given by the squared absolute value of the scalar product of the corresponding eigenstate $|\varphi\rangle$ and the state $|a\rangle$,

$$\mathbb{P}_a\left(o_\varphi\right) = \left|\langle a|\varphi\rangle\right|^2 . \tag{5.1}$$

In a more mathematical language: Since the operator $\mathcal{O}$ is hermitian, the state $|a\rangle$ induces a measure on the spectrum of $\mathcal{O}$. In physics, this measure is interpreted as the probability of the occurrence of certain eigenvalues of $\mathcal{O}$ if $\mathcal{O}$ is measured in the state $|a\rangle$.

The theorem we present below considers chains of quantum systems with nearest neighbor interactions and states that for a product state

$|a\rangle$, the measure (5.1) converges to a Gaussian normal distribution in the limit of infinitely many subsystems.

Further assumptions, which are needed to proof the theorem are very weak; the energy of each subsystem must not exceed a given bound and the width of (5.1) must grow with the number of subsystems. A precise formulation of these conditions will be given below along with the theorem. Before we state the theorem itself, we first introduce the model and the relevant notation.

5.1. Model and Notation

We consider a chain of quantum systems with nearest neighbor interactions. The entire system is described by a Hamiltonian H which is a linear, self-adjoint operator on a separable, complex Hilbert space $\mathscr{H}$. The Hilbert space $\mathscr{H}$ is a direct product of the Hilbert spaces of the subsystems,

$$\mathscr{H} \equiv \prod_{\mu=1}^{n} \otimes \mathscr{H}_\mu \,, \tag{5.2}$$

and the Hamiltonian may be written in the form,

$$H \equiv \sum_{\mu=1}^{n} \mathcal{H}_\mu \,, \tag{5.3}$$

with

$$\mathcal{H}_\mu \equiv \hat{1}^{\otimes\,\mu-1} \otimes H_\mu \otimes \hat{1}^{\otimes\,n-\mu} \;+\; \hat{1}^{\otimes\,\mu-1} \otimes I_{\mu,\mu+1} \otimes \hat{1}^{\otimes\,n-(\mu+1)} \,, \tag{5.4}$$

where H_μ is the proper Hamiltonian of subsystem μ, $I_{\mu,\mu+1}$ the interaction of subsystem μ with subsystem $\mu+1$ and $\hat{1}$ is the identity operator.

The theorem holds for periodic boundary conditions, $I_{n,n+1} = I_{n,1}$ as well as for fixed boundary conditions, $I_{n,n+1} = 0$. The proof in appendix A is only given for fixed boundary conditions, but the modification for periodic ones is straight forward.

Let furthermore E_φ be the eigenenergies and, using the Dirac notation [65], let $\{|\varphi\rangle\}$ be an orthonormal basis of $\mathscr{H}$ consisting of eigenstates of the total system.

$$H\,|\varphi\rangle = E_\varphi\,|\varphi\rangle \qquad \text{with} \qquad \langle\varphi|\varphi'\rangle = \delta_{\varphi\varphi'} \,, \tag{5.5}$$

where $\delta_{\varphi\varphi'}$ is the Kronecker delta. We denote by $|a\rangle$ the product state

$$|a\rangle \equiv \prod_{\mu=1}^{n} \otimes |a_\mu\rangle \,, \tag{5.6}$$

built up from some state $|a_\mu\rangle$ of each subsystem μ, $|a_\mu\rangle \in \mathscr{H}_\mu$.

In general, $|a\rangle$ is not an eigenstate of H and the total energy E does not have a sharp value in the state $|a\rangle$. We denote its expectation value and its squared width, respectively, by

$$\overline{E}_a \equiv \langle a| H |a\rangle \,, \tag{5.7}$$

$$\Delta_a^2 \equiv \langle a| H^2 |a\rangle - \langle a| H |a\rangle^2 \,. \tag{5.8}$$

Furthermore we introduce the operator

$$S_n \equiv \frac{H - \overline{E}_a}{\Delta_a} \,, \tag{5.9}$$

which is diagonal in the same basis as H. The operator S_n is defined such that its expectation value in the state $|a\rangle$ vanishes and its squared width is one,

$$\langle a| S_n |a\rangle = 0 \qquad \text{and} \qquad \langle a| S_n^2 |a\rangle = 1 \,. \tag{5.10}$$

Let s_φ denote its eigenvalues,

$$S_n |\varphi\rangle = s_\varphi |\varphi\rangle \,. \tag{5.11}$$

Note that H and therefore $\overline{E}_a$, Δ_a and s_φ as well as the basis $\{|\varphi\rangle\}$ depend on the number of subsystems n.

Since H and thus S_n are self-adjoint , $|a\rangle$ induces a measure on the spectrum of S_n and H. This measure of the quantum mechanical distribution of the eigenvalues of S_n in the state $|a\rangle$, is given by the usual formula [65],

$$\mathbb{P}_a \left(s_\varphi \in [s_1, s_2]\right) = \sum_{\{|\varphi\rangle : s_1 \leq s_\varphi \leq s_2\}} |\langle a|\varphi\rangle|^2 \,, \tag{5.12}$$

where the sum extends over all states $|\varphi\rangle$ with eigenvalues in the respective interval. $\mathbb{P}_a \left(s_\varphi \in [s_1, s_2]\right)$ is the probability that a value s_φ between s_1 and s_2 is obtained if S_n is measured in the state $|a\rangle$.

After having introduced the necessary notation and definitions, we now turn to formulate the theorem.

5.2. Theorem

If the operator H and the state $|a\rangle$ satisfy

$$\Delta_a^2 \geq n\, C \tag{5.13}$$

for all n and some $C > 0$ and if each operator $\mathcal{H}_\mu$ is bounded, i.e.

$$\langle\chi|\, \mathcal{H}_\mu\, |\chi\rangle \leq C' \tag{5.14}$$

for all normalized states $|\chi\rangle \in \mathscr{H}$ and some constant C', then the quantum mechanical distribution of the eigenvalues of S_n in the state $|a\rangle$ converges weakly to a Gaussian normal distribution:

$$\lim_{n\to\infty} \mathbb{P}_a\left(s_\varphi \in [s_1, s_2]\right) = \int_{s_1}^{s_2} \frac{\exp\left(-s^2/2\right)}{\sqrt{2\pi}}\, ds \tag{5.15}$$

for all real $-\infty < s_1 < s_2 < \infty$.

5.3. Sketch of the proof

The proof of the theorem 5.2 follows closely the proof of central limit theorems for mixing sequences of classical random variables; The weak convergence of the distributions is shown by proofing the pointwise convergence of the characteristic functions [32].

For every distribution $\mathbb{P}_a$, there exists a density, $w_a(s_\varphi)$, which is defined by

$$\mathbb{P}_a\left(s_\varphi \in [s_1, s_2]\right) \equiv \int_{s_1}^{s_2} w_a(s)\, ds\,. \tag{5.16}$$

The characteristic function is the Fourier transform of the density $w_a(s_\varphi)$:

$$\langle a|\, \mathrm{e}^{-\mathrm{i}rS_n}\, |a\rangle = \int_{s_1}^{s_2} w_a(s)\, \mathrm{e}^{-\mathrm{i}rs}\, ds\,. \tag{5.17}$$

Since the Fourier transform of a Gaussian is again a Gaussian, one can prove that the density converges to a Gaussian by proving that the characteristic function converges to a Gaussian.

To illustrate the basic idea of this proof, let us have a look at a simpler system: Consider therefore the operators

$$X_\mu = \frac{\mathcal{H}_\nu - \langle a|\,\mathcal{H}_\nu\,|a\rangle}{\Delta_a}\,, \qquad \text{where} \qquad S_n = \sum_{\mu=1}^{n} X_\mu\,. \tag{5.18}$$

Let us assume the X_μ to be independent, that is they commute, and that all mixed moments factorize,

$$[X_\mu, X_\nu] = 0\,, \qquad \text{and} \qquad \langle a|\,X_\mu^k X_\nu^l\,|a\rangle = \langle a|\,X_\mu^k\,|a\rangle\,\langle a|\,X_\nu^l\,|a\rangle\ . \tag{5.19}$$

for any integers k and l. As a second simplification, we assume that the state was translation invariant ($|a_\mu\rangle = |a_0\rangle$ for all μ),

$$|a\rangle = |a_0\rangle^{\otimes n}\ , \tag{5.20}$$

where the state $|a_0\rangle$ is not an eigenstate of the operators X_μ. For this system, which is of course much simpler than the system defined by equations (5.3) and (5.4), the limit of the characteristic function can be calculated as follows:

$$\begin{aligned}
\langle a|\,\mathrm{e}^{-\mathrm{i}rS_n}\,|a\rangle &= \langle a|\exp\left(-\mathrm{i}r\sum_{\mu=1}^{n} X_\mu\right)|a\rangle && (5.21)\\
&= \prod_{\mu=1}^{n}\langle a|\exp\left(-\mathrm{i}rX_\mu\right)|a\rangle && (5.22)\\
&= \prod_{\mu=1}^{n}\left(1 - \frac{r^2}{2}\,\langle a|\,X_\mu^2\,|a\rangle + \ldots\right) && (5.23)\\
&= \left(1 - \frac{r^2}{2}\,\langle a|\,S_n^2\,|a\rangle + \ldots\right) \xrightarrow[n\to\infty]{} \exp\left(-\frac{r^2}{2}\right) && (5.24)
\end{aligned}$$

The property (5.19) ensures that (5.22) holds, while the convergence in (5.24) is due to equation (5.20). In this special case here, we have $\Delta_a^2 \propto n$ and, since each X_μ carries a normalization factor Δ_a^{-1}, all moments of higher order vanish because the normalization factors grow faster than the number of terms as $n \to \infty$. The latter only ensures the convergence

because all appearing terms have comparable values, which is a consequence of the translation invariance of the system and the state. In the asymptotic relation (5.24) we have used equation (5.10).

For the much more general case, for which our theorem (5.15) applies, the proof works along the same lines as above. However, the proof of equality (5.22) and the asymptotic equality (5.24) is more subtle. Successively, one shows that

- the characteristic function does not change, if a few of the $\mathcal{H}_\mu$ are neglected, and that the characteristic function of the remainder of H factorizes, which establishes the equality (5.22),
- the remainder of H fulfills the Lyapunov condition [10] (see eq. (A.29)) and therefore, the entire characteristic function is of a Gaussian form, which establishes the asymptotic equality (5.24).

In this more general case, the Lyapunov condition plays the role of the translation invariance for the special case.

Since the characteristic function is the Fourier transform of the density of the distribution, the latter is of a Gaussian form whenever the characteristic function is, which completes the proof.

The complete, rigorous proof is given in appendix A, we thus refer the interested reader to this chapter.

5.4. Discussion of the Assumptions and Possible Generalizations

The above theorem is formulated for a linear chain of quantum systems with nearest neighbor interactions. As is obvious from its proof in section A, this is not the most general setup, where it holds.

First of all, the theorem is not only valid for a linear chain but also for lattices of arbitrary dimension. This is a straight forward generalization of the theorem and trivial to proof by simply mapping the indices to higher dimensional ones.

In addition, the interactions may be short range of the following type: Every subsystem interacts only with a fixed, limited number of neighboring subsystems. The crucial point here is, that the number of interaction partners must not depend on the total number of subsystems.

The conditions (5.13) and (5.14) deserve some further discussion, too. We first consider condition (5.13). Rewriting it in terms of the operators $X_\mu \equiv \mathcal{H}_\mu - \langle a| \mathcal{H}_\mu |a\rangle$ and using equation (A.26) we get

$$\sum_{\mu=1}^{n} \langle a| \frac{1}{2} \left(X_\mu^2 + X_{\mu+1}^2\right) + X_\mu X_{\mu+1} + X_{\mu+1} X_\mu |a\rangle \geq n\, C\,. \qquad (5.25)$$

Thus, every term in the sum in (5.25) having a finite value larger than zero is sufficient for (5.13) to be satisfied.

Condition (5.14) states that the energy of one subsystem must not exceed an upper bound, which in turn must not depend on the total number of subsystems. Physically, this means that for a diverging number of subsystems, the excitation energy, which then also diverges for most states, should not be concentrated in only a small part of the subsystems. While the condition is automatically fulfilled for all states if the subsystems have a finite spectrum, such as i.e. spins, it is violated for some states if the subsystems have an infinite spectrum, such as i.e. harmonic oscillators. For very large systems however, where our theorem applies, this is only a minor restriction since, due to combinatorial reasons, the fraction of states that do not fulfill condition (5.14) is vanishingly small.

Furthermore, the observable one considers need not be the Hamiltonian. Any other observable shows the same feature as long as conditions (5.13), (5.14), (A.25) and (A.26) are met.

Finally, conditions (5.13) and (5.14) may be relaxed, since the theorem still holds, whenever Lyapunov's condition, or even only Lindeberg's condition [10] (see eq. (A.32)), is fulfilled (see appendix A). We have chosen here stricter but simpler conditions to make it easier to check the applicability of our theorem.

After the discussion of our assumptions and possible generalizations of these, we now consider the application of the theorem to physical problems.

5.5. Applications in Physics

For applications in physics, where n is very large but finite, the density of the limit distribution (5.15) can be written as a function of the energy

E of the system,

$$\mathbb{P}_a(E \in [E_1, E_2]) = \int_{E_1}^{E_2} w_a(E)\, dE\,, \tag{5.26}$$

with

$$w_a(E) = \frac{1}{\sqrt{2\pi}\,\Delta_a}\, \exp\left(-\frac{\left(E - \overline{E}_a\right)^2}{2\,\Delta_a^2}\right)\,, \tag{5.27}$$

where we have substituted of the integration variable in equation (5.15) by

$$s = \frac{E - \overline{E}_a}{\Delta_a}\,. \tag{5.28}$$

As a consequence the expectation value of an operator $\mathcal{O}$, which is a function of H and thus diagonal in the eigenbasis, can be written

$$\langle a|\, \mathcal{O}\, |a\rangle = \int w_a(E)\, O(E)\, dE\,, \tag{5.29}$$

where $O(E)$ is the eigenvalue of $\mathcal{O}$ belonging to the energy E. If $\mathcal{O}$ is not a function of H, degenerate eigenvalues of H, for which $\mathcal{O}$ takes on different values, are problematic.

One application of the theorem is of course the calculation of the minimal length scales for the existence of local temperatures, which we will discuss in chapter 7. Two other applications of equation (5.29) are given in the next chapter, 6. Here, we will finally discuss some existing central limit theorems and their relation to ours.

5.6. Connection to Other Existing Theorems

Central limit theorems for the distribution of energy eigenvalues in quantum gases with Boltzmann statistics [27] as well as for Bose and Fermi statistics [26] have been discussed by M. Sh. Goldstein. His theorems apply for mixed states, namely classical mixtures of quantum states involving classical probabilities. These results are thus not comparable

to ours since they consider classical probabilities, while we consider a measure on the spectrum of an operator in a pure state.

Some extensions of the central limit theorem to quantum systems, with the state not necessarily being mixed, have been proven in the past [13, 2, 24, 25, 49, 58]. The version, which appears closest related to ours, has been published by Goderis and Vets in 1989 [25]. They consider a quantum lattice system and assume that the state and the operator they look at, are invariant under lattice translations. Their proof is then based on a set of "cluster conditions", which replace the mixing condition of the random variable case.

The assumptions we use are stricter with respect to the mixing behavior, nevertheless, they may still be weakened and generalized. On the other hand, neither the operator (Hamiltonian) nor the product state need to be invariant with respect to lattice translations. This point makes our theorem much more general than others and opens up a large field of applications [35].

Translation invariant product states are states $|a\rangle$, in which every subsystem is in the same state $|a_0\rangle$ ($|a_\mu\rangle = |a_0\rangle$ for all μ),

$$|a\rangle_{\text{trans. inv.}} = |a_0\rangle^{\otimes n} \ . \tag{5.30}$$

However, states of this type form only a small fraction of all possible product states. In particular for the case $n \gg 1$, this fraction is negligible. For applications of the theorem in physics it is thus very important that translation invariance need not be required.

6. Tests and Applications of the Quantum Central Limit Theorem

In this chapter, we apply the quantum central limit theorem (5.15) to the calculation of quantities, which are of interest in condensed matter physics. In particular, we calculate the spectral density and the partition function for a spin chain model, for which both quantities may also be evaluated exactly. Thus, by comparing the results we get a test of the theorem (5.15).

Nonetheless our aim here is twofold. On the one hand the applications of theorem (5.15) serve to check whether the theorem reproduces correctly the known exact results. On the other hand, since (5.15) is valid under very general assumptions, it allows to estimate quantities, such as the spectral density and the partition function, even for models, where they may not be obtained exactly. The theorem (5.15) is thus a very powerful tool for the calculation of collective properties of quantum many particle systems.

In order to study these systems in full detail, the respective Hamiltonians need to be diagonalized. With increasing dimension of the Hilbert space, the diagonalization of an operator becomes a very tedious task. For lattices or arrays of interacting subsystems or particles, the dimension of the Hilbert space scales as m^n, where m is the dimension of the Hilbert space of one particle and n is the number of particles. Thus, apart from some exceptions [46], it is even numerically impossible to exactly determine the eigenvalues of those models.

Fortunately, considerable understanding can be obtained already from functions of the eigenvalues without knowing each individual eigenvalue. For example all thermodynamical quantities of a system are determined by its partition function [69,48,40], while spectral densities reveal central

properties of the dynamics of a system.

We therefore rederive these two quantities here from our theorem (5.15) for a case, where they are well known and thus establish the theorem as an alternative method.

6.1. Spectral Densities

Spectra of energy levels and thus spectral densities are of immense interest in the theory of quantum systems. They play a central role, e.g. in the analysis of chaotic behavior [28].

For systems, where theorem (5.15) holds, the calculation of spectral densities is straight forward: Let us first consider the so-called counting function $N(E)$, that is the number of energy levels below a given threshold energy E. It is given by the trace of the operator $\Theta(E - H)$, where Θ is the Heaviside step function. Since the trace of an operator is invariant under basis transformations, we may choose to compute it in the basis formed by products of eigenstates of the local Hamiltonians H_μ (see equation (5.4)),

$$|a\rangle \equiv \prod_{\mu=1}^{n} \otimes \, |a_\mu\rangle \,, \quad \text{where } H_\mu \, |a_\mu\rangle = E_\mu \, |a_\mu\rangle \,. \tag{6.1}$$

For $N(E)$, we thus get

$$N(E) = \sum_{\{|a\rangle\}} \langle a| \, \Theta(E - H) \, |a\rangle \,, \tag{6.2}$$

where the sum extends over all states $|a\rangle$ of the type (6.1). According to equation (5.29), the expectation value of $\Theta(E-H)$ in the state $|a\rangle$ reads

$$\langle a| \, \Theta(E - H) \, |a\rangle = \int_{E_g}^{E} w_a(E') \, dE', \tag{6.3}$$

where E_g is the energy of the ground state of the system. The density of states η is given by the derivative of the counting function with respect to energy, $\eta(E) = dN(E)/dE$:

$$\eta(E) = \sum_{\{|a\rangle\}} w_a(E) = \sum_{\{|a\rangle\}} \frac{1}{\sqrt{2\pi}\,\Delta_a} \, \exp\left(-\frac{\left(E - \overline{E}_a\right)^2}{2\,\Delta_a^2} \right), \tag{6.4}$$

where $\overline{E}_a$ and Δ_a^2 are as defined in equations (5.7) and (5.8) respectively.

Since the convergence of the distribution is weak, i.e. only on intervals of nonzero length, the derivative should be understood according to its definition as a linear approximation on intervals of arbitrarily small but non-vanishing length.

6.2. Partition Sums

The thermodynamics of a physical system is completely determined by its partition function. It is therefore of fundamental relevance to know the partition function of the system of interest. For quantum systems its calculation is extremely demanding since it involves the complete diagonalization of the Hamiltonian. As the dimension of the Hilbert space grows exponentially with the number of subsystems, the diagonalization of the Hamiltonian quickly becomes impossible even with super computers.

Theorem (5.15) allows to give an analytical expression for the partition function at finite temperatures, which can easily be evaluated numerically. The partition function is given by the trace of the operator $\exp(-\beta H)$ with the inverse temperature β. We again express it in the basis $\{|a\rangle\}$ as defined in equation (6.1):

$$Z = \sum_{\{|a\rangle\}} \langle a| \, \mathrm{e}^{-\beta H} \, |a\rangle \tag{6.5}$$

The expectation values of $\exp(-\beta H)$ can be computed using equation (5.29) [30, 31], they read

$$\begin{aligned} \langle a| \, \mathrm{e}^{-\beta H} \, |a\rangle = \frac{1}{2} \, \exp\left(-\beta \overline{E}_a + \frac{\beta^2 \Delta_a^2}{2}\right) \times \\ \times \left[\operatorname{erfc}\left(\frac{E_g - \overline{E}_a + \beta \Delta_a^2}{\sqrt{2}\,\Delta_a}\right) - \operatorname{erfc}\left(\frac{E_u - \overline{E}_a + \beta \Delta_a^2}{\sqrt{2}\,\Delta_a}\right)\right], \end{aligned} \tag{6.6}$$

where $\overline{E}_a$ and Δ_a^2 are as defined in equations (5.7) and (5.8) and $\operatorname{erfc}(x)$ is the conjugate Gaussian error function [1]. E_g is the energy of the ground state and E_u the upper limit of the energy spectrum.

Expression (6.6) can be simplified further. The underlying central limit theorem is valid in the limit of a very large number of subsystems. In that limit, the argument of the second conjugate error function is always much larger than the argument of the first. Furthermore, it is always positive, which makes the second error function term negligible compared to the first [1].

Therefore, the partition function Z can be taken to read

$$Z = \sum_{\{|a\rangle\}} \exp\left(-\beta\left(\overline{E}_a - E_g\right) + \frac{\beta^2 \Delta_a^2}{2}\right) \frac{1}{2} \operatorname{erfc}\left(\frac{E_g - \overline{E}_a + \beta\Delta_a^2}{\sqrt{2}\,\Delta_a}\right), \tag{6.7}$$

where we have rescaled the energy in the first exponent, so that all appearing energies are positive and therefore $\exp\left(-\beta\left(\overline{E}_a - E_g\right)\right) \leq 1$. The ground state energy E_g in the error function is not a consequence of the rescaling but stems from a cutoff in the integral (5.29) similar to the one in (6.3).

In contrast to the expression for the density of states (6.4), there appears one quantity in equation (6.7) that cannot be obtained without diagonalizing the Hamiltonian. This is the ground state energy E_g.

The exact value of E_g however is not needed. The cutoff in (5.29) at E_g is only introduced because we are dealing with a finite number of subsystems. In the limit of infinite number of subsystems, it is irrelevant since the Gaussian function $w_a(E)$ decays strong enough, so that it becomes negligible at $E = E_g$. A sufficiently good estimate of E_g can be obtained from the spectral density (6.4).

However, since equation (5.15) is only an approximation to one term in the sum (6.7), errors due to the finite number of subsystems may add up. Nonetheless, the partition function divided by the number of states may be calculated instead (see section 6.4 for details).

We now turn to verify the validity of equations (6.4) and (6.7) for a model that can be treated exactly.

6.3. Numerical Verification

In this section we present numerical tests of the two equations (6.4) and (6.7) for an Ising spin chain in a transverse field. The Hamiltonian of

the chain reads

$$H = B\left(-\sum_{i=1}^{n}\sigma_i^z - K\sum_{i=1}^{n}\sigma_i^x \otimes \sigma_{i+1}^x\right). \tag{6.8}$$

Here, σ_i^x and σ_i^z are the Pauli matrices, $2B$ is the difference between local energy levels and KB the coupling strength. We chose periodic boundary conditions, $\sigma_{n+1}^x = \sigma_1^x$.

The model (6.8) can be diagonalized via successive Jordan-Wigner, Fourier and Bogoliubov transformations [64, 41] (see appendix B). The eigenvalues of the Hamiltonian (6.8) read

$$E_\varphi = \sum_{l=-(n/2)+1}^{n/2} \omega_l \left(n_l(\varphi) - \frac{1}{2}\right) \tag{6.9}$$

where the $n_l(\varphi)$ are fermionic occupation numbers that can take on the two values 0 and 1. The eigenfrequencies ω_l are given by

$$\omega_l = 2B\sqrt{K^2 + 1 - 2K\cos\left(\frac{2\pi l}{n}\right)}. \tag{6.10}$$

We chose units where Planck's and Boltzmann's constant are equal to one, $\hbar = k_B = 1$.

For a finite number of spins n, a "density of states" can be defined with respect to certain energy bins: We chose the size of the bins to be B, so that the density of states $\eta_n(E)$ is defined as

$$\eta_n(E) \equiv \frac{\text{number of eigenstates with } E_\varphi \in [E, E+B)}{B}. \tag{6.11}$$

The second quantity of interest, the partition function, is given by the standard expression [64]

$$Z_n = \prod_{l=-(n/2)+1}^{n/2} 2\cosh\left(\beta\frac{\omega_l}{2}\right), \tag{6.12}$$

where $\beta = T^{-1}$ is the inverse temperature. Note that the exact quantities, $\eta_n(E)$ and Z_n, carry an index n, reflecting the finite number of

spins, in contrast to the values of the asymptotic approximation, $\eta(E)$ and Z.

Before we proceed to calculate the density of states and the partition function for the model (6.8) with the help of equations (6.4) and (6.7), let us test whether the central limit theorem (5.15) is applicable at all, that is whether conditions (5.14) and (5.13) are satisfied.

The energy of each spin is at least $-B$ and at most B so that condition (5.14) is fulfilled. The squared width Δ_a^2 reads

$$\Delta_a^2 = n\, B^2\, K^2, \tag{6.13}$$

where n is the number of spins, and condition (5.13) is also met. For a large number of spins, the density of states and the partition function of the system at hand can thus, indeed, be calculated via equations (6.4) and (6.7).

The model (6.8) allows for a further simplification of equations (6.4) and (6.7): Since $\overline{E}_a = E_a$ and $\Delta_a^2 = const$, the sum over all states $|a\rangle$ can be transformed into a sum over all energies $E_a = k\,2\,B - n\,B$ with $k = 0, 1, \ldots, n$. Here, the number of states $|a\rangle$ with energy E_a is equal to the number of configurations with k spins pointing up, so that

$$\sum_{\{|a\rangle\}} = \sum_k \binom{n}{k}. \tag{6.14}$$

Using this transformation, the expressions (6.4) and (6.7) are now evaluated numerically and compared with the exact results (6.11) and (6.12).

Figure 6.1 shows the density of states $\eta_n(E)$ and its approximation $\eta(E)$ for a chain of 10 spins and for a chain of 15 spins. The approximation works well despite the still small number of spins; furthermore, the tendency that the approximation improves with increasing number of spins is evident. Figure 6.2 shows the partition function for a chain of 100 spins divided by the number of states, 2^{100}, as a function of temperature. The difference between the exact function Z_n and the approximation Z is not visible. To see whether the convergence improves with the number of spins, we have considered the maximal difference between Z_n and Z for all temperatures,

$$\delta(n) = \max_T \left| Z_n - Z \right|. \tag{6.15}$$

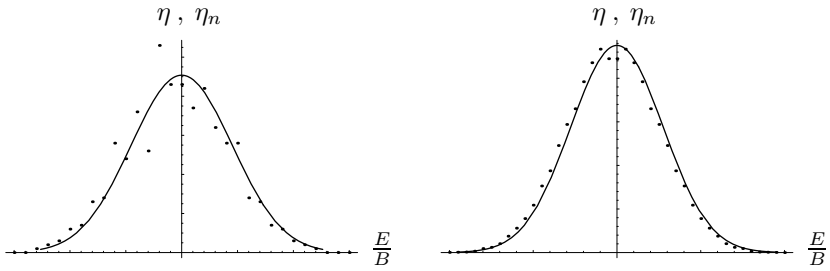

Figure 6.1.: Density of states for a chain of 10 spins and a chain with 15 spins for $B = K = 1$. The dots show the exact density η_n and the line the approximation η (η_n and η are defined in equations (6.11) and (6.4) respectively).

We have found the following values: $\delta(10) \sim 10^{-3}$, $\delta(100) \sim 10^{-8}$ and $\delta(1000) \sim 10^{-11}$.

6.4. Discussion and Limitations

The approximations of the quantities $\eta_n(E)$ and Z_n by equations (6.4) and (6.7) face some problems that cannot be avoided.

Firstly, the convergence in equation (5.15) is only weak, i.e. the lhs converges to the rhs for all intervals $[E_1, E_2]$ of nonzero length. The convergence is not pointwise. In the present case this means that, for example, the trace of a projector on a single eigenstate $P = |\varphi\rangle\langle\varphi|$ cannot be approximated. The problem becomes apparent, if one tries to calculate the partition function for zero temperature via (6.7), where only the ground state is occupied. In the present model, for example, this state is energetically separated from the other states that form a quasi continuous band. As a consequence quantum phase transitions [64] occuring at zero temperature can not be treated with our approach.

The second drawback of our approach is the following: Each term $\langle a| \mathcal{O} |a\rangle$ for some operator $\mathcal{O}$ that is a function of H is well approximated and the accuracy increases with the number of subsystems n. On the other hand, the number of terms in the sums (6.4) and (6.7) increases exponentially with the number of subsystems, for example with 2^n for the spin chain. Therefore, the quantities $\eta(E)$ and Z can only be in good

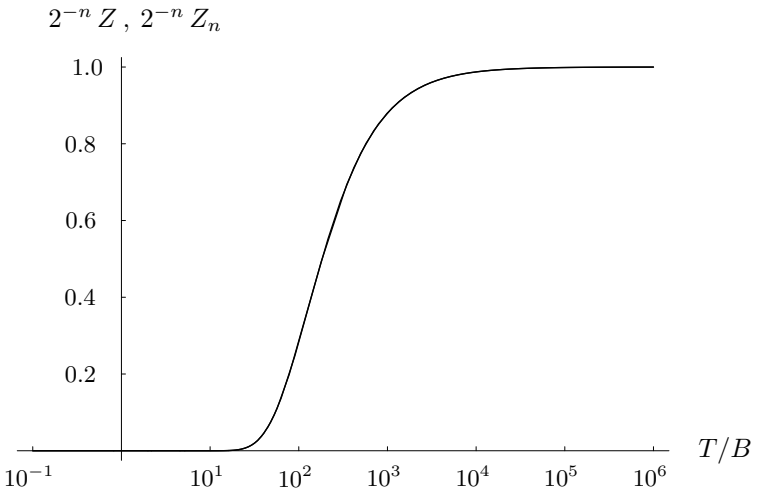

Figure 6.2.: Partition function for a chain of 100 spins with $B = K = 1$ divided by the number of states, 2^{100}. The difference between $2^{-n}\,Z_n$ and $2^{-n}\,Z$ is not visible (Z_n and Z are defined in equations (6.12) and (6.7) respectively).

accordance with $\eta_n(E)$ and Z_n, if both are divided by the dimension of the Hilbert space, i.e. the number of states $|a\rangle$.

This will not always be problematic, since the errors in each term $\langle a|\,\mathcal{O}\,|a\rangle$ need not all be of the same sign and may thus cancel each other, as in the calculation of the spectral densities.

In the calculation of the partition sum, however, there is the following problem: Every stable system has a finite minimal energy, the energy of the ground state. Nonetheless the probability density (5.27) is, albeit very small, nonzero for all energies. Therefore, one needs to introduce the cutoffs in the integral (5.29). As can be seen from expression (6.7), the upper limit of the integral does not matter. The lower limit on the other hand matters and becomes increasingly relevant at low temperatures. No matter what lower limit of the integral we take, the error of the approximation (6.7) always has the same sign.

Figure 6.3 shows the logarithm of the exact partition function of the spin chain and its approximation, each divided by the number of spins,

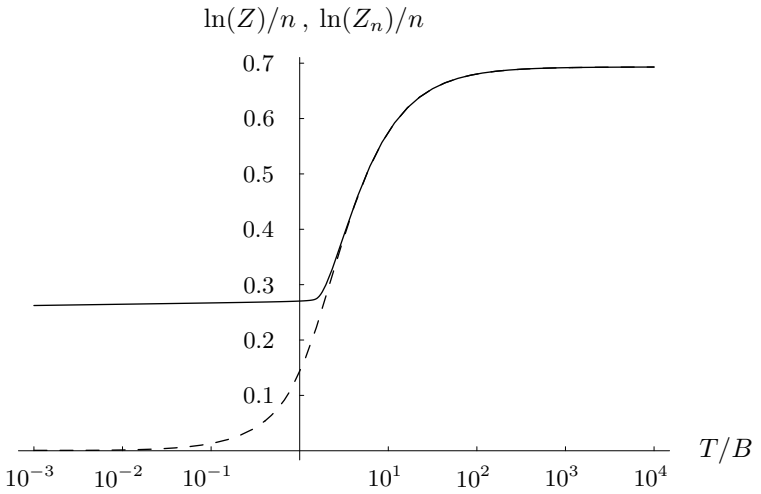

Figure 6.3.: Logarithm of the partition function divided by the number of spins for a chain of 1000 spins with $B = K = 1$. The dashed line shows the exact expression $\ln(Z_n)$ and the solid line the approximation $\ln(Z)$ (Z_n and Z are defined in equations (6.12) and (6.7) respectively).

for a chain of 1000 spins. The plot is done with the exact ground state energy. The approximation fails for low temperatures. In the present case ($B = K = 1$), deviations appear below $T \sim B$, while they start already at higher temperatures for stronger coupling, e.g. at $T \sim 10\,B$ for $K = 10$. Therefore, only the partition sum divided by the number of states can be accurately predicted.

7. General Theory for the Existence of Local Temperature

In this chapter we present the general theoretical considerations that determine the minimal length scale on which temperature can exist locally.

As discussed in chapter 3, we adopt the convention that temperature exists for a part of a larger system if that part is in a thermal, i.e. canonical, state. In order to determine whether temperature exists locally, we thus have to analyze under what conditions a canonical state exists locally.

As outlined in chapter 4, we focus on one dimensional systems which are in a canonical state on the global scale. We consider chains of particles with nearest neighbor interactions, partition them into N_G groups of n adjacent particles and test whether the diagonal elements of the reduced density matrices of the individual groups have a canonical form.

7.1. Model and Partition

We consider a homogeneous (i.e. translation invariant) chain of elementary quantum subsystems with nearest neighbor interactions. The Hamiltonian of our system is thus of the form [56],

$$H = \sum_i H_i + I_{i,i+1} \,, \tag{7.1}$$

where the index i labels the elementary subsystems. H_i is the Hamiltonian of subsystem i and $I_{i,i+1}$ the interaction between subsystem i and $i+1$. We assume periodic boundary conditions.

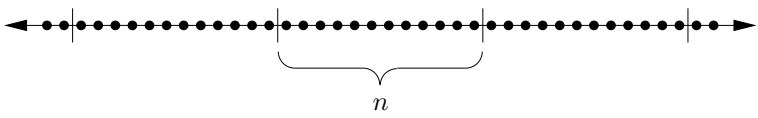

Figure 7.1.: Groups of n adjoining subsystems are formed.

We now form N_G groups of n subsystems each (index $i \to (\mu-1)n+j$; $\mu = 1, \ldots, N_G$; $j = 1, \ldots, n$) and split this Hamiltonian into two parts,

$$H = H_0 + I \,, \tag{7.2}$$

where H_0 is the sum of the Hamiltonians of the isolated groups,

$$\begin{aligned} H_0 &= \sum_{\mu=1}^{N_G} (\mathcal{H}_\mu - I_{\mu n, \mu n+1}) \qquad \text{with} \\ \mathcal{H}_\mu &= \sum_{j=1}^{n} H_{n(\mu-1)+j} + I_{n(\mu-1)+j,\, n(\mu-1)+j+1} \,, \end{aligned} \tag{7.3}$$

and I contains the interaction terms of each group with its neighbor group,

$$I = \sum_{\mu=1}^{N_G} I_{\mu n, \mu n+1} \,. \tag{7.4}$$

The eigenstates of the Hamiltonian H_0,

$$H_0 \, |a\rangle = E_a \, |a\rangle \,, \tag{7.5}$$

are products of group eigenstates of the individual groups (cf. chapt. 4),

$$|a\rangle = \prod_{\mu=1}^{N_G} \otimes \, |a_\mu\rangle \quad \text{with} \quad (\mathcal{H}_\mu - I_{\mu n, \mu n+1}) \, |a_\mu\rangle = E_\mu \, |a_\mu\rangle \,, \tag{7.6}$$

where E_μ is the energy of one subgroup only and $E_a = \sum_{\mu=1}^{N_G} E_\mu$.

7.2. Thermal State in the Product Basis

We assume that the total system is in a thermal state (cf. eq. (3.3)) with the density matrix

$$\hat{\rho} = \frac{\mathrm{e}^{-\beta H}}{Z} \,. \tag{7.7}$$

Here, Z is the partition sum and $\beta = (k_\mathrm{B} T)^{-1}$ the inverse temperature with Boltzmann's constant k_B and temperature T. Reduced density matrices of individual groups can only be calculated in the eigenbasis of H_0. We thus write the density matrix (7.7) in this basis. Its diagonal elements read

$$\langle a| \hat{\rho} |a\rangle = \langle a| \frac{\mathrm{e}^{-\beta H}}{Z} |a\rangle \,. \tag{7.8}$$

This is exactly a situation, for which the Quantum Central Limit Theorem of chapter 5 applies. One only has to take into account that the groups of the partition (7.2) now play the role of the subsystems in chapter 5. In this language, H describes a chain of groups interacting with their neighbor groups only and $|a\rangle$ is a product state with respect to this partition.

Thus, if conditions (5.13) and (5.14) are fulfilled, the theorem (5.15) holds and equation (5.29) can be used to calculate $\langle a| \hat{\rho} |a\rangle$ in the limit of infinite number of groups N_G since $\hat{\rho}$ is a function of the total Hamiltonian H.

$$\langle a| \hat{\rho} |a\rangle = \int_{E_0}^{E_1} w_a(E) \frac{\mathrm{e}^{-\beta E}}{Z} \, dE \,, \tag{7.9}$$

where E_0 is the energy of the ground state and E_1 the upper limit of the spectrum. For systems with an energy spectrum that does not have an upper bound, the limit $E_1 \to \infty$ should be taken. The distribution $w_a(E)$ reads

$$\lim_{N_G \to \infty} w_a(E) = \frac{1}{\sqrt{2\pi}\Delta_a} \exp\left(-\frac{\left(E - \overline{E}_a\right)^2}{2\,\Delta_a^2} \right) \,, \tag{7.10}$$

where the quantities $\overline{E}_a$ and Δ_a are defined in equations (5.7) and (5.8), respectively.

The expectation value of the entire Hamiltonian H in the state $|a\rangle$, $\overline{E}_a$, is the sum of the energy eigenvalue of the isolated groups E_a and a term that contains the interactions,

$$\overline{E}_a = E_a + \varepsilon_a \,, \tag{7.11}$$

Therefore, the two quantities ε_a and Δ_a^2 can also be expressed in terms of the interaction (see eq. (7.2)) only,

$$\varepsilon_a = \langle a| I |a\rangle \qquad \text{and} \tag{7.12}$$

$$\Delta_a^2 = \langle a| I^2 |a\rangle - \langle a| I |a\rangle^2 \,, \tag{7.13}$$

meaning that ε_a is the expectation value and Δ_a^2 the squared width of the interactions in the state $|a\rangle$. Note that ε_a has a classical counterpart while Δ_a^2 is purely quantum mechanical. It appears because the commutator $[H, H_0]$ is nonzero, and the distribution $w_a(E)$ therefore has nonzero width.

The applicability of theorem (5.15) depends on whether the two conditions (5.13) and (5.14) are fulfilled. In scenarios, where the energy spectrum of each elementary subsystem has an upper limit, such as spins, condition (5.14) is met a priori. For subsystems with an infinite energy spectrum, such as harmonic oscillators, we restrict our analysis to states where the energy of every group, including the interactions with its neighbor groups, is bounded. Thus, our considerations do not apply to product states $|a\rangle$, for which all the energy was located in only one group or only a small number of groups. The number of such states is vanishingly small compared to the number of all product states.

Provided that conditions (5.14) and (5.13) are met, equation (7.8) yields for $N_G \gg 1$,

$$\langle a| \hat{\rho} |a\rangle = \frac{1}{Z} \exp\left(-\beta\,(E_a + \varepsilon_a) + \frac{\beta^2 \Delta_a^2}{2}\right) \times$$

$$\times \frac{1}{2}\left[\operatorname{erfc}\left(\frac{E_0 - E_a - \varepsilon_a + \beta\Delta_a^2}{\sqrt{2}\,\Delta_a}\right) - \operatorname{erfc}\left(\frac{E_1 - E_a - \varepsilon_a + \beta\Delta_a^2}{\sqrt{2}\,\Delta_a}\right)\right] , \tag{7.14}$$

where $\operatorname{erfc}(x)$ is the conjugate Gaussian error function [1],

$$\operatorname{erfc}(x) = \frac{2}{\sqrt{\pi}} \int_x^\infty \mathrm{e}^{-s^2}\, ds \,. \tag{7.15}$$

The second error function appears only if the energy is bounded and the integration extends from the energy of the ground state E_0 to the upper limit of the spectrum E_1.

Note that $E_a + \varepsilon_a$ is a sum of N_G terms and that Δ_a fulfills equation (5.13). The arguments of the conjugate error functions thus grow proportional to $\sqrt{N_G}$ or stronger. If these arguments divided by $\sqrt{N_G}$ are finite (different from zero), the asymptotic expansion of the error function [1] may thus be used for $N_G \gg 1$:

$$\operatorname{erfc}(x) \approx \begin{cases} \dfrac{\exp\left(-x^2\right)}{\sqrt{\pi}\, x} & \text{for} \quad x \to \infty \\ 2 + \dfrac{\exp\left(-x^2\right)}{\sqrt{\pi}\, x} & \text{for} \quad x \to -\infty \end{cases} \tag{7.16}$$

After inserting this approximation into equation (7.14) and using $E_0 < E_a + \varepsilon_a < E_1$ it follows that the second conjugate error function, which contains the upper limit of the energy spectrum, can always be neglected compared to the first, which contains the ground state energy.

The same type of argument shows that the normalization of the Gaussian in equation (7.10) is correct although the energy range does not extend over the entire real axis $(-\infty, \infty)$.

Applying the asymptotic expansion (7.16), equation (7.14) can be taken to read

$$\langle a|\, \hat{\rho}\, |a\rangle = \frac{1}{Z} \exp\left[-\beta\left(E_a + \varepsilon_a - \frac{\beta\Delta_a^2}{2}\right)\right] \tag{7.17}$$

for

$$\frac{E_0 - E_a - \varepsilon_a + \beta\Delta_a^2}{\sqrt{2N_G}\,\Delta_a} < 0 \tag{7.18}$$

and

$$\langle a|\, \hat{\rho}\, |a\rangle = \frac{\exp\left(-\beta E_0 - \dfrac{(E_a + \varepsilon_a - E_0)^2}{2\Delta_a^2}\right)}{\sqrt{2\pi}\, Z\ \dfrac{E_0 - E_a - \varepsilon_a + \beta\Delta_a^2}{\Delta_a}} \tag{7.19}$$

for

$$\frac{E_0 - E_a - \varepsilon_a + \beta\Delta_a^2}{\sqrt{2N_G}\,\Delta_a} > 0\,. \tag{7.20}$$

The off diagonal elements $\langle a|\,\hat{\rho}\,|b\rangle$ vanish for $|E_a - E_b| > \Delta_a + \Delta_b$ because the overlap of the two Gaussian distributions becomes negligible. For $|E_a - E_b| < \Delta_a + \Delta_b$, the transformation involves an integral over frequencies and thus these terms are significantly smaller than the entries on the diagonal.

7.3. Conditions for Local Thermal States

We now test under what conditions the density matrix $\hat{\rho}$ may be approximated by a product of canonical density matrices with temperature $\beta_{\rm loc}$ for each subgroup $\mu = 1, 2, \ldots, N_G$. Since the trace of a matrix is invariant under basis transformations, it is sufficient to verify the correct energy dependence of the product density matrix. If we assume periodic boundary conditions, all reduced density matrices are equal and their product is of the form $\langle a|\,\hat{\rho}\,|a\rangle \propto \exp(-\beta_{\rm loc}E_a)$. We thus have to verify whether the logarithm of rhs of equations (7.17) and (7.19) is a linear function of the energy E_a,

$$\ln\left(\langle a|\,\hat{\rho}\,|a\rangle\right) \approx -\beta_{\rm loc}\,E_a + c\,, \tag{7.21}$$

where $\beta_{\rm loc}$ and c are constants.

Note that equation (7.21) does not imply that the occupation probability of an eigenstate $|\varphi\rangle$ with energy E_φ and a product state $|a\rangle$ with the same energy $E_a \approx E_\varphi$ are equal. Since $\beta_{\rm loc}$ and β enter into the exponents of the respective canonical distributions, the difference between both has significant consequences for the occupation probabilities; even if $\beta_{\rm loc}$ and β are equal with very high accuracy, but not exactly the same, occupation probabilities may differ by several orders of magnitude, provided that the energy range is large enough.

We exclude negative temperatures ($\beta_{\rm loc} > 0$). Equation (7.21) can only be true for

$$\frac{E_a + \varepsilon_a - E_0}{\sqrt{N_G}\,\Delta_a} > \beta\frac{\Delta_a^2}{\sqrt{N_G}\,\Delta_a}\,, \tag{7.22}$$

as can be seen from equations (7.17) and (7.19). In this case, $\langle a|\,\hat{\rho}\,|a\rangle$ is given by (7.17) and to satisfy (7.21), ε_a and Δ_a^2 furthermore have to be of the form,

$$-\varepsilon_a + \frac{\beta}{2}\,\Delta_a^2 \approx c_1 E_a + c_2\,, \tag{7.23}$$

where c_1 and c_2 are constants.

Note that ε_a and Δ_a^2 need not be functions of E_a and therefore in general cannot be expanded in a Taylor series.

To ensure that the density matrix of each subgroup μ is approximately canonical, one needs to satisfy (7.23) for each subgroup μ separately;

$$-\frac{\varepsilon_{\mu-1}+\varepsilon_\mu}{2} + \frac{\beta}{4}\,\left(\Delta_{\mu-1}^2 + \Delta_\mu^2\right) + \frac{\beta}{6}\,\tilde{\Delta}_\mu^2 \;\approx\; c_1\,E_\mu + c_2\,, \tag{7.24}$$

where $\varepsilon_\mu = \langle a|\,I_{\mu n,\mu n+1}\,|a\rangle$ with $\varepsilon_a = \sum_{\mu=1}^{N_G}\varepsilon_\mu$,

$$\Delta_\mu^2 = \langle a|\,\mathcal{H}_\mu^2\,|a\rangle - \langle a|\,\mathcal{H}_\mu\,|a\rangle^2 \qquad \text{and} \tag{7.25}$$

$$\tilde{\Delta}_\mu^2 = \sum_{\nu=\mu-1}^{\mu+1} \langle a|\,\mathcal{H}_{\nu-1}\mathcal{H}_\nu + \mathcal{H}_\nu\mathcal{H}_{\nu-1}\,|a\rangle - 2\,\langle a|\,\mathcal{H}_{\nu-1}\,|a\rangle\,\langle a|\,\mathcal{H}_\nu\,|a\rangle\;. \tag{7.26}$$

Temperature becomes intensive, if the constant c_1 vanishes,

$$|c_1| \ll 1 \qquad \Rightarrow \qquad \beta_{\rm loc} = \beta\,. \tag{7.27}$$

If this was not the case, temperature would not be intensive, although it might exist locally.

It is sufficient to satisfy conditions (7.22) and (7.24) for an adequate energy range $E_{\rm min} \le E_\mu \le E_{\rm max}$ only.

For large many body systems, the density of states is typically a rapidly growing function of energy [22, 70]. If the total system is in a thermal state, occupation probabilities decay exponentially with energy (cf. chapt. 3). The product of these two functions is thus sharply peaked at the expectation value of the energy $\overline{E}$ of the total system $\overline{E} + E_0 = {\rm Tr}(H\hat{\rho})$, with E_0 being the ground state energy (see figure 3.1). Hence, the energy range needs to be centered at this peak and large enough to sufficiently cover it. On the other hand it must not be

larger than the range of values E_μ can take on. Therefore a pertinent and "safe" choice for $E_{\min}$ and $E_{\max}$ is

$$\begin{aligned} E_{\min} &= \max\left([E_\mu]_{\min} \, , \, \frac{1}{\alpha}\frac{\overline{E}}{N_G} + \frac{E_0}{N_G} \right) \\ E_{\max} &= \min\left([E_\mu]_{\max} \, , \, \alpha\frac{\overline{E}}{N_G} + \frac{E_0}{N_G} \right) , \end{aligned} \tag{7.28}$$

where $\alpha \gg 1$ and $\overline{E}$ will in general depend on the global temperature β. In equation (7.28), $[E_\mu]_{\min}$ and $[E_\mu]_{\max}$ denote the minimal and maximal values E_μ can take on.

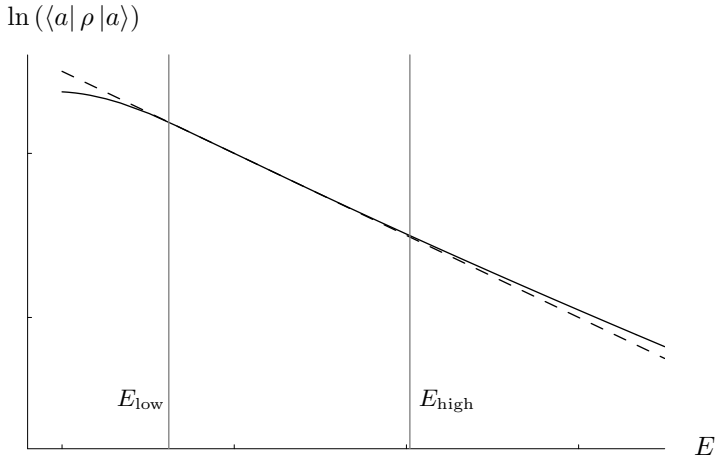

Figure 7.2.: $\ln(\langle a|\,\rho\,|a\rangle)$ for ρ as in equation (7.14) (solid line) and a canonical density matrix ρ (dashed line) for a harmonic chain.

Figure 7.2 shows the logarithm of equation (7.14) and the logarithm of a canonical distribution with the same β for the example of a harmonic chain. The actual density matrix is more mixed than the canonical one. In the interval between the two vertical lines, both criteria (7.22) and (7.24) are satisfied. For $E < E_{\text{low}}$ (7.22) is violated and (7.24) for

$E > E_{\text{high}}$. To allow for a description by means of canonical density matrices, the group size needs to be chosen such that $E_{\text{low}} < E_{\text{min}}$ and $E_{\text{high}} > E_{\text{max}}$.

For a model obeying equations (5.14) and (5.13), the two conditions (7.22) and (7.24), which constitute the general result of this chapter, must both be satisfied. In the following chapters, these fundamental criteria will be applied to some concrete examples.

8. Ising Spin Chain in a Transverse Field

In this chapter we apply the theory developed in chapter 7 to models, in which the elementary subsystems have finite dimension. We consider an Ising chain of $N_G \cdot n$ spins in a transverse field [34, 33, 29]. For this model the respective terms in the Hamiltonian (7.1) read

$$\begin{aligned} H_i &= -B\,\sigma_i^z \\ I_{i,i+1} &= -\frac{J_x}{2}\,\sigma_i^x \otimes \sigma_{i+1}^x - \frac{J_y}{2}\,\sigma_i^y \otimes \sigma_{i+1}^y\,, \end{aligned} \tag{8.1}$$

where σ_i^x, σ_i^y and σ_i^z are the Pauli matrices. B is the magnetic field and J_x and J_y are two coupling parameters. We will always assume $B > 0$.

We divide the chain into N_G groups of n adjoining spins to get a partition as considered in chapter 7.

The individual groups may be diagonalized via a Jordan-Wigner and a Fourier transformation (see appendix B). Using the abbreviations

$$K = \frac{J_x + J_y}{2\,B} \quad \text{and} \quad L = \frac{J_x - J_y}{2\,B}\,, \tag{8.2}$$

the energy E_a reads

$$E_a = 2B \sum_{\mu=1}^{N_G} \sum_k \left[1 - K\cos(k)\right] \left(n_k^a(\mu) - \frac{1}{2} \right)\,, \tag{8.3}$$

where $k = \pi l/(n+1)$ $(l = 1, 2, \ldots, n)$ and $n_k^a(\mu)$ is the fermionic occupation number of mode k of group μ in the state $|a\rangle$. It can take on the values zero and one.

For the Ising model at hand one has $\varepsilon_a = 0$ for all states $|a\rangle$, while the squared variance Δ_a^2 reads

$$\Delta_a^2 = \sum_{\mu=1}^{N_G} \Delta_\mu^2 \tag{8.4}$$

(implying $\tilde{\Delta}_\mu = 0$), with

$$\begin{aligned}\Delta_\mu^2 =& B^2 \left(\frac{K^2}{2} + \frac{L^2}{2}\right) - 2\,B^2 \left(K^2 - L^2\right) \times \\ & \times \left[\frac{2}{n+1} \sum_k \sin^2(k) \left(n_k^a(\mu) - \frac{1}{2}\right)\right] \times \\ & \times \left[\frac{2}{n+1} \sum_p \sin^2(p) \left(n_p^a(\mu+1) - \frac{1}{2}\right)\right], \end{aligned} \tag{8.5}$$

where the $n_k^a(\mu)$ are the same fermionic occupation numbers as in equation (8.3).

The conditions for the central limit theorem are met for the Ising chain apart from two exceptions. Condition (5.14) is always fulfilled as the Hamiltonian of a single spin has finite dimension. As follows from equations (8.4) and (8.5), condition (5.13) is satisfied except for one single state in the case $J_x = J_y$ ($L = 0$) and one in the case $J_x = -J_y$ ($K = 0$), respectively. These two states have $\Delta_\mu^2 = 0$ and thus $\Delta_a^2 < N_G C'$.

For $L = 0$, the state that violates (5.13) is the one where all occupation numbers $n_k^a(\mu)$ vanish. For $K = 0$, it is the state where all occupation numbers of one group are zero, $n_k^a(\mu) = 0$, all occupation numbers of the neighboring group are one, $n_k^a(\mu+1) = 1$, the occupation numbers of the next group are again zero, and so on and so forth. As there is at most one state that does not fulfill (5.13), the fraction of states where our theory does not apply is negligible for $N_G \gg 1$.

The entire chain with periodic boundary conditions may be diagonalized via successive Jordan-Wigner, Fourier and Bogoliubov transformations (see appendix B). The relevant energy scale is introduced via the thermal expectation value (without the ground state energy)

$$\overline{E} = \frac{n N_G}{2\pi} \int_{-\pi}^{\pi} dk\, \frac{\omega_k}{\exp(\beta\,\omega_k) + 1}\,, \tag{8.6}$$

where ω_k is given by

$$\omega_k = 2B\sqrt{[1 - K\cos k]^2 + [L \sin k]^2}\,, \tag{8.7}$$

(see equation (B.9)). The ground state energy E_0 is given by

$$E_0 = -\frac{n N_G}{2\pi} \int_{-\pi}^{\pi} dk\, \frac{\omega_k}{2}\,. \tag{8.8}$$

Since $N_G \gg 1$, the sums over all modes have been replaced by integrals.

We now turn to analyze conditions (7.22) and (7.24). Equation (8.5) shows that Δ_μ^2 cannot be expressed in terms of $E_{\mu-1}$ and E_μ. One would therefore have to check (7.22) and (7.24) for every state $|a\rangle$ separately. For the large systems with $N_G \gg 1$ considered here, this is an impossible task. Fortunately, one can get reliable order of magnitude estimates by approximating (7.22) and (7.24) with simpler expressions.

Let us first analyze condition (7.22). Since it cannot be checked for every state $|a\rangle$ we use the stronger condition

$$E_\mu - \frac{E_0}{N_G} > \beta \left[\Delta_\mu^2\right]_{\max} , \tag{8.9}$$

instead. It implies that (7.22) holds for all states $|a\rangle$. We require that (8.9) is true for all states with energies in the range (7.28). It is hardest to satisfy for $E_\mu = E_{\min}$, we thus get the condition on n:

$$n > \beta \frac{\left[\Delta_\mu^2\right]_{\max}}{e_{\min} - e_0} , \tag{8.10}$$

where $e_{\min} = E_{\min}/n$ and $e_0 = E_0/(nN_G)$.

We now turn to analyze condition (7.24). Equation (8.5) shows that the Δ_μ^2 do not contain terms which are proportional to E_μ. One thus has to determine, when the Δ_μ^2 are approximately constant. This is the case if

$$\beta \frac{\left[\Delta_\mu^2\right]_{\max} - \left[\Delta_\mu^2\right]_{\min}}{2} \ll \left[E_\mu\right]_{\max} - \left[E_\mu\right]_{\min} , \tag{8.11}$$

where $[x]_{\max}$ and $[x]_{\min}$ denote the maximal and minimal value x takes on in all states $|a\rangle$. As a direct consequence, we get

$$|c_1| \ll 1 , \tag{8.12}$$

which means that temperature is intensive (see equation (7.27)). Defining the quantity $e_\mu = E_\mu/n$, we can rewrite (8.11) as a condition on n,

$$n \geq \frac{\beta}{2\,\delta} \frac{\left[\Delta_\mu^2\right]_{\max} - \left[\Delta_\mu^2\right]_{\min}}{\left[e_\mu\right]_{\max} - \left[e_\mu\right]_{\min}} , \tag{8.13}$$

where the accuracy parameter $\delta \ll 1$ is equal to the ratio of the lhs and the rhs of (8.11).

Since equation (8.11) does not take into account the energy range (7.28), its application needs some further discussion. If the occupation number of one mode of a group is changed, say from $n_k^a(\mu) = 0$ to $n_k^a(\mu) = 1$, the corresponding Δ_μ^2 differ at most by

$$\frac{4}{n+1} B^2 \left| K^2 - L^2 \right| . \tag{8.14}$$

On the other hand,

$$\left[\Delta_\mu^2\right]_{\max} - \left[\Delta_\mu^2\right]_{\min} = B^2 \left| K^2 - L^2 \right| . \tag{8.15}$$

The state with the maximal Δ_μ^2 and the state with the minimal Δ_μ^2 thus differ in nearly all occupation numbers and therefore their difference in energy is close to $[E_\mu]_{\max} - [E_\mu]_{\min}$. On the other hand, states with similar energies E_μ also have a similar Δ_μ^2. Hence the Δ_μ^2 only change quasi continuously with energy and equation (8.11) ensures that the Δ_μ^2 are approximately constant even on only a part of the possible energy range.

To illustrate the scenarios that can occur, we are now going to discuss three special choices of parameters which represent extremal cases of the possible couplings in our model [34].

8.1. Coupling with Constant Width Δ_a: $J_y = 0$

If one of the coupling parameters vanishes ($J_x = 0$ or $J_y = 0$), $K = L$ and

$$\Delta_\mu^2 = B^2 K^2 \tag{8.16}$$

is constant. In this case only criterion (7.22) has to be satisfied, which then coincides with (8.10).

We calculate $e_{\min}$ from (8.6) and (8.8) and insert it, together with (8.16), into condition (8.10) to obtain the minimal number of spins per group, $n_{\min}$ Figure 8.1 shows $n_{\min}$ for weak coupling $K = L = 0.1$ and figure 8.2 for strong coupling $K = L = 10$ with $\alpha = 10$ as a function

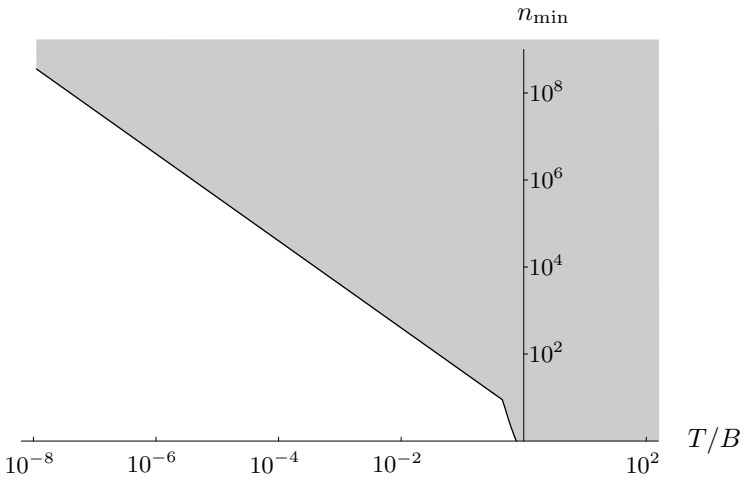

Figure 8.1.: $n_{\min}$ for constant width coupling according to eq. (8.10) for $K = L = 0.1$ as a function of T/B. $\alpha = 10$ (see eq. (7.28)). Local temperature exists in the shaded region.

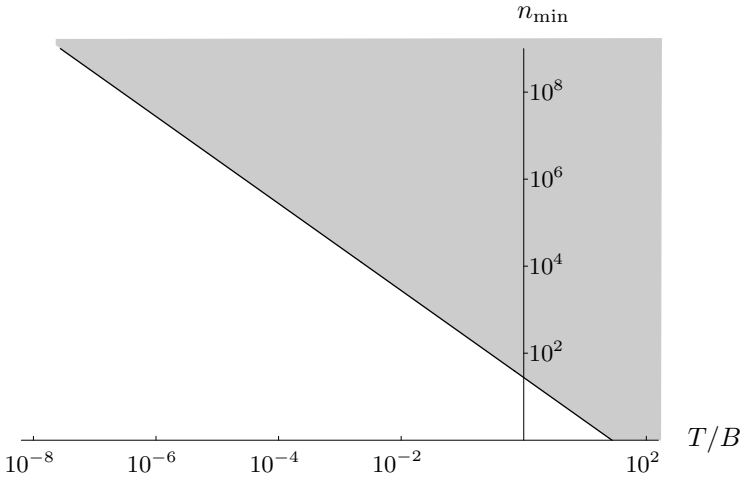

Figure 8.2.: $n_{\min}$ for constant width coupling according to eq. (8.10) for $K = L = 10$ as a function of T/B. $\alpha = 10$ (see eq. (7.28)). Local temperature exists in the shaded region.

of T/B. We choose units where Boltzmann's constant k_B is one. Local temperatures do exist in the shaded region.

Note that, since $\Delta_\mu = const$, condition (8.10) coincides with criterion (7.22) ($\Delta_\mu = const = [\Delta_\mu]_{\max}$), so that using (8.10) does not involve any approximations.

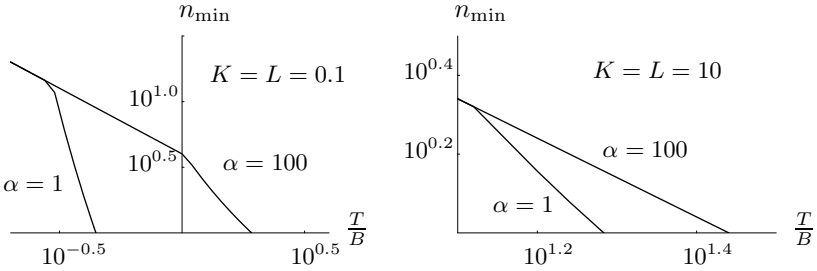

Figure 8.3.: $n_{\min}$ for constant width coupling as a function of T/B from eq. (8.10) for two values of the accuracy parameter α, $\alpha = 1$ and $\alpha = 100$. The left plot is for $K = L = 0.1$ and the right plot for $K = L = 10$. α is defined in eq. (7.28).

As condition (7.23) is automatically satisfied for the present model, the results do not depend on the accuracy parameter δ. The dependence of the results on α is shown in figure 8.3. The parameter α only plays a role where $E_{\min} = \overline{E}/(\alpha N_G) + E_0/N_G$ (cf. equation (7.28)). Then for smaller α, $n_{\min}$ eventually decays steeper and thus reaches $n_{\min} = 1$ already at lower temperatures. There is thus a temperature interval, where $n_{\min}$ is larger for larger α and vice versa. This means, the larger one chooses the energy range (7.28) where the condition (7.22) should be satisfied, the larger have to be the groups.

We finally discuss the dependence of $n_{\min}$ on the coupling strength K and L. Figure 8.4 shows $n_{\min}$ according to eq. (8.10) as a function of the coupling parameter K ($K = L$) and T/B for $\alpha = 10$. The range with $K < 1$ represents the weak coupling regime, since the local level splitting is larger than the coupling strength. As one would expect, $n_{\min}$ grows with increasing coupling K. At low temperatures, $n_{\min}$ does not smoothly approach 1 for $K \to 0$. This feature possibly originates from the $N_G \to \infty$ limit, we consider here.

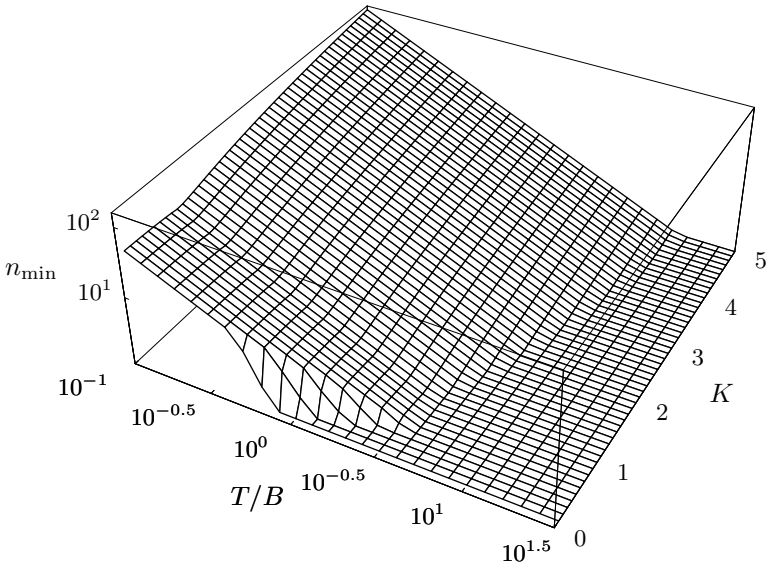

Figure 8.4.: $n_{\min}$ for constant width coupling according to eq. (8.10) as a function of the coupling parameter $K = L$ and T/B. $\alpha = 10$ is defined in eq. (7.28).

8.2. Fully Anisotropic Coupling: $J_x = -J_y$

If both coupling parameters are nonzero, the Δ_μ^2 are not constant. As an example, we consider here the case of fully anisotropic coupling, where $J_x = -J_y$, i. e. $K = 0$. Now both criteria, (8.10) and (8.13), have to be met.

For $K = 0$, one has the maximal and minimal width of the interaction

$$\left\{ \begin{array}{c} [\Delta_\mu^2]_{\max} \\ [\Delta_\mu^2]_{\min} \end{array} \right\} = B^2 \left\{ \begin{array}{c} L^2 \\ 0 \end{array} \right\}, \tag{8.17}$$

while the maximum and minimum of e_μ are

$$\left\{ \begin{array}{c} [e_\mu]_{\max} \\ [e_\mu]_{\min} \end{array} \right\} = \left\{ \begin{array}{c} + \\ - \end{array} \right\} B\,. \tag{8.18}$$

We insert these results together with $e_{\min}$ derived from (8.18), (8.6) and (8.8) into (8.13) and (8.10) to calculate the minimal number of spins per group, $n_{\min}$.

Figure 8.5 shows $n_{\min}$ according to criterion (8.10) and according to criterion (8.13) separately, for weak coupling $L = 0.1$ with $\alpha = 10$ and $\delta = 0.01$ as a function of T/B. Local temperatures exist in the shaded area.

Figure 8.6 shows $n_{\min}$ according to criterion (8.10) and (8.13), for strong coupling $L = 10$ with $\alpha = 10$ and $\delta = 0.01$ as a function of T/B. Local temperatures exist in the shaded area.

In the present case, all occupation numbers $n_k^a(\mu)$ are zero in the ground state of a group. In this state, Δ_μ^2 is maximal ($\Delta_\mu^2 = B^2\,L^2$) as can be seen from (8.5). Therefore criterion (8.10) is equivalent to criterion (7.22) for low temperatures, where $E_{\min} = [E_\mu]_{\min}$. For high temperatures, where $E_{\min} = \overline{E}/(\alpha N_G)$, condition (8.10) is slightly stronger than (7.22). For the present model, this is only the case for $L = 0.1$ (dashed line) and $T \gtrsim 0.45B$.

In figures 8.5 and 8.6, the results obtained from equation (8.13) are proportional to δ^{-1} (dashed lines), while those obtained from equation (8.10) (solid lines) have the same dependency on α as shown in figure 8.3.

Figure 8.7 shows $n_{\min}$ according to equations (8.10) and (8.13) as a function of the coupling parameter K and T/B for $\alpha = 10$. Again, $L < 1$ represents the weak coupling regime, where the local level splitting is larger than the coupling strength. As in the previous case, $n_{\min}$ is a monotonic increasing function of L but shows a non-smooth transition to the uncoupled ($L = 0$) case. The latter may again be due to the $N_G \to \infty$ limit.

8.3. Isotropic Coupling: $J_x = J_y$

As a second example of models where both coupling parameters are nonzero, we consider the isotropic coupling case, where $J_x = J_y$, i. e. $L = 0$. Again, both criteria (8.10) and (8.13) have to be met.

In this case, the maximal and minimal widths of the interaction are

$$\left\{ \begin{array}{c} [\Delta_\mu^2]_{\max} \\ [\Delta_\mu^2]_{\min} \end{array} \right\} = B^2 \left\{ \begin{array}{c} K^2 \\ 0 \end{array} \right\} . \tag{8.19}$$

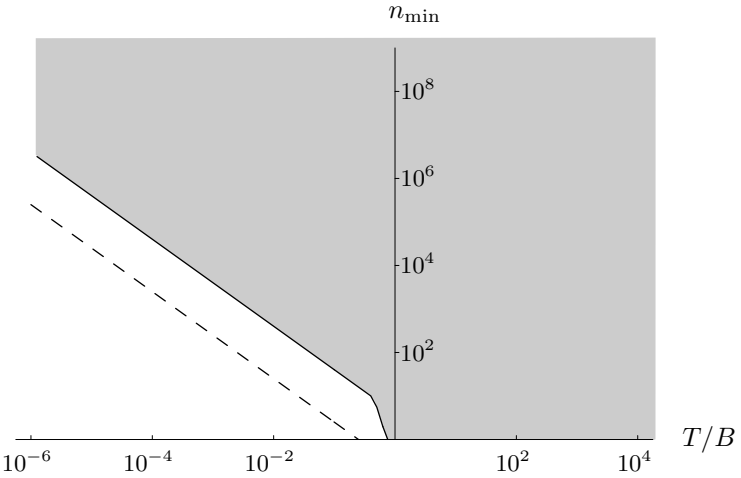

Figure 8.5.: $n_{\min}$ for fully anisotropic coupling ($K = 0$) according to eq. (8.10) (solid line) and eq. (8.13) (dashed line) for $L = 0.1$ as a function of T/B. $\alpha = 10$ and $\delta = 0.01$ (see eqs. (7.28) and (8.13)). Local temperatures exist in the shaded area.

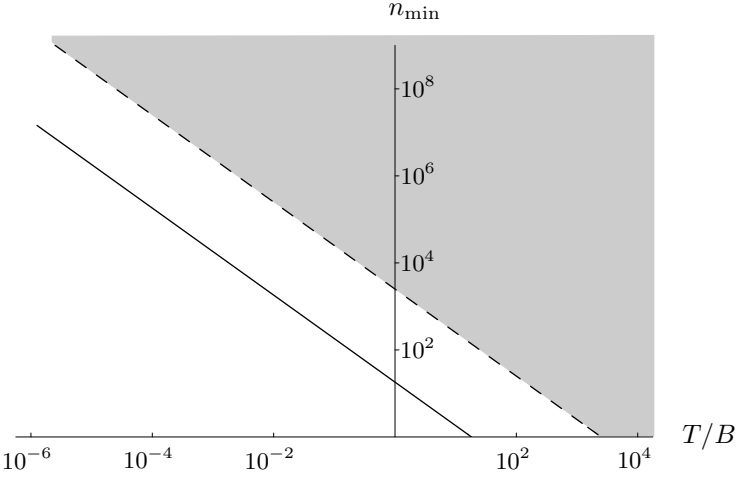

Figure 8.6.: $n_{\min}$ for fully anisotropic coupling ($K = 0$) according to eq. (8.10) (solid line) and eq. (8.13) (dashed line) for $L = 10$ as a function of T/B. $\alpha = 10$ and $\delta = 0.01$ (see eqs. (7.28) and (8.13)). Local temperatures exist in the shaded area.

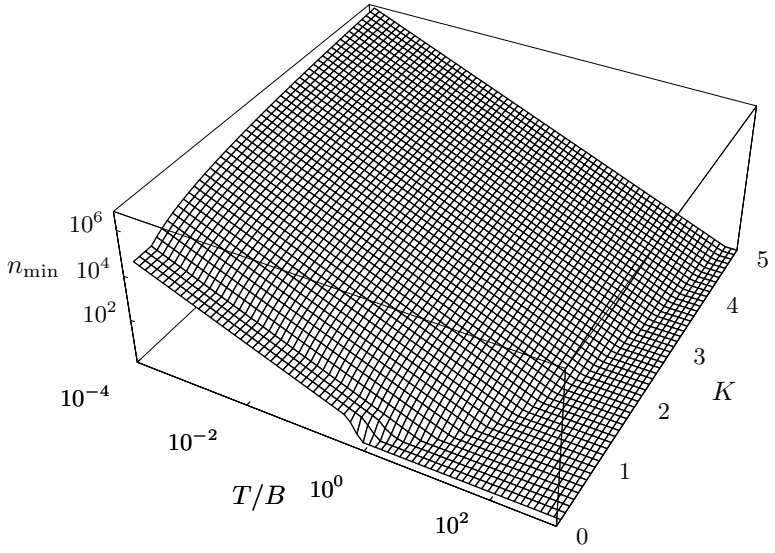

Figure 8.7.: $n_{\min}$ for fully anisotropic coupling according to eq. (8.10) and eq. (8.13) as a function of the coupling parameter L and T/B. $K = 0$, $\alpha = 10$ and $\delta = 0.01$. α and δ are defined in eqs. (7.28) and (8.13) respectively.

while the maxima and minima of e_μ are

$$\left\{ \begin{array}{c} [e_\mu]_{\max} \\ [e_\mu]_{\min} \end{array} \right\} = \left\{ \begin{array}{c} + \\ - \end{array} \right\} B \,, \tag{8.20}$$

for $|K| < 1$ and

$$\left\{ \begin{array}{c} [e_\mu]_{\max} \\ [e_\mu]_{\min} \end{array} \right\} = \left\{ \begin{array}{c} + \\ - \end{array} \right\} B \, \frac{2}{\pi} \left[\sqrt{K^2 - 1} + \arcsin\left(\frac{1}{|K|} \right) \right] , \tag{8.21}$$

for $|K| > 1$.

For the present model with $L = 0$ and $|K| < 1$ all occupation numbers $n_k^a(\mu)$ are zero in the ground state and thus $\Delta_\mu^2 = 0$. As a consequence,

condition (8.10) cannot be used instead of (7.22). We therefore argue as follows:

In the ground state $E_\mu - E_0/N_G = 0$ as well as $\Delta_\mu^2 = 0$ and all occupation numbers $n_k^a(\mu)$ are zero. If one occupation number is then changed from 0 to 1, Δ_μ^2 changes at most by $4\,B^2\,K^2/(n+1)$ and E_μ changes at least by $2\,B\,(1-|K|)$. Therefore (7.22) will hold for all states except the ground state if

$$n > 2\,B\,\beta\,\frac{K^2}{1-|K|} \tag{8.22}$$

The minimal number of spins per group for $|K| < 1$ can now be calculated from equation (8.22) and equation (8.13) with $\left[\Delta_\mu^2\right]_{\max}$, $\left[\Delta_\mu^2\right]_{\min}$, $[e_\mu]_{\max}$, and $[e_\mu]_{\min}$ given by equations (8.19) and (8.20) respectively. Figure 8.8 shows $n_{\min}$ according to criteria (8.22) and (8.13) for weak coupling $K = 0.1$ with $\alpha = 10$ and $\delta = 0.01$ as a function of T/B. Local temperatures exist in the shaded area.

Equation (8.22) does not take into account the relevant energy range (7.28), it is therefore possible that a weaker condition could be sufficient in that case. However, since (8.13) is a stronger condition than (8.22) for $K = 0.1$, this possibility has no relevance.

If $|K| > 1$, occupation numbers of modes with $\cos(k) < 1/|K|$ are zero in the ground state and occupation numbers of modes with $\cos(k) > 1/|K|$ are one. Δ_μ^2 for the ground state then is $\left[\Delta_\mu^2\right]_{\rm gs} \approx \left[\Delta_\mu^2\right]_{\max}/2$ and (8.10) is a good approximation of condition (7.22). Inserting $\left[\Delta_\mu^2\right]_{\max}$, $\left[\Delta_\mu^2\right]_{\min}$, $[e_\mu]_{\max}$, and $[e_\mu]_{\min}$ given by equations (8.19) and (8.21) respectively and $e_{\min}$ as derived from (8.20), (8.6) and (8.8) into (8.13) and (8.10) for $|K| > 1$, the minimal number of spins per group can be calculated.

Figure 8.9 shows $n_{\min}$ according to criteria (8.10) and (8.13) for strong coupling $K = 10$ with $\alpha = 10$ and $\delta = 0.01$ as a function of T/B. Local temperatures exist in the shaded area.

For the present model, the dependence of the results on the accuracy parameters α and δ is as follows: Results obtained from equation (8.13) are proportional to δ^{-1} (dashed lines), while the result obtained from equation (8.10) (solid line in figure 8.9) has the same dependency on α as shown in figure 8.3. For weak coupling and low temperatures (solid line in figure 8.8) $n_{\min}$ does not depend on the two accuracy parameters.

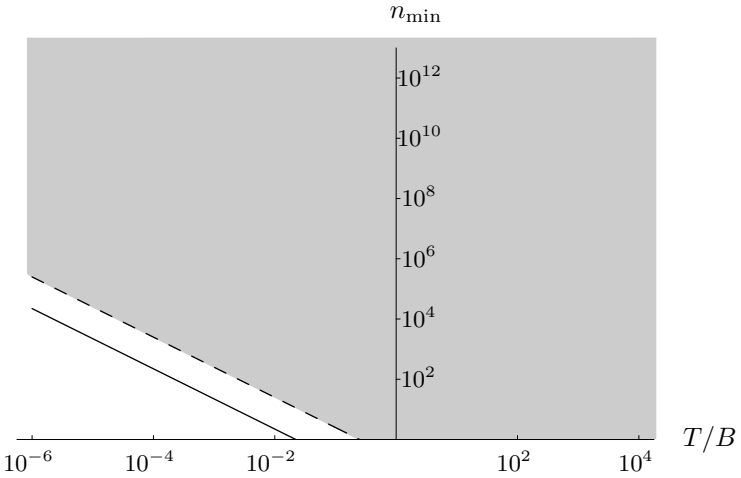

Figure 8.8.: $n_{\min}$ for isotropic coupling ($L = 0$) according to eq. (8.22) (solid line) and eq. (8.13) (dashed line) for $K = 0.1$ as a function of T/B. $\alpha = 10$ and $\delta = 0.01$ (see eqs. (7.28) and (8.13)). Local temperatures exist in the shaded area.

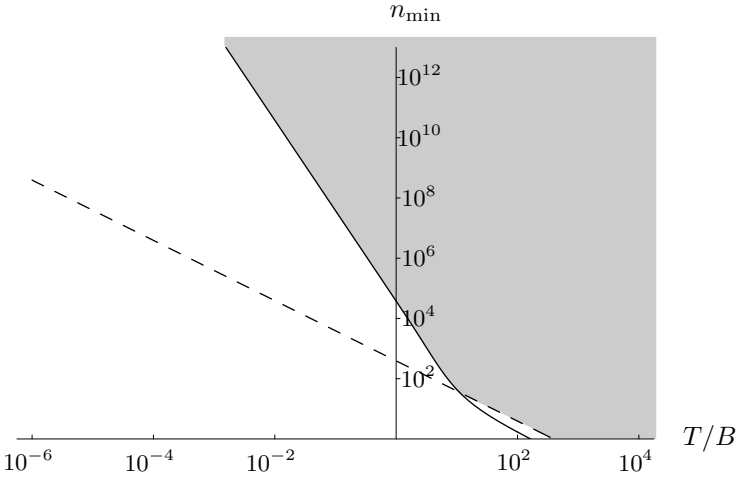

Figure 8.9.: $n_{\min}$ for isotropic coupling ($L = 0$) according to eq. (8.10) (solid line) and eq. (8.13) (dashed line) for $K = 10$ as a function of T/B. $L = 0$, $\alpha = 10$ and $\delta = 0.01$ (see eqs. (7.28) and (8.13)). Local temperatures exist in the shaded area.

For the isotropic coupling $L = 0$, we only present the results for the two limiting cases of weak coupling ($K = 0.1$) and strong coupling ($K = 10$). For $K \sim 1$, the simple approximations to criterion (7.22) do not work and the analysis of (7.22) becomes rather tedious.

Next, we apply our general result, conditions (7.22) and (7.24) to a model, where the subsystems have infinite dimension, a harmonic chain.

9. Harmonic Chain

In this chapter, we apply the theory of chapter 7 to a representative for the class of systems with an infinite energy spectrum:

We consider a harmonic chain of $N_G \cdot n$ particles of mass m and spring constant $\sqrt{m}\,\omega_0$ [31,33]. In this case, the respective terms in the Hamiltonian (7.1) read

$$H_i = \frac{m}{2}\,p_i^2 + \frac{m}{2}\,\omega_0^2\,q_i^2 \tag{9.1}$$

$$I_{i,i+1} = -m\,\omega_0^2\,q_i\,q_{i+1}\,, \tag{9.2}$$

where p_i is the momentum of the particle at site i and q_i the displacement from its equilibrium position $i \cdot a_0$ with a_0 being the distance between neighboring particles at equilibrium. We divide the chain into N_G groups of n particles each and thus get a partition of the type considered in chapter 7.

The Hamiltonian of one group is diagonalized by a Fourier transform and the definition of creation and annihilation operators $a_k^\dagger$ and a_k for the Fourier modes (see appendix C).

$$E_a = \sum_{\mu=1}^{N_G} \sum_k \omega_k \left(n_k^a(\mu) + \frac{1}{2} \right)\,, \tag{9.3}$$

where $k = \pi l/(a_0\,(n+1))$ $(l = 1, 2, \ldots, n)$ and the frequencies ω_k are given by

$$\omega_k^2 = 4\,\omega_0^2\,\sin^2\left(\frac{k\,a_0}{2}\right)\,. \tag{9.4}$$

$n_k^a(\mu)$ is the occupation number of mode k of group μ in the state $|a\rangle$. We choose units, where $\hbar = 1$. Let us first verify, that the central limit theorem (5.15) applies to this model, i.e. that conditions (5.13) and (5.14) are met.

To see that the model satisfies the condition (5.13) one needs to express the group interaction $V(q_{\mu n}, q_{\mu n+1})$ in terms of $a_k^\dagger$ and a_k, which yields $\tilde{\Delta}_\mu = 0$ for all μ and therefore

$$\Delta_a^2 = \sum_{\mu=1}^{N_G} \Delta_\mu^2 \,, \tag{9.5}$$

where Δ_μ, the width of one group interaction, reads

$$\Delta_\mu^2 = \left(\frac{2}{n+1}\right)^2 \left[\sum_k \cos^2\left(\frac{k\,a_0}{2}\right)\,\omega_k\,\left(n_k + \frac{1}{2}\right)\right] \times \\ \times \left[\sum_p \cos^2\left(\frac{p\,a_0}{2}\right)\,\omega_p\,\left(m_p + \frac{1}{2}\right)\right] . \tag{9.6}$$

In equation (9.6), k labels the modes of group μ with occupation numbers n_k and p the modes of group $\mu+1$ with occupation numbers m_p.

Δ_μ^2 has a minimum value since all $n_k \geq 0$ and all $m_p \geq 0$ and the width Δ_a^2 thus fulfills condition (5.13).

Since the spectrum of every single oscillator is infinite, condition (5.14) can only be satisfied for states, for which the energy of the system is distributed among a relevant fraction of the groups. As discussed in chapter 7, these states constitute only a negligible fraction of all product states $|a\rangle$.

The expectation values of the group interactions vanish, $\varepsilon_\mu = 0$, while the widths Δ_μ^2 depend on the occupation numbers n_k and therefore on the energies E_μ. We thus apply both conditions, (7.22) and (7.24). To analyze them, we make use of the continuum or Debye approximation [45], requiring $n \gg 1$, $a_0 \ll l$, where $l = n\,a_0$, and the length of the chain to be finite. As will become clear below, the resulting minimal group sizes $n_{\min}$ are larger than 10^3 for all temperatures and the application of the Debye approximation is well justified.

Using this approximation we now have $\omega_k = v\,k$ with the constant velocity of sound $v = \omega_0\,a_0$ and $\cos(k\,a_0/2) \approx 1$. The width of the group interaction thus translates into

$$\Delta_\mu^2 = \frac{4}{n^2}\,E_\mu\,E_{\mu+1}\,, \tag{9.7}$$

where $n+1 \approx n$ has been used.

The relevant energy scale is introduced by the thermal expectation value of the entire chain

$$\overline{E} = N_G n k_B \Theta \left(\frac{T}{\Theta}\right)^2 \int_0^{\Theta/T} \frac{x}{\mathrm{e}^x - 1}\, dx\,, \tag{9.8}$$

and the ground state energy is given by

$$E_0 = N_G n k_B \Theta \left(\frac{T}{\Theta}\right)^2 \int_0^{\Theta/T} \frac{x}{2}\, dx = \frac{N_G n k_B \Theta}{4}\,, \tag{9.9}$$

where Θ is the Debye temperature [45].

We first consider the criterion (7.22). For a given $E_a = \sum_\mu E_\mu$, the squared width Δ_μ^2 is largest if all E_μ are equal, $\tilde{E} \equiv E_\mu \,\forall \mu$. Thus (7.22) is hardest to satisfy for that case, where it reduces to

$$\tilde{E} - \frac{E_0}{N_G} - \frac{4\beta}{n^2}\tilde{E}^2 > 0\,. \tag{9.10}$$

Equation (9.10) sets a lower bound on n. For temperatures where $\overline{E} < E_0$, this bound is strongest for low energies $\tilde{E}$, while at $\overline{E} > E_0$ it is strongest for high energies $\tilde{E}$. Since condition (7.24) is a stronger criterion than condition (7.22) for $\overline{E} > E_0$, we only consider (9.10) at temperatures where $\overline{E} < E_0$. In this range, (9.10) is hardest to satisfy for low energies, i.e. at $\tilde{E} = (\overline{E}/\alpha N_G) + (E_0/N_G)$, where it reduces to

$$n > \frac{\Theta}{T}\,\frac{\alpha}{4\overline{e}}\left(\frac{4\overline{e}}{\alpha} + 1\right)^2 \tag{9.11}$$

with $\overline{e} = \overline{E}/(n N_G k_B \Theta)$.

To test condition (7.24) we take the derivative with respect to E_μ on both sides,

$$\frac{\beta}{n^2}\left(E_{\mu-1} + E_{\mu+1} - 2\,\frac{E_0}{N_G}\right) + \frac{2\beta}{n^2}\frac{E_0}{N_G} \approx c_1\,, \tag{9.12}$$

where we have separated the energy dependent and the constant part in the lhs. (9.12) is satisfied if the energy dependent part is much smaller than one,

$$\frac{\beta}{n^2}\left(E_{\mu-1} + E_{\mu+1} - 2\frac{E_0}{N_G}\right) \leq \delta \ll 1\,, \tag{9.13}$$

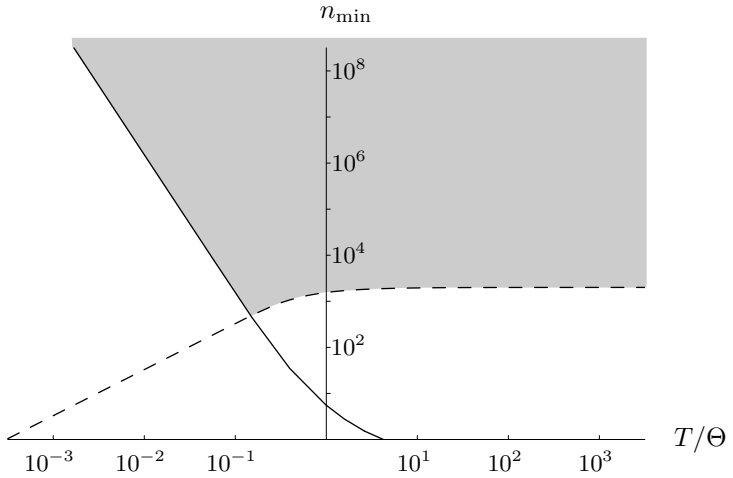

Figure 9.1.: $n_{\min}$ from eq. (9.11) (solid line) and $n_{\min}$ from eq. (9.14) (dashed line) for $\alpha = 10$ and $\delta = 0.01$ as a function of T/Θ for a harmonic chain. δ and α are defined in equations (9.14) and (7.28), respectively. Local temperature exists in the shaded region.

which is hardest to fulfill for high energies $E_{\mu-1}$ and $E_{\mu+1}$. Thus taking $E_{\mu-1}$ and $E_{\mu+1}$ equal to the upper bound of the range (7.28), this yields

$$n > \frac{2\alpha}{\delta}\,\frac{\Theta}{T}\,\overline{e}\,, \tag{9.14}$$

where the accuracy parameter $\delta \ll 1$ quantifies the value of the energy dependent part in (9.12).

Since the constant part in the lhs of (9.12) satisfies

$$\frac{2\beta}{n^2}\frac{E_0}{N_G} < \frac{\sqrt{\delta}}{\alpha}\left(\frac{1}{\sqrt{2}} - \frac{\sqrt{\delta}}{\alpha}\right) \ll 1\,, \tag{9.15}$$

the temperature is intensive, $\beta_{\mathrm{loc}} = \beta$ (see eq. (7.27)).

Inserting equation (9.8) into equation (9.11) and (9.14) one can now calculate the minimal n for given δ, α, Θ and T. Figure 9.1 shows $n_{\min}$

for $\alpha = 10$ and $\delta = 0.01$ given by criterion (9.11) and (9.14) as a function of T/Θ.

For high (low) temperatures $n_{\min}$ can thus be estimated by

$$n_{\min} \approx \begin{cases} \dfrac{2\,\alpha}{\delta} & \text{for} \quad T > \Theta \\ \dfrac{3\alpha}{2\,\pi^2}\,\dfrac{\Theta^3}{T^3} & \text{for} \quad T < \Theta \end{cases} \tag{9.16}$$

The temperature dependence of $n_{\min}$ for low temperatures, $n_{\min} \propto T^{-3}$, is the same as for the Ising spin chain for $L = 0$ and $|K| > 1$. This agreement is to be expected: The two couplings have the same form, when expressed in creation and annihilation operators, and the upper limit of the spectrum of the spin chain becomes irrelevant at low temperatures.

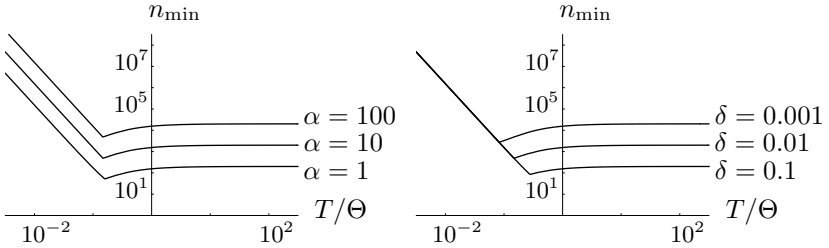

Figure 9.2.: Left plot: $n_{\min}$ for $\delta = 0.01$ and $\alpha = 1$, 10 and 100.
Right plot: $n_{\min}$ for $\alpha = 10$ and $\delta = 0.1$, 0.01 and 0.001.

We finally turn to discuss the dependence of the results on the accuracy parameters α and δ. The asymptotic dependencies for low and high temperatures T can be read off from (9.16): $n_{\min} \propto \alpha$, in other words, the larger one chooses the energy range where (7.22) and (7.24) should be fulfilled, the larger has to be the number of particles per group. Furthermore, for high temperatures only, $n_{\min} \propto \delta^{-1}$, which simply states that one needs more particles per group to obtain a canonical state with better accuracy.

Figure 9.2 shows the minimal group size $n_{\min}$ for different values of α and δ. In these two figures, we have only plotted $n_{\min}$ as given by the criterion ((7.22) or (7.24)) which is stronger in the respective temperature range, i.e. (7.22) for low and (7.24) for high temperatures. The effect of

varying α or δ at temperatures $T \sim \Theta$ is essentially the same as in the asymptotic cases.

Since solids can be well described by harmonic lattice models, we use the results of this chapter to obtain estimates for the corresponding length scales in real existing materials in the following chapter.

10. Estimates for Real Materials

Thermal properties of insulating solids can successfully be described by harmonic lattice models. Probably the best known example of such a successful modeling is the correct prediction of the temperature dependence of the specific heat based on the Debye theory [45]. We therefor expect our approach to give reasonable estimates for real existing materials, when applied to harmonic lattice models.

In this chapter, we take the results obtained in chapter 9 for the harmonic chain and insert the corresponding parameters of real existing materials. In particular, we insert the Debye temperature of the corresponding material, which can be found tabulated [45], and obtain a length scale by multiplying $n_{\min}$ with the corresponding lattice constant. The minimal length scale on which intensive temperatures exist in insulating solids is thus given by

$$l_{\min} = n_{\min}\, a_0, \tag{10.1}$$

where a_0 is the lattice constant, the distance between neighboring atoms.

Since $n_{\min}$ has been calculated for a one dimensional model, the results, we obtain here, should be valid for one dimensional or at least quasi one dimensional structures of the respective materials. Let us consider some examples:

10.1. Silicon

Silicon is used in many branches of technology. In its crystalline form, it has a Debye temperature of $\Theta \approx 645\,\mathrm{K}$ and its lattice constant is $a_0 \approx 2.4\,\text{Å}$. Using these parameters, figure 10.1 shows the minimal length-scale on which temperature can exist in a one-dimensional silicon wire as a function of global temperature. Here, the accuracy parameters α and δ are chosen to be $\alpha = 10$ and $\delta = 0.01$. Local temperature exists in the shaded area.

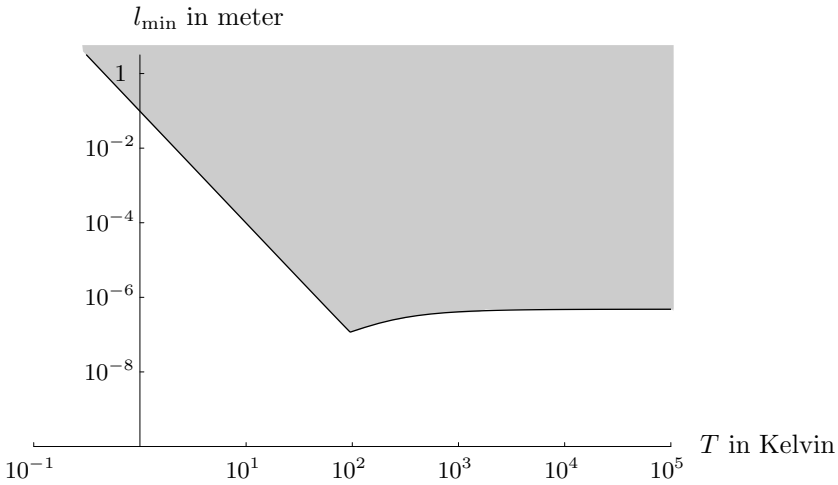

Figure 10.1.: $l_{\min}$ as a function of temperature T for crystalline silicon. $a_0 \approx 2.4\,\text{Å}$, $\Theta \approx 645\,\text{K}$, $\alpha = 10$ and $\delta = 0.01$. Local temperature exists in the shaded area.

10.2. Carbon

Recently, carbon has been investigated for the fabrication of nano structured devices [15, 14]. We consider two of its possible structures: Diamond, which is the crystalline form of carbon appearing in nature, and nanotubes, which are widely used in nano-technological experiments.

10.2.1. Diamond

Diamond is a very stiff crystalline form of carbon. It has a very high Debye temperature of $\Theta \approx 2230\,\text{K}$ and a lattice constant of $a_0 \approx 1.5\,\text{Å}$.

Figure 10.2 shows the minimal length-scale on which temperature can exist in a (quasi) one-dimensional diamond device as a function of global temperature. Again, the accuracy parameters α and δ are chosen to be $\alpha = 10$ and $\delta = 0.01$. Local temperature exists in the shaded area.

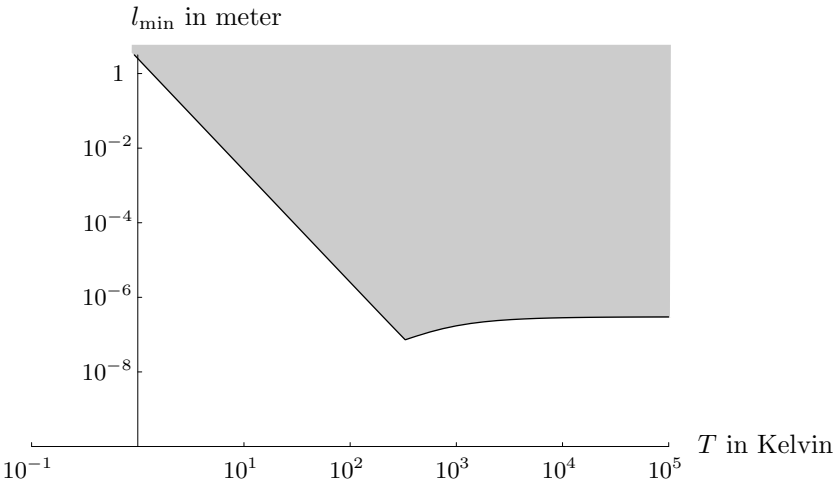

Figure 10.2.: $l_{\min}$ as a function of temperature T for diamond. $a_0 \approx 1.5\,\text{Å}$, $\Theta \approx 2230\,\text{K}$, $\alpha = 10$ and $\delta = 0.01$. Local temperature exists in the shaded area.

10.2.2. Carbon Nanotube

Carbon nanotubes have diameters of only a few nanometers. Measurements of their specific heat have shown, that their thermal properties can be accurately modeled with one-dimensional harmonic chains [37]. Our results can thus be expected to be accurately applicable to them. Carbon nanotubes have a Debye temperature of $\Theta \approx 1100\,\text{K}$ and a lattice constant of $a_0 \approx 1.4\,\text{Å}$.

Figure 10.3 shows the minimal length-scale on which temperature can exist in a carbon nanotube as a function of global temperature. It provides a good estimate of the maximal accuracy, with which temperature profiles in such tubes can be meaningfully discussed [12]. Again, the accuracy parameters α and δ are chosen to be $\alpha = 10$ and $\delta = 0.01$. Local temperature exists in the shaded area.

Of course the validity of the harmonic lattice model will eventually break down at high but finite temperatures. The estimates drawn from our approach, in particular the results presented in figures 10.1, 10.2 and 10.3, will then no longer apply.

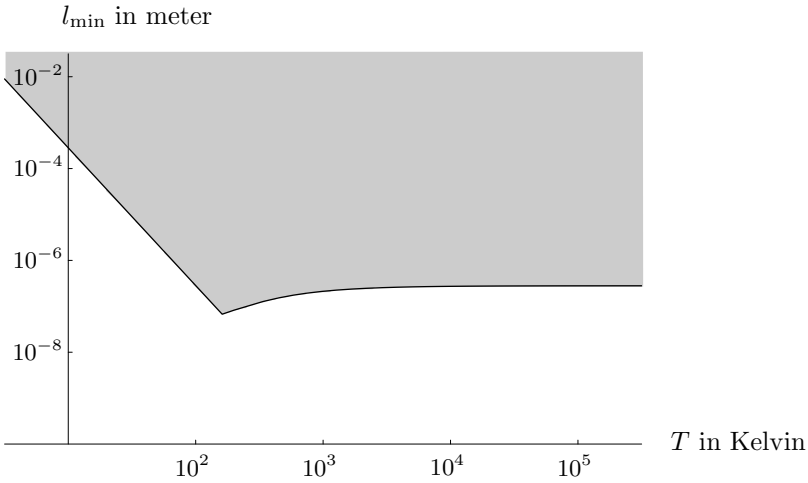

Figure 10.3.: $l_{\min}$ as a function of temperature T for a carbon nanotube. $a_0 \approx 1.4\,\text{Å}$, $\Theta \approx 1100\,\text{K}$, $\alpha = 10$ and $\delta = 0.01$. Local temperature exists in the shaded area.

The above results and those for spin chains and the harmonic chain are discussed in the next chapter.

11. Discussion of the Length Scale Results

The length scales we obtain here are, in particular for low temperatures, surprisingly large. One might thus wonder whether our approach really captures the relevant physics. Let us therefore discuss some possible limitations of it:

Firstly, taking the limit of an infinite number of groups, as it is required for the central limit theorem, may not correspond to the physically relevant situations. However, having in mind, that we intended to analyze when a small part of a larger system can be in a thermal state, taking this limit should be well justified.

Secondly, we consider strictly one-dimensional models. A real physical system, even if it is of a very prolate shape, is always three-dimensional. A generalization of our approach to those models is thus of high interest. Let us stress here, that the general conditions (7.22) and (7.24) apply to systems of arbitrary dimension, it is only the application to specific models, which needs to be generalized.

Thirdly, the question, whether a local spectrum can be meaningfully defined is not clear a priori. In order to decide, whether the local density matrix is canonical, two quantities need to be considered: The reduced (local) density matrix itself, which can be unambigously determined by tracing over the degrees of freedom of the surrounding, and the eigenvalues of the local Hamiltonian. In systems of strongly interacting particles, it is not clear how to define the latter and one might wonder whether two different choices of it could lead to a local thermal state respectively a non-thermal state for the same system. However, since we analyse the conditions, under which interactions with the surrounding are small enough such that they do not perturb the local thermal state, the possible modification of the local Hamiltonian can be expected to be negligible, too.

Furthermore, all the models we have considered here, can be mapped

to systems of non-interacting particles. For the harmonic chain this means, that no phonon scattering does occur. The purely harmonic model does, for example, not predict any expansion or shrinking of the material caused by heating or cooling. It is therefore possible that the harmonic model fails to accurately describe the questions we were interested in. The difference to a model with additional non-harmonic interactions could be significant since, in particular at low temperatures, entanglement plays an important role and this effect can be highly non-linear.

Finally, one might speculate whether the length scales could significantly change if the assumption of a global equilibrium state was relaxed. This possibility of course exists, nonetheless one would expect our estimates to still apply as long as temperature gradients are small. Imagine, there are two baths attached to one of the considered chains[1] of chapter 8 or 9. If both baths have the same temperature, the chain is in a "global" equilibrium state and our results are valid. If one now continously increased the temperature of one bath, the density matrix of the chain would change continously, too. Hence, the minimal group sizes would also change continuously and our results are still good estimates, at least for small temperature gradients.

To clarify whether our findings are in agreement or in conflict with experiments, their measurability needs to be considered in more detail. We proceed to do this in the next chapter.

[1] For this consideration, the chains are of course no longer assumed to have periodic boundary conditions.

12. Consequences for Measurements

In this chapter, we give some examples of possible experimental consequences of the local breakdown of the temperature concept at small length scales, i.e. of the fact that the respective individual subsystems or even subgroups of those cannot reach a canonical state. The experimental data we eventually consider are not new, however, they have not been analyzed and interpreted in the present context. First we consider temperature measurements with very small "thermometers" which use a standard technique.

12.1. Standard Temperature Measurements

Temperature is always measured indirectly via observables, which, in quantum mechanics, are represented by hermitian operators. Usually, one is interested in measuring the temperature of a system in a stationary state. The chosen observable should therefore be a conserved quantity, i.e. its operator should commute with the Hamiltonian of the system.

A conventional technique, e.g., is to bring the piece of matter, the temperature T of which is to be measured, in thermal contact with a box (volume V) of an ideal gas (number of particles n) and to measure the pressure p of the gas, which is related to its temperature by $n\,k_{\mathrm{B}}\,T = p\,V$ (k_{B} is Boltzmann's constant). Since the gas is in thermal equilibrium with the considered piece of matter, both substances have the same temperature. A measurement of p for constant V allows to infer the global temperature T of the piece of matter.

One might wonder, whether a small (maybe even microscopic) thermometer, which is locally coupled to one subsystem of the large chain considered in chapter 7, is capable of measuring a local temperature or whether the measurement would show any indications of a possible local

breakdown of temperature.

A prerequisite for the above gas thermometer to work properly is that the thermometer does not significantly perturb the system. For our class of models this means that the thermometer system should only be weakly coupled to the respective subsystem of the chain and that it should be significantly smaller than the latter. These two requirements ensure that the energy exchange between system and thermometer would not significantly alter the energy contained in the system. Therefore, this measurement scenario can be accurately modeled as follows:

Let the thermometer be represented by a single spin, which is locally coupled to a harmonic chain, say. The Hamiltonian of this model reads,

$$H = \Omega\sigma_t^z + \lambda\sigma_t^x q_0 + \sum_{j=0}^{n} \left(\frac{m}{2} p_j^2 + \frac{m}{2} \omega_0^2 \, (q_j - q_{j+1})^2 \right) , \tag{12.1}$$

where the first term describes the thermometer, the second its interaction with oscillator number 0 and the third the chain of oscillators[1]. The latter can also be written in terms of phonon creators and annihilators $a_k^\dagger$ and a_k (see appendix C)[2],

$$H = \Omega\sigma_t^z + \sigma_t^x \sum_k \lambda_k \left(a_k + a_k^\dagger \right) + \sum_k \omega_k \left(a_k^\dagger a_k - \frac{1}{2} \right) . \tag{12.2}$$

Since the coupling is assumed to be weak, $\lambda \ll \Omega$ or $\lambda_k \ll \Omega$ for all k, and the chain is assumed to be very large, $n \gg 1$, and in a thermal state, the present model can accurately be treated with a master equation approach [74]. In this approximation, we obtain for the reduced density matrix of the spin (the thermometer) the equation of motion [21],

$$\begin{aligned} \dot\rho = &- \mathrm{i} \, [\omega \, \sigma_t^z, \rho] + \\ &+ \frac{\pi \, \lambda(\Omega)^2}{2} \, \frac{1}{\exp(\beta\Omega) - 1} \, \left(2\sigma_t^- \rho \sigma_t^+ - \sigma_t^+ \sigma_t^- \rho - \rho \sigma_t^+ \sigma_t^- \right) \\ &+ \frac{\pi \, \lambda(\Omega)^2}{2} \, \frac{1}{1 - \exp(\beta\Omega)} \, \left(2\sigma_t^+ \rho \sigma_t^- - \sigma_t^- \sigma_t^+ \rho - \rho \sigma_t^- \sigma_t^+ \right) , \end{aligned} \tag{12.3}$$

[1] For the present purpose, it is irrelevant what kind of boundary conditions are chosen for the chain, since the master equation approach assumes the number of oscillators to be very large, $n \gg 1$.

[2] $\hbar = 1$

where we have set $\hbar = 1$. This equation describes the relaxation of the reduced density matrix into the stationary state,

$$\rho_{t\to\infty} = \frac{\exp(-\beta\Omega\sigma_t^z)}{\mathrm{Tr}\left(\exp(-\beta\Omega\sigma_t^z)\right)}\,. \tag{12.4}$$

The spin (thermometer) thus approaches a canonical state with the same temperature as the total chain, β, even for perfectly local coupling.

Note that one would obtain the same result for a thermometer with more than only two energy levels.

As long as the chain is in a global equilibrium state, a temperature measurement of this type thus does not have any spatial resolution at all. It is only capable of measuring the global temperature of the chain. Neither can any local temperatures be measured nor any signatures of their breakdown be detected.

This conclusion obviously cannot hold anymore for scenarios with only local but no global equilibrium. Macroscopic temperature profiles are measured, with the standard technique described above, every day. Whether such measurements of temperature profiles are still possible for much smaller systems and what their maximally possible spatial resolution is in that case should be subject of further investigations.

According to the above considerations, one might think that the question of local temperatures for systems in global equilibrium was an irrelevant issue since it has no observable consequences. This, however is not the case. In the following we turn to discuss an example of such measurable consequences of the local breakdown of the concept of temperature.

12.2. Non-thermal Local Properties

We now consider observables of the object (chain) itself, which can be used to measure local temperatures T_{loc}, i.e. temperatures of subsystems, provided the subsystems are in a canonical state. In turn, if the respective subsystems are not in a canonical state, this fact should modify the measurement results for those observables.

The minimal group sizes calculated in chapter 7 depend on the global temperature and on the strength of the interactions between neighboring subsystems. Furthermore, local temperatures can even exist for single subsystems if these are finite dimensional, as we have seen in chapter

8. For systems composed of finite dimensional subsystems, local temperatures do thus exist for single subsystems at relatively low global temperatures if the coupling is weak, while they do not if the coupling is strong.

Pertinent systems, for which such effects can easily by studied, are magnetic materials. These can in many cases be described by spin lattice or spin chain models. Since, as we will see below, properties of single spins can be infered from measurements of even macroscopic magnetic observables, those materials thus allow to study the existence of temperature, as defined by the existence of a canonical state, on the most local scale possible, i.e. for single spins.

Since, for a spin-1/2 system, it is always possible to assign a Boltzmann factor and thus a local temperature to the ratio of the occupation probability of the higher and lower level[3], we consider, as our model, a homogeneous chain of spin-1 particles interacting with their nearest neighbors. For the interactions, we assume a Heisenberg model. The Hamiltonian of this system reads [71]:

$$H = B \sum_{j=1}^{n} \tilde{\sigma}_j^z + J \sum_{j=1}^{n} \tilde{\sigma}_j^x \tilde{\sigma}_{j+1}^x + \tilde{\sigma}_j^y \tilde{\sigma}_{j+1}^y + \tilde{\sigma}_j^z \tilde{\sigma}_{j+1}^z \,, \tag{12.5}$$

where $\tilde{\sigma}_j^x$, $\tilde{\sigma}_j^y$ and $\tilde{\sigma}_j^z$ are the spin-1 matrices (see D.2). B is an applied magnetic field, J the coupling and n the number of spins. The coupling J is taken to be positive, $J > 0$. The spins thus tend to align anti-parallelly and the material is anti-ferromagnetic. The local Hamiltonian of subsystem j is $H_j = B\,\tilde{\sigma}_j^z$. The system has periodic boundary conditions and is thus translation invariant.

As in the previous chapters, we assume that the entire system (12.5) is in a thermal state (see equation (3.3)). Because of the translational invariance, all reduced density matrices of single subsystems are equal. We represent them in the eigenbasis of the respective subsystem Hamiltonian, say H_j. Let its diagonal matrix elements be p_α. It is convenient to introduce a spectral temperature T_{spec}, which would coincide with T_{loc}

[3]For a spin-1/2 system, the spectral temperature (12.6) is always a local temperature, $T_{\text{spec}} = T_{\text{loc}}$ and the deviations ς vanish, $\varsigma = 0$.

if the local state was canonical but which formally exists for any state:

$$\frac{1}{T_{\text{spec}}} \equiv -k_{\text{B}} \sum_{\alpha>0} \frac{p_\alpha}{1-p_0} \, \frac{\ln(p_\alpha) - \ln(p_0)}{E_\alpha - E_0} \,. \tag{12.6}$$

Here the E_α are the spectrum of the isolated subsystem; E_0 denotes the ground state. The factor $(1-p_0)^{-1}$ is the normalization. The description of the local state may thus be condensed into T_{spec} and a parameter ς describing mean relative square deviations of the occupation probabilities p_α from those of a canonical state, p_α^c, with $T_{\text{loc}} = T_{\text{spec}}$,

$$\varsigma^2 \equiv \sum_\alpha p_\alpha \left(\frac{p_\alpha - p_\alpha^c}{p_\alpha} \right)^2 , \tag{12.7}$$

where

$$p_\alpha^c = \frac{\exp\left(-\dfrac{E_\alpha}{k_{\text{B}}\, T_{\text{spec}}} \right)}{\displaystyle\sum_\alpha \exp\left(-\frac{E_\alpha}{k_{\text{B}}\, T_{\text{spec}}} \right)} \,. \tag{12.8}$$

Note that T_{spec} and ς depend on the global temperature T **and** the type and strength of subsystem interactions.

Figure 12.1 shows the spectral temperature T_{spec}, the global temperature T and the deviations ς of the local state from a canonical state with T_{spec} as a function of T for a spin-1 chain of 4 particles with the Hamiltonian (12.5). While the deviations ς are small at high T, they become larger for low T, where the spectral temperature T_{spec} starts to rise again as T is lowered further. For $T = 0$, ς vanishes, since a completely mixed state corresponds to a canonical one with $T_{\text{spec}} \to \infty$. A signature of these local deviations from a canonical state ($\varsigma \neq 0$) can be measured.

As an example of such an experiment, we will now consider two different magnetic observables of a spin-1 system with the Hamiltonian (12.5). The first observable is the magnetization in the direction of the applied

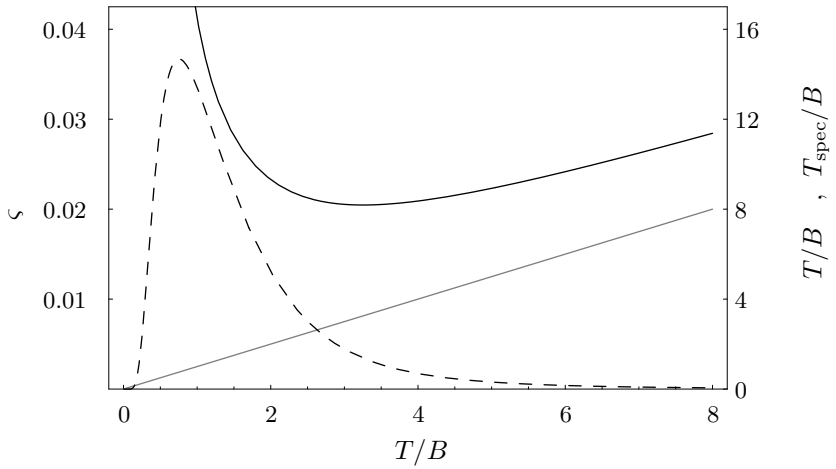

Figure 12.1.: T_{spec} (solid line), T (gray line) and ς (dashed line) as a function of temperature T for a spin-1 chain of 4 particles. T_{spec} and T are given in units of B and $J = 2 \times B$.

field[4], m_z, which we define to be the total magnetic moment per particle:

$$m_z \equiv \frac{1}{n} \Big\langle \sum_{j=1}^{n} \tilde{\sigma}_j^z \Big\rangle \,, \tag{12.9}$$

where $\langle \mathcal{O} \rangle$ is the expectation value of the operator $\mathcal{O}$, i.e. $\langle \mathcal{O} \rangle = \mathrm{Tr}(\rho\, \mathcal{O})$. In the translation invariant state ρ, the reduced density matrices of all individual spins are equal, and the magnetization (12.9) can be written as

$$m_z = \langle \tilde{\sigma}_k^z \rangle \,, \tag{12.10}$$

for any $k = 1, 2, \ldots, n$. The magnetization, although defined macroscopically, is thus actually a property of a single spin, i.e. a strictly local property.

[4]The two other components of the magnetization, m_x and m_y, vanish due to symmetry reasons.

As our second observable we choose the occupation probability, p, of the $s_z = 0$ level (averaged over all spins),

$$p = \frac{1}{n}\Big\langle \sum_{j=1}^{n} |0_j\rangle\langle 0_j| \Big\rangle . \tag{12.11}$$

Similar to m_z according to equation (12.10), p may be written as

$$p = \langle |0_k\rangle\langle 0_k| \rangle , \tag{12.12}$$

for any $k = 1, 2, \ldots, n$ and is thus strictly local, too.

Now, if each single spin was in a canonical state with $\varsigma = 0$ and a temperature $T_{\mathrm{loc}} = T_{\mathrm{spec}}$, m_z and p would both have to be monotonic functions of T_{loc}. Consequently, T_{loc} could, after calibration, be infered from measurements of m_z or p. Note, that m_z is proportional to the local energy, the average energy of one subsystem.

Figure 12.2, shows m_z and p as a function of the global temperature T for a spin-1 chain of 4 particles with the Hamiltonian (12.5) for weak interactions, $J = 0.1 \times B$. Both quantities are monotonic functions of each other.

The situation changes drastically when the spins are strongly coupled. In this case the concept of temperature breaks down locally due to correlations of each single spin with its environment.

Figure 12.3 shows m_z and p as a function of temperature T for a spin-1 chain of 4 particles with the Hamiltonian (12.5) for strong interactions $J = 2 \times B$. Both quantities are non-monotonic functions of T and therefore no mapping between m_z and p exists.

How could a local observer determine whether the system he observes, a single spin, is in a thermal state and can therefore be characterized by a temperature? The local observer needs to compare two situations:

In the first situation, the spin is weakly coupled to a larger system, the heat bath. In this situation, the local observer could measure m_z and p as functions of the temperature of the heat bath and would get a result similar to figure 12.2. This result would not be sensitive to the details of the coupling to the heat bath. The local observer would thus recognize this situation as a particular one and might term it the "thermal" situation.

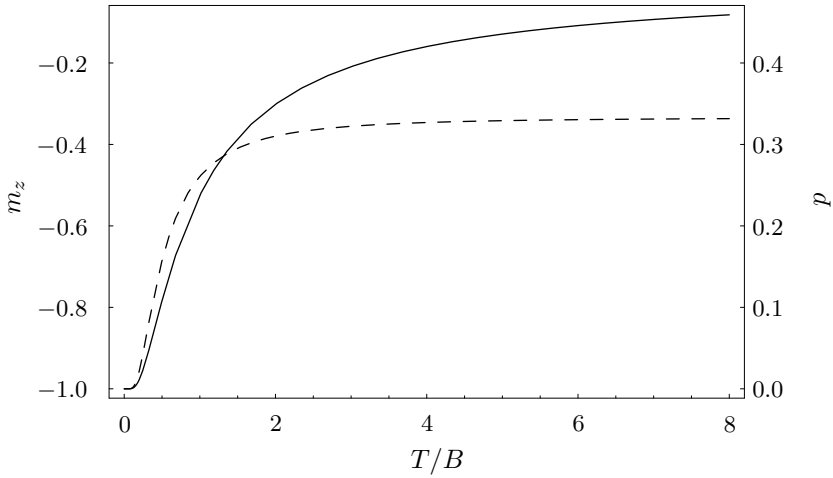

Figure 12.2.: m_z (solid line) and p (dashed line) as a function of temperature T for a spin-1 chain of 4 particles. T is given in units of B and $J = 0.1 \times B$.

The second situation is fundamentally different. The spin is now strongly coupled to its surrounding. If the local observer again measures m_z and p as functions of the temperature of the surrounding, he gets the result of figure 12.3.

The observer can tell the difference between both situations, even if he has no access to the temperature T of the surrounding. In the first case he can construct a mapping from say m_z to p, i.e. $p(m_z)$, or vice versa, $m_z(p)$, in the second he cannot: Here the concept of a local temperature breaks down at least on the level of individual particles, since temperature measurements via different local observables would contradict each other.

The question, whether and on what scale local temperatures can exist in systems, which are in a global equilibrium state is thus indeed physically relevant. The purpose of the concept of temperature is that it allows to predict several physical properties of the considered system. This is only possible if different properties (expectation values of observ-

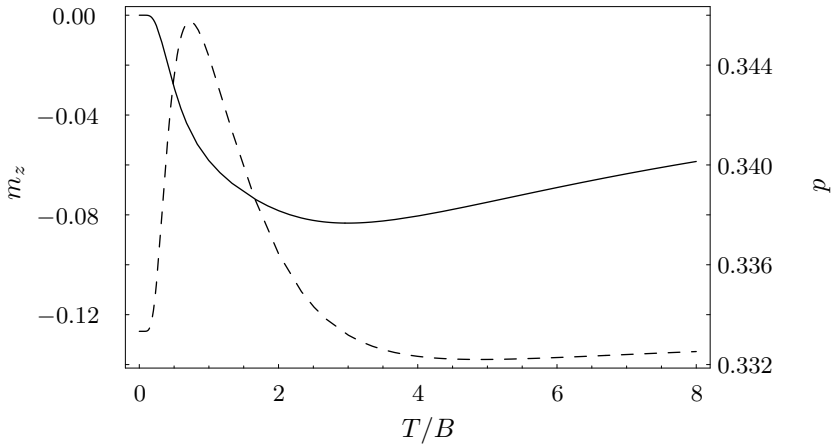

Figure 12.3.: m_z (solid line) and p (dashed line) as a function of temperature T for a spin-1 chain of 4 particles. T is given in units of B and $J = 2 \times B$.

ables) map one to one on each other as in figure 12.2. The following example illustrates the situation:

Consider a piece of metal, say a wire. Assume , its temperature is measured via its electrical resistance. Why are we interested in this temperature? We are interested in it because it allows us to predict how the wire behaves with respect to other physical processes. For example, if we know its temperature, we can tell whether the wire is going to melt or not. Effectively, we thus have a mapping of the resistance onto the fact that the wire is going to melt or is not going to melt. In a more mathematical language, we can construct a function: melting as a function of the resistance[5]. Analogously, for the scenario of figure 12.2, a local observer is able to construct a function $m_z(p)$.

What happens if such functions can no longer be constructed? In this situation, the concept of temperature becomes useless. Assume our

[5]In the present case this would of course be a step function, which would be smeared out a little.

wire had such properties. We could still measure its resistance and, if we wished, could assign a "temperature value" to it. This "temperature value", however, would be of no further use, since it would not allow us to predict whether the wire is going to melt or not. A situation where such problems do really occur is the scenario of figure 12.3.

12.3. Potential Experimental Tests

Finally, we address the question of whether the effects described here could be observed in real experiments. Indeed, pertinent experiments are available and have partly already been carried out:

A realization of a quasi one dimensional anti-ferromagnetic spin-1 Heisenberg chain is the compound $CsNiCl_3$ [42,4,8]. Here the coupling is $J \approx 2.3$ meV. To achieve a detectable modulation of m_z and p, the spins should be significantly polarized for $T > 0$. Therefore a sufficiently strong applied magnetic field is needed. For $CsNiCl_3$, a field of roughly 9.8 Tesla would correspond to $J = 4 \times B$.

The magnetization in an applied field can be measured with high precision with a SQUID [54]. The occupation probability of the $s_z = 0$ states, on the other hand, is accessible via neutron scattering experiments [43, 55]. The differential cross section for neutron scattering of spin-systems is given by [9]

$$\frac{\partial^2 \tilde{\sigma}}{\partial \Omega \, \partial E_\mathrm{f}} \sim \left| f(\vec{q})^2 \right| \frac{\left| \vec{k}_\mathrm{f} \right|}{\left| \vec{k}_\mathrm{i} \right|} \sum_{a,b} \left(\delta_{a,b} - \frac{\vec{q}_a}{|\vec{q}_a|} \cdot \frac{\vec{q}_b}{|\vec{q}_b|} \right) S^{ab}(\vec{q}, \omega) \,, \qquad (12.13)$$

where E_i, E_f, $\vec{k}_\mathrm{i}$ and $\vec{k}_\mathrm{f}$ are the initial and final energies and momenta of the scattered neutrons. $a, b = x, y, z$, $\omega = E_\mathrm{f} - E_\mathrm{i}$, $\vec{q} = \vec{k}_\mathrm{f} - \vec{k}_\mathrm{i}$ and $f(\vec{q})$ is the magnetic form factor, which can be found tabulated [11]. The dynamic structure factor $S^{ab}(\vec{q}, \omega)$ is the Fourier transform of the spin-spin correlation function,

$$S^{ab}(\vec{q}, \omega) = \frac{1}{2\pi} \int dt \sum_{\vec{r}, \vec{r}'} e^{i\vec{q}(\vec{r} - \vec{r}') - i\omega t} \langle \tilde{\sigma}^a_{\vec{r}}(0) \, \tilde{\sigma}^b_{\vec{r}'}(t) \rangle \,. \qquad (12.14)$$

If we only consider events, where the difference in momentum is along the z-axis, $\vec{q} = q_z \vec{e}_z$, only S^{xx}, S^{xy}, S^{yx} and S^{yy} contribute in equation

(12.13). Since the applied field B is along the z-axis, S^{xy} and S^{yx} are zero due to symmetry. Summing up over all $\vec{q}$ and all ω and using our knowledge of $\vec{k}_{\mathrm{i}}$, $\vec{k}_{\mathrm{f}}$ and $f(\vec{q})$ we can obtain information about the quantity

$$\frac{1}{n}\sum_{\vec{r}}\langle\tilde{\sigma}^x_{\vec{r}}(0)\,\tilde{\sigma}^x_{\vec{r}}(0)+\tilde{\sigma}^y_{\vec{r}}(0)\,\tilde{\sigma}^y_{\vec{r}}(0)\rangle = 1+p \tag{12.15}$$

from the measurement data. Therefore, p is measurable in neutron scattering experiments.

Such experiments or a combination thereof could thus be used to demonstrate the non-existence of local temperature.

13. Conclusion and Outlook

In the present work, we have considered the minimal spatial length scales on which local temperature can meaningfully be defined. For large systems in a global equilibrium state, we have derived two criteria which are valid for all quantum many body systems with nearest neighbor interactions[1] and discussed the physical relevance of the existence and non-existence of local temperatures. A generalization to scenarios with only local but no global equilibrium remains an interesting issue for future research.

We have started our treatment of the global equilibrium case with a description of a recent experiment, in which the existence of local temperatures is an open and relevant question. Although this experiment deals with the non-equilibrium case, it impressively shows the need for better understanding of the microscopic limits of the applicability of the concept of temperature.

For the determination of the length scales on which temperature can exist, a precise definition of the notion of temperature is of crucial relevance. Real physical systems are never perfectly isolated, but do always interact with their surrounding, even if the interaction is only via the substrate they sit on or the trap they are in. For these situations, Statistical Mechanics predicts that the equilibrium state is a canonical one. We have thus defined the existence of local temperature to be the existence of a local canonical state. This definition has been discussed in chapter 3, where we have also mentioned some rather "practical" arguments for it. These include the existence of one-to-one mappings between expectation values of observables and temperature[2].

In chapter 4, we have outlined our approach to determine the length

[1] The conditions apply to an even larger class of models. Next nearest neighbor interaction and all systems where each subsystem has only a finite number of interaction partners are also permitted

[2] We have treated physical consequences of the existence and non-existence of these mappings again, and in more detail, in chapter 12.

scales in question. We have considered a large homogeneous quantum many body system with nearest neighbor interactions and assumed it to be in a thermal, i.e. canonical state. We have then divided this system into adjoining groups of n elementary subsystems each and derived criteria, when the groups themselves are in canonical states. In doing so, we have focused on the diagonal elements of the reduced density matrices of the groups because the off-diagonal elements are significantly smaller.

The key step of our approach is a central limit theorem for interacting quantum many body systems, which we have discussed in chapter 5. If a quantum observable is measured for a system, which is not in an eigenstate of the observable, eigenvalues of the latter are obtained with certain probabilities[3]. The theorem states, that the distribution of these probabilities converges to a Gaussian normal distribution for a many body system with nearest neighbor interactions in a product state. Among the known central limit theorems for this type of quantum systems, it is, to the best of our knowledge, the only one which does not require a translation invariant product state. This generalization however is crucial for applications in physics since, for example a chain of 100 spins has 2^{100} product states but only 2 of them are translation invariant.

Having established the theorem, it has then been applied to several interesting problems in physics. First we have used it to rederive the spectral density and partition function of a spin chain, for which both quantities can be computed exactly, in chapter 6. In the present case this was intended to confirm the validity of the theorem, but in others, the theorem may open up a new approach to calculate such quantities. In the present work, the most important application of the theorem is the derivation of criteria for the existence of local temperatures, which has been presented in chapter 7. The criteria can be expressed in only two conditions for each product state (equations (7.22) and (7.24)), which relate the expectation value and the squared width of the corresponding energy distribution with the global temperature. In particular, the temperature only appears in terms that depend on the squared width. Since the latter is only nonzero because the local Hamiltonians do not commute with the global one ($[H_0, H] \neq 0$), the temperature dependence can be regarded as a pure quantum phenomenon [73, 39, 6, 59].

[3]These probabilities are given by the squared absolute value of the scalar products of the eigenstates and the state the system is in.

We have then applied the general method to several types of Ising spin chains (chapter 8) and a harmonic chain (chapter 9). Since, for systems with short range interactions, the energy in one group is n times the average energy per subsystem, while the energy contained in the group interactions is independent of the group size (interactions only take place at the two ends), interactions become less relevant as the group size increases. Therefore, conditions (7.22) and (7.24) determine a minimal group size and thus a minimal length scale on which temperature may be defined according to the concept we adopt. Grains of size below these length scales are no more in a thermal state and temperature measurements with a higher resolution should no longer be interpreted in a standard way.

The most striking difference between the spin chains and the harmonic chain is that the energy spectrum of the spin chains is limited, while it is infinite for the harmonic chain. For spins at very high global temperatures, the total density matrix is thus almost completely mixed, i. e. proportional to the identity matrix, and therefore does not change under basis transformations. Hence, there are global temperatures which are high enough, so that local temperatures exist even for single spins.

For the harmonic chain, this feature does not appear, since the relevant energy range increases indefinitely with growing global temperature, leading to the constant minimal length scale in the high energy range.

Since harmonic lattice models in Debye approximation have proven to be successful in modeling thermal properties of insulators (e.g. the heat capacity) [45], our calculation for the harmonic chain provides a first estimate of the minimal length scale on which intensive temperatures exist in insulating solids of a quasi one-dimensional shape. As possible applications one may, for example, think of carbon nanotubes [14]. Some examples of these estimates are given in chapter 10, which also contains a discussion of the feasibility of our results.

Although in the present treatment only equilibrium cases have been considered, the calculated length scales should also constrain the way one can meaningfully define temperature profiles in non-equilibrium scenarios.

In chapter 12, finally, we have discussed possible "local" temperature measurements. The standard technique with a small thermometer weakly and locally coupled to a large system should not show any spatial resolution as long as the large system is in a global equilibrium

state, contrary to situations with thermal equilibrium states only on the local but not on the global scale. On the other hand, there are physical properties which are strictly local and which therefore reveal local temperatures and their eventual breakdown. As examples, we have considered magnetic properties of salts. For large structures, which may accurately be modeled by periodic boundary conditions, properties like the magnetization are, due to the translational invariance, strictly local. Nevertheless, they are accessible by macroscopic measurements. We have considered a spin-1 compound and shown that its magnetization cannot be taken to be a function of the occupation probability of the $s_z = 0$ level. This clearly shows that the concept of temperature has become meaningless for single spins in this case. Temperature only is a useful concept if it allows to predict several physical properties of a system. If one uses property a to measure temperature (i.e. assign a temperature value to measurement results of a), this concept is only useful if a different property b can be predicted from the temperature. This means, that one should be able to construct a function $b(a)$. However, in our example this is not possible.

We have thus been able to clarify some questions related to the microscopic limit of the applicability of Thermodynamics. Nevertheless, some open problems remain and even new ones appeared as we worked out the present approach.

First of all, the generalization of our calculations to scenarios with only local but no global equilibrium is an issue of significant importance. One might expect that the length scales do no longer depend on the interactions and the global temperature only, but that the temperature gradient becomes relevant, too.

For global non-equilibrium, local temperature measurements of the standard type are very interesting and important issues on their own. As we have discussed here, these measurements have no spatial resolution if the sample is in a global equilibrium state. On the other hand, local temperature measurements with spatial resolution are being done for macroscopic setups and nobody would dare to question their validity. Therfore the maximal spatial resolution of this kind of measurements is an interesting question and the present understanding of this topic is quite poor.

A second promising field for future research could be concerned with new physics that might show up for small entities, which are in contact

with a thermal surrounding, but which show non-thermal physics due to the breakdown of temperature on the respective scale. One example for this are the observable features discussed in chapter 12. However, one might think about more surprising phenomena, as for example anomalous pressure fluctuations in nanoscopic gas bubbles enclosed in a piece of solid. With respect to future nanotechnologies, such phenomena could equally be harmful or useful, depending on whether one is able to design the devices in the pertinent way.

Furthermore, our mathematical technique, the central limit theorem, is of interest on its own. As already indicated in chapter 5.4, there are many possibilities for generalizations of the theorem. Furthermore, the applications discussed in chapter 6 could proof useful in the analysis of quantum phases of strongly correlated many particle systems. In this field, analytical results are quite rare, while numerical ones are always limited to small systems or subtle approximations. The significant advantage of our approach in this context is that it is not limited to systems with nearest neighbor interactions but can also be applied to frustrated ones.

Finally, possible generalizations of Thermodynamics, that could apply on even smaller scales seem to be interesting. In the present work, we have considered the microscopic limit of usual thermal behavior in quantum systems, i.e. Quantum Thermodynamics [22], where effective interactions among the considered parts are small. One might thus wonder, whether only partitions with weak effective couplings can be considered within such a "universal" description, that does not depend on the details of the microscopic constituents, or whether there also exists an intermediate level of description, which is not as universal as standard Thermodynamics but which, on the other hand, applies on smaller scales. Since, in standard Thermodynamics, equilibrium states are fully characterized by one single parameter, temperature (cf. equation (3.3)), one could for example imagine that there exists a class of generalized equilibrium states, which require say two or three parameters for their characterization. Some phenomenological attempts in this direction have already been made [36, 61]. Nonetheless, justification of these attempts from an underlying theory, i.e. Quantum or Classical Mechanics, is still missing.

14. Deutsche Zusammenfassung

14.1. Einleitung

Thermodynamik beschreibt die physikalischen Eigenschaften von Systemen, die aus einer sehr großen Anzahl von Teilchen bestehen. Nachdem sie anfangs eine rein phänomenologische Wissenschaft war, wurde sie später, beginnend mit den Arbeiten von Joule und Boltzmann, im Rahmen der Statistischen Mechanik auf die zugrundeliegende Theorie für die einzelnen Teilchen zurückgeführt. Während die Begründung des irreversiblen Strebens ins Gleichgewicht (Zweiter Hauptsatz) noch heute debattiert wird, ist die Existenz thermodynamischer Größen, der Thermodynamische Limes, für makroskopische System geklärt.

Eine fundamentale, bis heute ungeklärte Frage ist hingegen, wie groß Systeme mindestens sein müssen, um thermodynamisch beschreibbar zu sein. Diese Frage hat in jüngster Zeit stark an Wichtigkeit gewonnen, da sie seit der Entwicklung der Nanotechnologie immer mehr von experimenteller Relevanz ist. Die Möglichkeiten, Materialien mit Strukturen im Nanometerbereich herzustellen und experimentell zu untersuchen haben in den letzten Jahren entscheidend zugenommen und Messungen thermodynamischer Größen auf Nanoskalen erscheinen möglich. In diesem Zusammenhang ist eine Frage besonders wichtig und interessant: Kann Temperatur auf diesen Skalen sinnvoll definiert werden?

Die vorliegende Doktorarbeit untersucht diese Frage quantitativ und geht dabei wie folgt vor:

Wir betrachten ein quantenmechanisches Vielteilchensystem, von dem wir annehmen, es befände sich in einem thermischen (hier kanonischen) Zustand. Dann zerteilen wir das System gedanklich in gleich große Stücke, Gruppen von n aneinanderliegenden Teilchen, und analysieren, ab welcher Größe die einzelnen Stücke bzw. Gruppen ebenfalls in einem lokalen thermischen Zustand sind.

Die betrachteten Vielteilchensysteme haben Nächste-Nachbar-Wechsel-

wirkungen. Die Wechselwirkungen einer Gruppe mit ihrer Umgebung finden daher nur an der Oberfläche der Gruppe statt, wohingegen sich die Energie in der Gruppe auf das ganze Volumen erstreckt. Da aber die Oberfläche einer Region mit zunehmender Größe langsamer wächst als das Volumen (in einer Dimension ist z.B. die Oberfläche konstant während das Volumen linear wächst) werden die Wechselwirkungen für größere Gruppen immer in-effektiver. Durch dieses Skalierungsverhalten gibt es eine minimale Gruppengröße $n_{\min}$, ab der die Wechselwirkungen und damit auch die Korrelationen effektiv so klein sind, dass die einzelnen Gruppen sich in thermischen Zuständen befinden und somit eine lokale Temperatur existiert. Um dieses Verhalten quantitativ zu analysieren muss zunächst die Existenz lokaler Temperatur präzise definiert sein.

14.2. Lokale Temperatur

Die Existenz lokaler Temperatur definieren wir als die Existenz eines lokalen thermischen Zustandes. Demnach existiert eine lokale Temperatur dann und nur dann, wenn die entsprechende reduzierte Dichtematrix von kanonischer Form ist.

Neben ihrer Begründung aus der Statistischen Mechanik gibt es noch weitere, eher praktische, Argumente für diese Definition. Der kanonische Zustand ist durch zwei Eigenschaften ausgezeichnet, er ist durch einen einzigen Parameter, die Temperatur, charakterisiert und die enthaltenen Besetzungswahrscheinlichkeiten sind eine exponentiell abfallende Funktion der Energie.

Ersteres sorgt dafür, dass es eindeutige Abbildungen zwischen der Temperatur und Erwartungswerten von Observablen gibt. Da Temperatur immer indirekt über Erwartungswerte von Observablen gemessen wird, hat diese Eigenschaft zur Folge, dass man bei Messungen über verschiedene Observable stets den selben Wert für die Temperatur erhält.

Die zweite Eigenschaft, das exponentielle Abfallen den Besetzungswahrscheinlichkeiten, bewirkt, dass Erwartungswerte von Observablen "scharf" sind, da für Vielteichensysteme die Zustandsdichte mit der Energie stark anwächst und somit ihr Produkt mit einer exponentiell abfallenden Funktion eine sehr schmale Verteilung mit stark ausgeprägtem

Maximum bildet (vgl. Abbildung 3.1).

Mit dieser Definition der Existenz lokaler Temperatur berechnen wir im folgende die Längenskalen, auf denen solch eine Temperatur existieren kann. Der zentrale Schritt hierbei ist ein zentraler Grenzwertsatz für quantenmechanische Vielteilchensysteme.

14.3. Zentraler Grenzwertsatz für quantenmechanische Vielteilchensysteme

Für ein quantenmechanisches Vielteilchensystem mit Nächster-Nachbar-Wechselwirkung kommutieren die Hamiltonoperatoren H_μ der einzelnen Teilchen nicht mit dem Hamiltonoperator des gesamten Systems H.

$$H = \sum_\mu H_\mu + I_{\mu,\mu+1} \qquad \text{wobei} \qquad [H_\mu, H] \neq 0\,. \tag{14.1}$$

Hierbei sind die $I_{\mu,\mu+1}$ die Wechselwirkungen zwischen den Teilchen μ und $\mu+1$. Bezeichnet man die Energieeigenzustände des Teichens μ mit $|a_\mu\rangle$,

$$H\,|a_\mu\rangle = E_\mu\,|a_\mu\rangle\ , \tag{14.2}$$

so gibt es Produktzustände

$$|a\rangle \equiv \prod_{\mu=1}^{n} \otimes\ |a_\mu\rangle\ . \tag{14.3}$$

Befindet sich das System nun in dem Zustand $|a\rangle$ so treten die Eigenwerte des gesamten Hamiltonoperators mit bestimmten Wahrscheinlichkeiten auf. Der, hier beschriebene zentrale Grenzwertsatz besagt nun, dass die Verteilung dieser Wahrscheinlichkeiten $w_a(E)$ im Limes unendlich vieler Teilchen gegen eine Gaußsche Normalverteilung konvergiert:

$$w_a(E) \longrightarrow \frac{1}{\sqrt{2\pi}\,\Delta_a}\ \exp\left(-\frac{\left(E-\overline{E}_a\right)^2}{2\,\Delta_a^2}\right)\ , \tag{14.4}$$

wobei der Erwartungswert durch $\overline{E}_a = \langle a|\,H\,|a\rangle$ und die Varianz durch $\Delta_a^2 = \langle a|\,H^2\,|a\rangle - \langle a|\,H\,|a\rangle^2$ gegeben sind.

Neben der Betrachtung, wann lokale Temperaturen existieren oder nicht, hat dieser Satz noch weitere interessante Anwendungen in der Physik. Der interessierte Leser sei hierzu auf Kapitel 6 verwiesen. Im nächsten Abschnitt skizzieren wir nun die allgemeinen Kriterien für die Existenz von lokaler Temperatur.

14.4. Allgemeine Theorie zur Existenz lokaler Temperatur

Wie bereits erwähnt, analysieren wir die Existenz lokaler Temperaturen für ein quantenmechanisches Vielteilchensystem, welches sich in einem thermischen Zustand befindet, indem wir es in gleich große Gruppen von Teilchen zerteilen und testen ob die reduzierten Dichtematrizen von kanonischer Form sind. Der thermisch Zustand des Gesamtsystems ist gegeben durch,

$$\hat{\rho} = \frac{\mathrm{e}^{-\beta H}}{Z}\,, \tag{14.5}$$

wobei β die inverse Temperatur und Z die Zustandssumme sind. Die oben beschriebene Partitionierung in Gruppen von n aneinanderliegenden Teilchen definiert Produktzustände der Form (14.3), wobei hier die $|a_\mu\rangle$ nicht mehr Eigenzustände einzelner Teilchen sondern Eigenzustände der Gruppen von n Teilchen sind. Um die reduzierten Dichtematrizen zu berechnen muss der Zustand (14.5) in der Basis dieser Produktzustände dargestellt werden. Wir beschränken uns hierbei auf die Diagonalelemente:

$$\langle a|\,\hat{\rho}\,|a\rangle = \int_{E_0}^{E_1} w_a(E)\,\frac{\mathrm{e}^{-\beta E}}{Z}\,dE\,. \tag{14.6}$$

Unter Verwendung des oben beschriebenen zentralen Grenzwertsatzes kann dieses Integral leicht berechnet werden.

Wir bezeichnen den Hamiltonoperator einer Gruppe μ mit H_μ. Sind alle Gruppen in einem kanonischen Zustand, so hat das Produkt ihrer Dichtematrizen die Form:

$$\prod_\mu \frac{\mathrm{e}^{-\beta H_\mu}}{Z_\mu}\,. \tag{14.7}$$

Gleichung (14.6) stimmt mit den Diagonalelementen von (14.7) überein, falls

$$\langle a|\,\hat{\rho}\,|a\rangle \propto \exp\left(-\beta \sum_{\mu} E_\mu\right) \tag{14.8}$$

ist, wobei die E_μ in (14.2) definiert sind. Gleichung (14.8) ist erfüllt sobald

$$E_\mu - \overline{E}_\mu + \frac{\beta}{2}\,\Delta_\mu^2 \;\approx\; c_1 E_\mu + c_2 \qquad \text{und} \tag{14.9}$$

$$\overline{E}_\mu - \frac{E_0}{N_G} \;>\; \beta\Delta_\mu^2 \tag{14.10}$$

gelten, wobei $\Delta_\mu^2 = \langle a_\mu|\,(H_\mu + I_{\mu,\mu+1})^2\,|a_\mu\rangle - \langle a_\mu|\,H_\mu + I_{\mu,\mu+1}\,|a_\mu\rangle^2$, $\overline{E}_\mu = \langle a_\mu|\,H_\mu + I_{\mu,\mu+1}\,|a_\mu\rangle$, E_0 die Grundzustandsenergie des Gesamtsystems, N_G die Anzahl der Gruppen und c_1 sowie c_2 beliebige reelle Konstanten sind. Die Bedingungen (14.9) und (14.10) sind das zentrale Ergebnis dieser Arbeit. Im Folgenden wenden wir sie auf konkrete Modelle an und bekommen somit quantitative Abschätzungen für die betrachteten Längenskalen.

14.5. Anwendung auf konkrete Modelle

Unter Berücksichtigung des eingangs diskutierten Skalierungsverhaltens der Wechselwirkungen lässt sich die minimale Teilchenzahl $n_{\min}$ einer Gruppe, die notwendig ist um die Bedingungen (14.9) und (14.10) zu erfüllen, abschätzen.

Wir betrachten hier eine harmonische Kette der Form

$$H = \sum_{\mu} \frac{p_\mu^2}{2m} + \frac{m}{2}\omega_0^2\,(q_\mu - q_{\mu+1})^2\ . \tag{14.11}$$

Dabei bezeichnen m die Massen, die p_μ die Impulse und die q_μ die Orte der Teilchen. ω_0 ist die Frequenz eines Oszillators.

Wir behandeln diese Kette in der Kontinuums- oder Debye-Näherung [45]. Das Ergebnis für $n_{\min}$ in Abhängigkeit von der globalen Temperatur T ist in Abbildung 9.1 dargestellt. Die Debye-Temperatur Θ ist eine Materialkonstante. Für Temperaturen unter der Debye-Temperatur ist $n_{\min}$

proportional zu T^{-3} und für Temperaturen über der Debye-Temperatur konstant.

Im nächsten Abschnitt untersuchen wir die experimentelle Relevanz dieser Ergebnisse.

14.6. Experimentelle Relevanz

Nachdem wir berechnet haben, auf welchen Längenskalen lokale Zustände in einem global thermischen System nicht mehr thermisch sind, beschäftigen wir uns nun mit der Frage ob und wie die nicht-thermischen Eigenschaften dieser Zustände messbar sind.

Betrachten wir zunächst eine herkömmliche Temperaturmessung: Ein kleines Sensorsystem wird lokal mit der oben betrachteten Kette in thermischen Kontakt gebracht, also schwach angekoppelt. Wir wissen aus Studien von System-Bad-Szenarien, dass das Sensorsystem unabhängig von den Kopplungen innerhalb der Kette und der Lokalität seiner Ankopplung an diese immer in einen kanonischen Zustand mit der globalen Temperatur der Kette relaxiert. Solange die Kette global in einem Gleichgewichtszustand ist besitzt diese Messung keine räumliche Auflösung. Ist die Kette global nicht mehr in einem Gleichgewichtszustand, so wie beim Wärmetransport, ist es unstrittig, dass zumindest auf makroskopischer Skala solche Temperaturmessungen eine räumliche Auflösung haben.

Diese Betrachtung bedeutet jedoch nicht, dass die Frage der Existenz lokaler Temperatur bei globalem Gleichgewicht physikalisch irrelevant wäre. Es gibt Observablen, die durch die lokalen Zustände bestimmt sind und die somit auch deren nicht-thermischen Charakter widerspiegeln.

Als Beispiel betrachten wir hier eine antiferromagnetische Spin-1-Heisenberg-Kette in einem Magnetfeld.

$$H = B \sum_{j=1}^{n} \tilde{\sigma}_j^z + J \sum_{j=1}^{n} \tilde{\sigma}_j^x \tilde{\sigma}_{j+1}^x + \tilde{\sigma}_j^y \tilde{\sigma}_{j+1}^y + \tilde{\sigma}_j^z \tilde{\sigma}_{j+1}^z \,, \tag{14.12}$$

Dabei sind B das Magnetfeld, $J > 0$ die Kopplungsstärke und die $\tilde{\sigma}$ die jeweiligen Spin-1-Matrizen.

Wenn die Kette sehr lang ist und Randeffekte vernachlässigbar sind, haben die Magnetisierung m_z und die mittlere Besetzungswahrscheinlichkeit p des $s_z = 0$ Niveaus folgende Eigenschaft:

$$m_z \equiv \frac{1}{n}\Big\langle \sum_{j=1}^{n} \tilde{\sigma}_j^z \Big\rangle = \langle \tilde{\sigma}_k^z \rangle \qquad \text{bzw.} \tag{14.13}$$

$$p \equiv \frac{1}{n}\Big\langle \sum_{j=1}^{n} |0_j\rangle\langle 0_j| \Big\rangle = \langle |0_k\rangle\langle 0_k| \rangle\,, \tag{14.14}$$

für einen beliebigen Spin k. Sie sind dadurch streng lokale Größen (Einzelspingrößen), können jedoch beide in makroskopischen Experimenten (Magnetisierungsmessung mit einem SQUID bzw. Neutronen-Streuexperiment) gemessen werden.

Für eine Kette mit schwacher Kopplung ($J \ll B$) ist zu erwarten, dass die lokalen Zustände thermisch sind, während für eine stark gekoppelte Kette ($J > B$) dies nicht mehr gilt und das Konzept der Temperatur lokal nicht mehr existiert. Abbildungen 12.2 und 12.3 zeigen jeweils m_z und p für schwache und starke Kopplung als Funktion der globalen Temperatur T.

Ein lokaler Beobachter kann nun feststellen, dass er im Fall schwacher Kopplung aus seinen Messwerten eine Funktion $m_z(p)$ konstruieren kann während dies im Fall starker Kopplung nicht geht, da diese Funktion mehrdeutig wäre. Diese Feststellung kann der lokale Beobachter machen ohne die globale Temperatur zu kennen und er kann somit den fundamentalen Unterschied zwischen der thermischen und der nicht-thermischen Situation experimentell nachweisen.

Die erwähnte Abbildbarkeit einer Observablen auf eine andere, die das thermische Szenario auszeichnet, ist Voraussetzung dafür, dass die Definition einer Temperatur nützlich ist. Wird eine Temperatur definiert, so muss sie über eine Observable gemessen werden, muss es dann aber auch ermöglichen Vorhersagen über eine andere Observable zu treffen, sonst wäre sie nutzlos. Es muss also effektiv eine Abbildung von der ersten auf die zweit Observable bestehen. Für die stark gekoppelte Heisenberg-Kette gibt es diese Abbildung zwischen den beiden betrachteten Größen nicht.

14.7. Diskussion und Ausblick

In der vorliegenden Arbeit haben wir die minimalen Längenskalen, auf denen Temperatur sinnvoll definiert werden kann, betrachtet. Für große Systeme in einem globalen Gleichgewichtszustand haben wir hierfür zwei Kriterien gefunden, die für alle Quanten-Vielteilchensysteme mit Nächster-Nachbar-Wechselwirkung anwendbar sind, und die physikalisch Relevanz der Existenz bzw. der Nicht-Existenz von lokaler Temperatur diskutiert.

Wir haben dazu die Existenz lokaler Temperatur als die Existenz einer reduzierten Dichtematrix von kanonischer Form auf der entsprechenden Skala definiert. Der Kern der Herleitung der Kriterien ist ein zentraler Grenzwertsatz für quantenmechanische Vielteilchensysteme, der besagt, dass die Verteilung der Gesamtenergie in einem Produktzustand gegen eine Gaußsche Normalverteilung konvergiert, wenn die Zahl der Teichen gegen unendlich geht.

Mit Hilfe dieses Satzes erhält man zwei Bedingungen die, wenn sie auf ein konkretes System angewandt werden, eine quantitative Abschätzung der betrachteten Längenskalen erlauben. Für quasi eindimensionale Festkörper, die sich durch eine Harmonische Kette in Debye-Näherung beschreiben lassen, ist die Skala, auf der lokale Temperatur existiert, konstant für Temperaturen über der Debye-Temperatur und proportional zu T^{-3} für Temperaturen unter der Debye-Temperatur. Die Temperaturabhängigkeit der Längenskala hängt direkt mit der Nicht-Kommutativität des gesamten Hamiltonoperators und der Ein-Teilchen-Hamiltonoperatoren zusammen und ist somit ein Quanteneffekt.

Obwohl der vorliegende Zugang von einem globalen Gleichgewichtszustand ausgeht, ist zu erwarten, dass die Ergebnisse auch auf globale Nichtgleichgewichtszustände mit kleinen Temperaturgradienten anwendbar sind.

Im Weiteren haben wir die experimentelle Relevanz dieser Ergebnisse diskutiert. Eine herkömmliche Temperaturmessung hat für den Fall des globalen Gleichgewichts keine räumliche Auflösung und ist somit nicht in der Lage das Zusammenbrechen des Konzepts lokaler Temperatur festzustellen. Es gibt jedoch Observablen, deren Erwartungswerte durch die lokalen Zustände bestimmt sind. Vergleicht man zwei Observablen dieses Typs, so lassen sich ihre Erwartungswerte im lokal thermischen Fall stets aufeinander abbilden, im nicht-thermischen Fall jedoch nicht. Dies ist ein messbarer, fundamentaler Unterschied zwischen beiden Szenarien.

Neben den Punkten, die in der vorliegenden Arbeit geklärt werden konnten, bleiben noch einige offene Fragen bzw. haben sich während der Ausarbeitung neue Fragen ergeben. Wir erwähnen hier die, die uns am interessantesten und wichtigsten erscheinen.

Zunächst wäre es wichtig den vorliegenden Zugang auf Systeme, die global nicht im Gleichgewicht sind, zu erweiteren. In diesem Zusammenhang ist die Frage der möglichen räumlichen Auflösung einer Temperaturmessung ebenfalls von hohem Interesse.

Weiterhin sind Verallgemeinerungen und weitere Anwendungen des zentralen Grenzwertsatzes denkbar und könnten sehr nützlich sein.

Ein großer Bereich offener Probleme ist auch die Physik, die lokal auf Skalen, auf denen die Zustände trotz thermischer Umgebung nicht mehr thermisch sind, auftritt. Hier könnten kleine Systeme die in eine thermische Umgebung stark wechselwirkend eingebettet, von dieser aber physikalisch unterscheidbar sind, interessant sein.

Zu guter letzt, könnten auch mögliche Verallgemeinerungen der Thermodynamik untersucht werden, die evtl. auf kleineren Skalen anwendbar sind als die herkömmliche Theorie. Die Gleichgewichtszustände wären dann möglicherweise nicht mehr nur durch einen Parameter charakterisiert, wie im kanonischen Fall.

A. Proof of the Quantum Central Limit Theorem

In this chapter we give the proof of the Quantum Central Limit Theorem (QCLT) of chapter 5. We prove the weak convergence of the distributions via the pointwise convergence of their characteristic functions, which is shown in three steps.

First, we show that the characteristic function of S_n does not change if a few of the $\mathcal{H}_\mu$ are neglected. Second, we prove, that the characteristic function of the remainder of S_n factorizes. It is thus a product of several characteristic functions. In the next step, we show that our system fulfills the Lyapunov condition [10]. This means that each of the individual characteristic functions is fully determined by its first two moments, which makes it a Gaussian. Being a product of Gaussians, the characteristic function of S_n is thus itself a Gaussian.

In the last section we then prove that the pointwise convergence of characteristic functions implies the weak convergence of the distributions.

Before we present the main part of the proof, we give two useful lemmas.

A.1. Two Useful Lemmas

Lemma A.1 *Let $z_1, \ldots, z_m$ and $w_1, \ldots, w_m$ be complex numbers of modulus smaller or equal to 1, $|z_j| \leq 1$ and $|w_j| \leq 1$; then*

$$|z_1 \cdots z_m - w_1 \cdots w_m| \leq \sum_{k=1}^{m} |z_k - w_k| \tag{A.1}$$

PROOF: Applying the triangle-inequality, the lemma follows by induction from

$$z_1 \cdots z_m - w_1 \cdots w_m = (z_1 - w_1)(z_2 \cdots z_m) + w_1 (z_2 \cdots z_m) \quad \text{(A.2)}$$

■

Lemma A.2 *If a real random variable X has a moment of order m, then for real r*

$$\left| \mathbb{E}\left[\mathrm{e}^{-\mathrm{i}rX}\right] - \sum_{k=0}^{m} \frac{(-\mathrm{i}r)^k}{k!} \mathbb{E}\left[X^k\right] \right| \leq \mathbb{E}\left[min\left\{ \frac{|rX|^{m+1}}{(m+1)!}, \frac{2\,|rX|^m}{m!} \right\} \right], \quad \text{(A.3)}$$

where $\mathbb{E}[X]$ is the expectation value of X.

PROOF: Integration by parts shows that for real s and x,

$$\int_0^x (x-s)^m \,\mathrm{e}^{-\mathrm{i}s}\, ds = \frac{x^{m+1}}{m+1} + \frac{-\mathrm{i}}{m+1} \int_0^x (x-s)^{m+1} \,\mathrm{e}^{-\mathrm{i}s}\, ds, \quad \text{(A.4)}$$

and by induction

$$\mathrm{e}^{-\mathrm{i}x} = \sum_{k=0}^{m} \frac{(-\mathrm{i}x)^k}{k!} + \frac{(-\mathrm{i})^{m+1}}{m!} \int_0^x (x-s)^m \, e^{-\mathrm{i}s}\, ds. \quad \text{(A.5)}$$

Replacing m with $m-1$ in equation (A.4), solving for the integral on the right and substituting it for the integral in equation (A.5) yields

$$\mathrm{e}^{-\mathrm{i}x} = \sum_{k=0}^{m} \frac{(-\mathrm{i}x)^k}{k!} + \frac{(-\mathrm{i})^m}{(m-1)!} \int_0^x (x-s)^{m-1} \left(\mathrm{e}^{\mathrm{i}s} - 1\right) ds. \quad \text{(A.6)}$$

Estimating the integrals in equations (A.5) and (A.6) leads to

$$\left| \mathrm{e}^{-\mathrm{i}x} - \sum_{k=0}^{m} \frac{(-\mathrm{i}x)^k}{k!} \right| \leq \min\left\{ \frac{|x|^{m+1}}{(m+1)!}, \frac{2\,|x|^m}{m!} \right\}, \quad \text{(A.7)}$$

from which the lemma follows by application of the triangle-inequality. ■

Having proved these two lemmas, we now turn to the main part of the proof. First we prove the pointwise convergence of the characteristic function.

A.2. The Pointwise Convergence of the Characteristic Function

We start by introducing some notation.

A.2.1. Notation

Define the operators

$$X_\mu \equiv \mathcal{H}_\mu - \langle a| \mathcal{H}_\mu |a\rangle \tag{A.8}$$

and consider the sum

$$S_n = \sum_{\mu=1}^{n} \frac{X_\mu}{\Delta_a}. \tag{A.9}$$

In the state $|a\rangle$ its first moment vanishes and the second is equal to one.

$$\langle a| S_n |a\rangle = 0 \quad \text{and} \quad \langle a| S_n^2 |a\rangle = 1 \tag{A.10}$$

Now split the sum S_n into alternate blocks of length $k-1$ (large blocks) and of length 1 (small blocks). The large blocks are given by

$$\xi_j = \sum_{l=1}^{k-1} \frac{X_{(j-1)\cdot k+l}}{\Delta_a} \quad \text{for} \quad j = 1, \ldots, [n/k] \quad \text{and} \tag{A.11}$$

$$\xi_{[n/k]+1} = \sum_{l=1}^{q} \frac{X_{[n/k]\cdot k+l}}{\Delta_a} \quad \text{with} \quad q = n - k\,[n/k], \tag{A.12}$$

where $[x]$ means the integer part of x.
The small blocks are the $X_{j\cdot k}$ with $j = 1, \ldots, [n/k]$.

Sum up all large blocks and all small blocks separately,

$$S'_n = \sum_{j=1}^{[n/k]+1} \xi_j \quad \text{and} \quad S''_n = \sum_{j=1}^{[n/k]} \frac{X_{j\cdot k}}{\Delta_a}, \tag{A.13}$$

so that $S_n = S'_n + S''_n$. The integer block length k is chosen to depend on n ($k = k(n)$) such that

$$\lim_{n\to\infty} \frac{n}{k^2} = 0 \quad \text{and} \quad \lim_{n\to\infty} \frac{k}{n} = 0, \tag{A.14}$$

with $k = \left[n^{3/4}\right]$ being a possible realization.

A.2.2. Proof

Consider the characteristic function

$$\langle a| \, \mathrm{e}^{-\mathrm{i}rS_n} \, |a\rangle \tag{A.15}$$

where r is real.
The objective is now to show that:

$$\langle a| \exp\left(-\mathrm{i}\, r\, S_n\right) |a\rangle = \langle a| \exp\left(-\mathrm{i}\, r \sum_{j=1}^{[n/k]+1} \xi_j\right) |a\rangle + \mathcal{O}(1) \tag{A.16}$$

$$= \prod_{j=1}^{[n/k]+1} \langle a| \, \mathrm{e}^{-\mathrm{i}r\xi_j} \, |a\rangle + \mathcal{O}(1) \tag{A.17}$$

$$= \prod_{j=1}^{[n/k]+1} \left(1 - \frac{1}{2} r^2 \langle a| \, \xi_j^2 \, |a\rangle\right) + \mathcal{O}(1) \tag{A.18}$$

$$= \prod_{j=1}^{[n/k]+1} \exp\left(-\frac{r^2}{2} \langle a| \, \xi_j^2 \, |a\rangle\right) + \mathcal{O}(1) \tag{A.19}$$

$$= \exp\left(-\frac{r^2}{2}\right) + \mathcal{O}(1) \tag{A.20}$$

The first asymptotic relation (A.16) is established by the following proposition:

Propositon A.1 *For all real r and $n \to \infty$:*

$$\langle a|\, \mathrm{e}^{-\mathrm{i}rS_n}\, |a\rangle \to \langle a|\, \mathrm{e}^{-\mathrm{i}rS'_n}\, |a\rangle \tag{A.21}$$

Proof: Using the operator identity [17]

$$\mathrm{e}^{-\mathrm{i}r(A+B)} = \mathrm{e}^{-\mathrm{i}rA} - \mathrm{i}\int_0^r \mathrm{e}^{-\mathrm{i}(r-s)(A+B)} B \mathrm{e}^{-\mathrm{i}sA} ds, \tag{A.22}$$

the triangle- and the Schwarz-inequality, one gets

$$\begin{aligned} \left|\langle a|\, \mathrm{e}^{-\mathrm{i}rS_n} - \mathrm{e}^{-\mathrm{i}rS'_n}\, |a\rangle\right| &\leq \int_0^r ds \sqrt{\langle a|\, \mathrm{e}^{\mathrm{i}sS_n} \left(S''_n\right)^2 \mathrm{e}^{-\mathrm{i}sS_n}\, |a\rangle} \\ &\leq r\sqrt{\left(\frac{1}{n}\left[\frac{n}{k}\right]^2\right)\frac{(2C')^2}{C}}, \end{aligned} \tag{A.23}$$

where the second inequality in (A.23) follows from conditions (5.13) and (5.14). The rhs of (A.23), indeed, converges to zero for $n \to \infty$. ■

The next proposition proves the asymptotic relation (A.17).

Propositon A.2 *The characteristic function of S'_n factorizes.*

$$\langle a|\, \mathrm{e}^{-irS'_n}\, |a\rangle = \prod_{j=1}^{[n/k]+1} \langle a|\, \mathrm{e}^{-ir\xi_j}\, |a\rangle \tag{A.24}$$

Proof: First note two important properties that arise due to the next neighbor interaction and the product property of the state $|a\rangle$: For $|\mu - \nu| > 1$ and any two integers k and l, we have

$$[\mathcal{H}_\mu, \mathcal{H}_\nu] = 0 \tag{A.25}$$

$$\langle a|\, (\mathcal{H}_\mu)^k (\mathcal{H}_\nu)^l\, |a\rangle = \langle a|\, (\mathcal{H}_\mu)^k\, |a\rangle\ \langle a|\, (\mathcal{H}_\nu)^l\, |a\rangle\,. \tag{A.26}$$

Therefore, for all (i, j) and any two integers k and l,

$$[\xi_i, \xi_j] = 0 \tag{A.27}$$

$$\langle a|\, (\xi_i)^k (\xi_j)^l\, |a\rangle = \langle a|\, (\xi_i)^k\, |a\rangle\ \langle a|\, (\xi_j)^l\, |a\rangle\,, \tag{A.28}$$

and equation (A.24) follows as a direct consequence. ■

To prove the remaining three asymptotic relations (A.18), (A.19) and (A.20), we need to show that the random variables associated to the operators ξ_j fulfill the Lindeberg condition. Therefore we first show, that they satisfy a quantum analog of the Lyapunov condition.

Propositon A.3 (Lyapunov Condition) *The operators ξ_j as defined in (A.11) fulfill*

$$\lim_{n\to\infty} \sum_{j=1}^{[n/k]+1} \langle a| \, |\xi_j|^{2+m} \, |a\rangle = 0 \tag{A.29}$$

for some $m > 0$.

Proof: Note that due to equation (A.21), $\langle a| \left(S_n'\right)^2 |a\rangle \to 1$ as $n \to \infty$ and therefore equation (A.29) is, indeed, the Lyapunov condition for the ξ_j [38, 10]. We verify the condition for $m = 2$. To this end, consider

$$\langle a| \, \xi_j^4 \, |a\rangle = \sum_{\mu,\nu,\rho,\tau=1}^{k-1} \langle a| \, X_{(j-1)k+\mu} \, X_{(j-1)k+\nu} \, X_{(j-1)k+\rho} \, X_{(j-1)k+\tau} \, |a\rangle \, . \tag{A.30}$$

Since $\langle a| \, X_\mu \, |a\rangle = 0$ and because of equations (A.27) and (A.28), only those terms are nonzero, for which all the X_μ are identical or neighbors or where two pairs of identical or neighboring X_μ appear. For example $\langle a| \, X_\mu X_{\mu+1} X_{\mu+2} X_{\mu-1} \, |a\rangle \neq 0$ while $\langle a| \, X_\mu X_{\mu+1} X_{\mu+3} X_{\mu-1} \, |a\rangle = 0$ or $\langle a| \, X_\mu X_{\mu+1} X_{\nu-1} X_\nu \, |a\rangle \neq 0$ while $\langle a| \, X_\mu X_\nu X_\mu X_{\nu+2} \, |a\rangle = 0$. Using this fact and the conditions (5.13) and (5.14) one realizes that

$$\sum_{j=1}^{[n/k]+1} \langle a| \, \xi_j^4 \, |a\rangle \leq \left(\left[\frac{n}{k} \right] + 1 \right) \frac{\left((k-1)^2 + 3 \cdot 5 \cdot 7 \cdot 3! \cdot (k-1) \right) (2C')^4}{n^2 C^2} \tag{A.31}$$

where the assumptions (5.13) and (5.14) have been used. The rhs vanishes in the limit $n \to \infty$. Note that $\langle a| \, \xi_{[n/k]+1}^4 \, |a\rangle$ contains less terms

than $\langle a| \xi_j^4 |a\rangle$ for $j < [n/k] + 1$ and is therefore bounded by the same expression. ■

Next, we show that the Lyapunov condition implies the Lindeberg condition.

Propositon A.4 (Linderberg Condition) *If the operators ξ_j fulfill the Lyapunov condition, then they also fulfill the Lindeberg Condition:*

$$\lim_{n\to\infty} \sum_{j=1}^{[n/k]+1} \int\limits_{|x_j|\geq\varepsilon} x_j^2 \, d\mathbb{P}_a(x_j) \tag{A.32}$$

where the real numbers x_j are the eigenvalues of the ξ_j in the state $|a\rangle$, $\xi_j |a\rangle = x_j |a\rangle$.

Proof: This follows directly by observing

$$\sum_{j=1}^{[n/k]+1} \int\limits_{|x_j|\geq\varepsilon} x_j^2 \, d\mathbb{P}_a(x_j) \leq \sum_{j=1}^{[n/k]+1} \int\limits_{|x_j|\geq\varepsilon} \frac{x_j^{2+m}}{\varepsilon^m} \, d\mathbb{P}_a(x_j) \leq$$

$$\leq \frac{1}{\varepsilon^m} \sum_{j=1}^{[n/k]+1} \langle a| \, |\xi_j|^{2+m} \, |a\rangle \tag{A.33}$$

■

We now turn to prove the remaining three asymptotic relations (A.18), (A.19) and (A.20). This part of the proof closely follows the standard proof of the central limit theorem for a mixing sequence of random variables [10].

Lemma A.2 states that

$$\left| \langle a| \, \mathrm{e}^{-\mathrm{i}r\xi_j} \, |a\rangle - \left(1 - \frac{1}{2} r^2 \, \langle a| \, \xi_j^2 \, |a\rangle\right) \right| \leq \langle a| \min\left\{ |r\xi_j|^2 , |t\xi_j|^3 \right\} |a\rangle \, , \tag{A.34}$$

which is a finite value. For positive ε the right hand side is at most

$$\begin{aligned}\int_{|x_j|<\varepsilon} |rx_j|^3 \, d\mathbb{P}_a(x_j) \; + \; \int_{|x_j|\geq\varepsilon} |rx_j|^2 \, d\mathbb{P}_a(x_j) \leq \\ \leq \varepsilon |r|^3 \; \langle a| \, \xi_j^2 \, |a\rangle \; + \; r^2 \int_{|x_j|\geq\varepsilon} x_j^2 \, d\mathbb{P}_a(x_j)\end{aligned} \tag{A.35}$$

Since the $\langle a| \, \xi_j^2 \, |a\rangle$ add up to 1 and ε is arbitrary, it follows by the Lindeberg condition that

$$\sum_{j=1}^{[n/k]+1} \left| \langle a| \, \mathrm{e}^{-\mathrm{i}r\xi_j} \, |a\rangle - \left(1 - \frac{1}{2} r^2 \, \langle a| \, \xi_j^2 \, |a\rangle\right)\right| \to 0 \tag{A.36}$$

for each fixed r. For ε positive,

$$\langle a| \, \xi_j^2 \, |a\rangle \leq \varepsilon^2 + \int\limits_{|x_j|\geq\varepsilon} x_j^2 \, d\mathbb{P}_a(x_j), \tag{A.37}$$

and so it, again, follows by the Lindeberg condition that

$$\max_{1\leq j\leq n} \; \langle a| \, \xi_j^2 \, |a\rangle \to 0 \tag{A.38}$$

For large enough n, the $1 - (r^2/2) \, \langle a| \, \xi_j^2 \, |a\rangle$ are all between 0 and 1 and by virtue of lemma A.1,

$$\prod_{j=1}^{[n/k]+1} \langle a| \exp(-\mathrm{i}r\xi_j) \, |a\rangle \qquad \text{and} \qquad \prod_{j=1}^{[n/k]+1} \left(1 - \frac{1}{2} r^2 \, \langle a| \, \xi_j^2 \, |a\rangle\right)$$

differ at most by the sum in (A.36). This establishes the asymptotic relation (A.18).

Now lemma A.1 also implies that

$$\begin{aligned}\left| \prod_{j=1}^{[n/k]+1} \exp\left(-\frac{1}{2} \, r^2 \, \langle a| \, \xi_j^2 \, |a\rangle\right) - \prod_{j=1}^{[n/k]+1} \left(1 - \frac{1}{2} \, r^2 \, \langle a| \, \xi_j^2 \, |a\rangle\right)\right| \leq \\ \leq \sum_{j=1}^{[n/k]+1} \left| \exp\left(-\frac{1}{2} \, r^2 \, \langle a| \, \xi_j^2 \, |a\rangle\right) - 1 + \frac{1}{2} \, r^2 \, \langle a| \, \xi_j^2 \, |a\rangle\right|.\end{aligned} \tag{A.39}$$

For complex z

$$|\mathrm{e}^z - 1 - z| \leq |z|^2 \sum_{k=2}^{\infty} \frac{|z|^{k-2}}{k!} \leq |z|^2 \, \mathrm{e}^{|z|}. \tag{A.40}$$

Plugging this into the rhs of (A.39) bounds it by

$$r^4 \, \mathrm{e}^{r^2} \sum_{j=1}^{[n/k]+1} \langle a| \, \xi_j^2 \, |a\rangle^2 \,, \tag{A.41}$$

by (A.38) and (A.10), this sum goes to 0, from which the asymptotic equality (A.19) follows. ■

In summary, the characteristic function of S_n converges pointwise to

$$\lim_{n\to\infty} \langle a| \exp\left(-\mathrm{i}\, r \, S_n\right) |a\rangle = \exp\left(-\frac{r^2}{2}\right). \tag{A.42}$$

for all real r. To prove the theorem (5.15), we still have to show, that the pointwise convergence of the characteristic function implies the weak convergence of the distribution. This is done in the next section.

A.3. The Convergence of the Distributions

Finally, we prove that the pointwise convergence of the characteristic functions, established above, implies the weak convergence of the distributions.

In monographs on probability theory such as [10], this statement usually forms part of the so called continuity theorem. We prove here only the statement which is relevant for our purposes [16]. Our proof is based on the fact that Schwarz functions are dense in the set of indicator functions [62].

Propositon A.5 *Let the real numbers z be the eigenvalues of the operator S_n and let the characteristic function of S_n have the pointwise limit (A.42), then*

$$\lim_{n\to\infty} \mathbb{P}_a \left(z \in [z_1, z_2]\right) = \int_{z_1}^{z_2} f(z) \, dz \tag{A.43}$$

for all real $-\infty < z_1 < z_2 < \infty$, where $f(z)$ is the Fourier transform of the asymptotic characteristic function

$$f(z) = \frac{1}{2\pi} \int_{-\infty}^{\infty} \mathrm{e}^{\mathrm{i}rz} \lim_{n\to\infty} \langle a| \, \mathrm{e}^{-\mathrm{i}rS_n} \, |a\rangle \; dr \tag{A.44}$$

PROOF: The measure $\mathbb{P}_a$ can be represented via indicator functions

$$\mathbb{P}_a \left(z \in [z_1, z_2] \right) = \mathbb{E} \left(\mathbb{1}_{[z_1,z_2]} \right), \tag{A.45}$$

where $\mathbb{1}_{[z_1,z_2]}(z) = 1$ if $z \in [z_1, z_2]$ and $\mathbb{1}_{[z_1,z_2]}(z) = 0$ else. $\mathbb{E}$ denotes the expectation value,

$$\mathbb{E} \left(\mathbb{1}_{[z_1,z_2]} \right) = \int \mathbb{1}_{[z_1,z_2]} \, d\mathbb{P}_a(z) = \int_{z_1}^{z_2} d\mathbb{P}_a(z). \tag{A.46}$$

For every $\varepsilon > 0$, the indicator function $\mathbb{1}_{[z_1,z_2]}$ can be a sandwiched between two Schwarz functions Φ^- and Φ^+ such that

$$\Phi^- < \mathbb{1}_{[z_1,z_2]} < \Phi^+ \qquad \text{and} \qquad \int dx \left| \Phi^+ - \Phi^- \right| < \varepsilon \tag{A.47}$$

for any $\varepsilon > 0$. Schwarz functions are infinitely many times differentiable ($\mathcal{C}^\infty$), where all the derivatives vanish faster than polynomial as $|x| \to \infty$. As a consequence of equation (A.47), we have

$$\mathbb{E} \left(\Phi^- \right) \leq \mathbb{P}_a \left(z \in [z_1, z_2] \right) \leq \mathbb{E} \left(\Phi^+ \right) \tag{A.48}$$

where for Φ^+ and Φ^-,

$$\mathbb{E} \left(\Phi^\pm \right) = \int \Phi^\pm(z) \, d\mathbb{P}_a(z). \tag{A.49}$$

Representing Φ via its Fourier transform $\tilde{\Phi}$

$$\Phi(z) = \int \mathrm{e}^{-\mathrm{i}rz} \, \tilde{\Phi}(r) \, dr, \tag{A.50}$$

we can write

$$\mathbb{E} \left(\Phi \right) = \int \int \mathrm{e}^{-\mathrm{i}rz} \tilde{\Phi}(r) \, dr \, d\mathbb{P}_a(z) \tag{A.51}$$

Since, in equation (A.51), all functions are square integrable, integrations may be interchanged, and by Lebesgue's theorem of dominated convergence, it follows that:

$$\begin{aligned}\lim_{n\to\infty} \mathbb{E}\left(\Phi\right) &= \int\int \tilde{\Phi}(r)\, \mathrm{e}^{-\mathrm{i}rz}\, d\mathbb{P}_a(z)\, dr = \int \tilde{\Phi}(r)\, \mathrm{e}^{-\frac{r^2}{2}}\, dr = \\ &= \frac{1}{2\pi} \int\int \mathrm{e}^{\mathrm{i}rz}\, \Phi(z)\, \mathrm{e}^{-\frac{r^2}{2}}\, dr\, dz = \int \Phi(z)\, \frac{\mathrm{e}^{-\frac{z^2}{2}}}{\sqrt{2\pi}}\, dz.\end{aligned} \tag{A.52}$$

We therefore have

$$\int \Phi^-(z)\, \frac{\mathrm{e}^{-\frac{z^2}{2}}}{\sqrt{2\pi}}\, dz \leq \mathbb{P}_a\left(z \in [z_1, z_2]\right) \leq \int \Phi^+(z)\, \frac{\mathrm{e}^{-\frac{z^2}{2}}}{\sqrt{2\pi}}\, dz \tag{A.53}$$

Observing equation (A.47) the proposition follows. ■

The pointwise convergence of the characteristic functions (A.42) thus implies the weak convergence of the distribution which completes the proof of the quantum central limit theorem (QCLT) (5.15).

B. Diagonalization of the Ising Chain

The Hamiltonian of the Ising chain is diagonalized via a Jordan-Wigner transformation [41, 53] which maps it to a fermionic system.

$$\begin{aligned} c_i &= \left(\prod_{j<i} \sigma_j^z\right) \frac{\sigma_i^x + \mathrm{i}\sigma_i^y}{2} \\ c_i^\dagger &= \left(\prod_{j<i} \sigma_j^z\right) \frac{\sigma_i^x - \mathrm{i}\sigma_i^y}{2} \end{aligned} \tag{B.1}$$

The operators c_i and $c_i^\dagger$ fulfill fermionic anti-commutation relations

$$\begin{aligned} \{c_i, c_j\} &= 0 \\ \{c_i, c_j^\dagger\} &= \delta_{ij} \end{aligned} \tag{B.2}$$

and the Hamiltonian reads

$$\begin{aligned} H = B \Bigg[\sum_j \left(2c_j^\dagger c_j - 1\right) - \\ -K \sum_j \left(c_j^\dagger c_{j+1} + \text{h.c.}\right) - L \sum_j \left(c_j^\dagger c_{j+1}^\dagger + \text{h.c.}\right) \Bigg] \end{aligned} \tag{B.3}$$

with $K = (J_x + J_y)/(2B)$ and $L = (J_x - J_y)/(2B)$. In the case of periodic boundary conditions a boundary term is neglected in equation (B.3). For long chains ($nN_G \to \infty$) this term is suppressed by a factor $(nN_G)^{-1}$. The Hamiltonian now describes Fermions which interact with their nearest neighbors. As for the bosonic system, a Fourier transformation maps the system onto noninteracting fermions. For the whole

chain with periodic boundary conditions,

$$\left\{ \begin{array}{c} c_j^\dagger \\ c_j \end{array} \right\} = \frac{1}{\sqrt{nN_G}} \sum_k \left\{ \begin{array}{c} d_k^\dagger \exp\left(\mathrm{i}kj\right) \\ d_k \exp\left(-\mathrm{i}kj\right) \end{array} \right\}, \tag{B.4}$$

with $k = (2\pi l)/(nN_G)$ where $l = 0, \pm 1, \ldots, \pm(nN_G - 2)/2, (nN_G)/2$ for nN_G even, and

$$\left\{ \begin{array}{c} c_j^\dagger \\ c_j \end{array} \right\} = \sqrt{\frac{2}{n+1}} \sum_k \sin(kj) \left\{ \begin{array}{c} d_k^\dagger \\ d_k \end{array} \right\}, \tag{B.5}$$

with $k = (\pi l)/(n+1)$ and $(l = 1, 2, \ldots, n)$ for one single group.

In the case of periodic boundary conditions, fermion interactions of the form $d_k^\dagger d_{-k}^\dagger$ and $d_k d_{-k}$ remain. Therefore, one still has to apply a Bogoliubov transformation to diagonalize the system, i.e.

$$\begin{aligned} d_k^\dagger &= u_k b_k^\dagger - \mathrm{i}v_k b_{-k} \\ d_k &= u_k b_k + \mathrm{i}v_k b_{-k}^\dagger \end{aligned} \tag{B.6}$$

where $u_k = u_{-k}$, $v_k = -v_{-k}$ and $u_k^2 + v_k^2 = 1$. With the definitions $u_k = \cos(\Theta_k/2)$ and $v_k = \sin(\Theta_k/2)$ the interaction terms disappear for

$$\cos(\Theta_k) = \frac{1 - K\cos k}{\sqrt{[1 - K\cos k]^2 + [L\sin k]^2}} \tag{B.7}$$

In the case of the finite chain of one group, the Bogoliubov transformation is not needed, since the corresponding terms are of the form $d_k^\dagger d_k^\dagger$ and $d_k d_k$ and vanish by virtue of equation (B.2).

The Hamiltonians in the diagonal form read

$$H = \sum_k \omega_k \left(b_k^\dagger b_k - \frac{1}{2} \right) \tag{B.8}$$

where the frequencies are

$$\omega_k = 2B\sqrt{[1 - K\cos k]^2 + [L\sin k]^2} \tag{B.9}$$

with $k = (2\pi l)/(nN_G)$ for the periodic chain and

$$\omega_k = 2B\left(1 - K\cos k\right) \tag{B.10}$$

with $k = (\pi l)/(n+1)$ for the finite chain.

For the finite chain the occupation number operators may also be chosen such that ω_k is always positive. Here, the convention at hand is more convenient, since the same occupation numbers also appear in the group interaction and thus in Δ_μ.

C. Diagonalization of the Harmonic Chain

The Hamiltonian of a harmonic chain is diagonalized by a Fourier transformation and the definition of creation and annihilation operators [19].

For the entire chain with periodic boundary conditions, the Fourier transformation reads

$$\left\{ \begin{array}{c} q_j \\ p_j \end{array} \right\} = \frac{1}{\sqrt{nN_G}} \sum_k \left\{ \begin{array}{c} u_k \, \exp(\mathrm{i}a_0 kj) \\ v_k \, \exp(-\mathrm{i}a_0 kj) \end{array} \right\} \tag{C.1}$$

with $k = 2\pi l/(a_0\, n\, N_G)$ and $(l = 0, \pm 1, \ldots, \pm(nN_G - 2)/2, (nN_G)/2$, where nN_G has been assumed to be even.

For the diagonalization of one single group, the Fourier transformation is

$$\left\{ \begin{array}{c} q_j \\ p_j \end{array} \right\} = \sqrt{\frac{2}{n+1}} \sum_k \left\{ \begin{array}{c} u_k \\ v_k \end{array} \right\} \sin(a_0 kj) \tag{C.2}$$

with $k = \pi l/(a_0\,(n+1))$ and $(l = 1, 2, \ldots, n)$.

The definition of the creation and annihilation operators is in both cases

$$\left\{ \begin{array}{c} a_k^\dagger \\ a_k \end{array} \right\} = \frac{1}{\sqrt{2m\omega_k}} \left(m\omega_k u_k \left\{ \begin{array}{c} - \\ + \end{array} \right\} i v_k \right) \tag{C.3}$$

where the corresponding u_k and v_k have to be inserted. The frequencies ω_k are given by $\omega_k^2 = 4\omega_0^2 \sin^2(ka_0/2)$ in both cases..

The operators $a_k^\dagger$ and a_k satisfy bosonic commutation relations

$$\begin{array}{rcl} [a_k, a_p] & = & 0 \\ [\, a_k, a_p^\dagger \,] & = & \delta_{kp} \end{array} \tag{C.4}$$

and the diagonalized Hamiltonian reads

$$H = \sum_k \omega_k \left(a_k^\dagger a_k + \frac{1}{2} \right) \tag{C.5}$$

D. Definitions and Properties of Special Functions and Operators

D.1. Gaussian Error Functions

The Gaussian error function is defined by the integral

$$\operatorname{erf}(x) = \frac{2}{\sqrt{\pi}} \int_0^x \mathrm{e}^{-s^2}\, ds \tag{D.1}$$

and the conjugate Gaussian error function by the integral

$$\operatorname{erfc}(x) = \frac{2}{\sqrt{\pi}} \int_x^\infty \mathrm{e}^{-s^2}\, ds\,. \tag{D.2}$$

Both functions are related by

$$\operatorname{erfc}(x) = 1 - \operatorname{erf}(x)\,. \tag{D.3}$$

The conjugate error function obeys the transformation formula

$$\operatorname{erfc}(-x) = 2 - \operatorname{erfc}(x) \tag{D.4}$$

and has the asymptotic expansions for $|x| \to \infty$,

$$\operatorname{erfc}(x) \approx \begin{cases} \dfrac{\exp\left(-x^2\right)}{\sqrt{\pi}} \left(\dfrac{1}{x} - \dfrac{1}{2\,x^3} + \mathcal{O}\left(\dfrac{1}{x^4}\right)\right) & \text{for} \quad x \to \infty \\ 2 + \dfrac{\exp\left(-x^2\right)}{\sqrt{\pi}} \left(\dfrac{1}{x} - \dfrac{1}{2\,x^3} + \mathcal{O}\left(\dfrac{1}{x^4}\right)\right) & \text{for} \quad x \to -\infty \end{cases} \tag{D.5}$$

D.2. Spin-1 Operators

The spin-1 operators $\tilde{\sigma}^x$, $\tilde{\sigma}^y$ and $\tilde{\sigma}^z$ can be defined via their representations in the eigenbasis of $\tilde{\sigma}^z$:

$$\tilde{\sigma}^x = \frac{1}{\sqrt{2}} \begin{pmatrix} 0 & 1 & 0 \\ 1 & 0 & 1 \\ 0 & 1 & 0 \end{pmatrix} \tag{D.6}$$

$$\tilde{\sigma}^x = \frac{1}{\sqrt{2}} \begin{pmatrix} 0 & -\mathrm{i} & 0 \\ \mathrm{i} & 0 & -\mathrm{i} \\ 0 & \mathrm{i} & 0 \end{pmatrix} \tag{D.7}$$

$$\tilde{\sigma}^z = \begin{pmatrix} 1 & 0 & 0 \\ 0 & 0 & 0 \\ 0 & 0 & -1 \end{pmatrix} \tag{D.8}$$

List of Previously Published Articles

[1] M. Hartmann and G. Mahler:
Measurable Consequences of the Local Breakdown of the Concept of Temperature
Europhys. Lett., accepted (2005), cond-mat/0410526.

[2] M. Hartmann, G. Mahler and O.Hess:
Nano-Thermodynamics: On the minimal length scale for the existence of temperature
Proceedings of the FQMT04 conference, July 2004 in Prague, Czech Republic
Physica E, accepted (2005).

[3] M. Hartmann, G. Mahler and O.Hess:
On Which Length Scales Can Temperature Exist in Quantum Systems?
Proceedings of the SPQS conference, July 2004 in Sendai, Japan
J. Phys. Soc. Jpn., accepted (2005).

[4] M. Hartmann, G. Mahler and O.Hess:
Spectral Densities and Partition Functions of a Modular Quantum System as Derived from a Central Limit Theorem
J. Stat. Phys., accepted (2005), cond-mat/0406100.

[5] M. Hartmann, G. Mahler and O.Hess:
Local Versus Global Thermal States: Correlations and the Existence of Local Temperatures
Phys. Rev. E **70**, 066148 (2004).

[6] M. Hartmann, G. Mahler and O.Hess:
Fundamentals of Nano-Thermodynamics
in Handbook of Theoretical and Computational Nanotechnology, M. Rieth and W. Schommers (Eds), American Scientific Publishers (2004).

[7] M. Hartmann, G. Mahler and O.Hess:
Existence of Temperature on the Nanoscale
Phys. Rev. Lett. **93**, 080402 (2004),
selected for the Virtual Journal of Nanoscale Science & Technology.

[8] M. Hartmann:
On the Existence of Local Temperatures
in Quantum Thermodynamics, J. Gemmer, M. Michel and G. Mahler, Lecture Notes in Physics **657**, Springer (2004).

[9] M. Hartmann, G. Mahler and O.Hess:
Gaussian Quantum Fluctuations in Interacting Many Particle Systems
Lett. Math. Phys. **68**, 103 (2004).

[10] M. Hartmann, J. Gemmer, G. Mahler and O.Hess:
Scaling behavior of interactions in a modular quantum system and the existence of local temperature
Europhys. Lett. **65**, 613 (2004).

[11] M. Michel, M. Hartmann, J. Gemmer and G. Mahler:
Fourier's law confirmed for a class of small quantum systems
Eur. Phys. J. B **34**, 325 (2003).

Bibliography

[1] M. Abramowitz and I. Stegun. *Handbook of Mathematical Functions*. Dover Publ., New York, 9th edition, 1970.

[2] L. Accardi and A. Bach. Quantum Central Limit Theorems for Strongly Mixing Random Variables. *Z. Wahrsch. verw. Geb.*, 68:393, 1985.

[3] G. Adam and O. Hittmair. *Wärmetheorie*. Vieweg, Braunschweig, Wiesbaden, 4. edition, 1992.

[4] I. Affleck. Quantum spin chains and the Haldane gap. *J. Phys.: Condens. Matter*, 1:3047, 1989.

[5] A. E Allahverdyan and Th. M Nieuwenhuizen. Extraction of Work from a Single Thermal Bath in the Quantum Regime. *Phys. Rev. Lett.*, 85:1799–1802, 2000.

[6] A. E. Allahverdyan and Th. M. Nieuwenhuizen. Testing the Violation of the Clausius Inequality in Nanoscale Electric Circuits. *Phys. Rev. B*, 66:115309, 2002.

[7] J. Aumentado, J. Eom, V. Chandrasekhar, P.M. Baldo, and L.E. Rehn. Proximity effect thermometer for local electron temperature measurements on mesoscopic samples. *Appl. Phys. Lett.*, 75:3554, 1999.

[8] O. Avenel et al. Low-temperature magnetic measurements of an S=1 linear-chain Heisenberg antiferromagnet. *Phys. Rev. B*, 46:8655, 1992.

[9] E. Balcar and S.W. Lovesey. *Theory of Magnetic Neutron and Photon Scattering*. Oxford Series on Neutron Scattering in Condensed Matter. Oxfrod University Press, Oxford, 1989.

[10] P. Billingsley. *Probability and Measure*. John Wiley & Sons, New York, 3rd edition, 1995.

[11] P.J. Brown. *Magnetic form factors*, volume C of *International tables for crystallography*, chapter 4.4.5, pages 391–399. Reidel, Dordrecht, 1999.

[12] D. Cahill, W. Ford, K. Goodson, G. Mahan, A. Majumdar, H. Maris, R. Merlin, and S. Phillpot. Nanoscale thermal transport. *J. Appl. Phys.*, 93:793, 2003.

[13] C.D. Cushen and R.L. Hudson. A Quantum-Mechanical Central Limit Theorem. *J. Appl. Probability*, 8:454, 1971.

[14] M.S. Dresselhaus, editor. *Carbon Nanotubes*, volume 80 of *Topics in Applied Physics*. Springer, Berlin, 2001.

[15] M.S. Dresselhaus, G. Dresselhaus, and P.C. Eklund. *Science of Fullerenes and Carbon Nanotubes*. Academic Press, San Diego, 1996.

[16] D. Dürr. *Die Mathematische und Physikalische Beschreibung der Wahrscheinlichkeit*. Script of lectures on probability theory. 1996.

[17] E. Fick and G. Sauermann. *The Quantum Statistics of Dynamic Processes*. Springer, Berlin, Heidelberg, 1990.

[18] M.E. Fisher. The Free Energy of a Macroscopic System. *Arch. Ratl. Mech. Anal.*, 17:377, 1964.

[19] G.W. Ford, M. Kac, and P. Mazur. Statistical Mechanics of Assenblies of Coupled Oscillators. *J. Math. Phys.*, 6:504, 1965.

[20] Y. Gao and Y. Bando. Carbon nanothermometer containing gallium. *Nature*, 415:599, 2002.

[21] C.W. Gardiner and P. Zoller. *Quantum Noise*. Springer, Berlin, 2nd edition, 2000.

[22] J. Gemmer, M. Michel, and G. Mahler. *Quantum Thermodynamics*, volume 657 of *Lecture Notes in Physics*. Springer, Berlin, 2004.

[23] J. Gemmer, A. Otte, and G. Mahler. Quantum approach to a derivation of the second law of thermodynamics. *Phys. Rev. Lett.*, 86:1927–1930, 2001.

[24] D. Goderis, A. Verbeure, and P. Vets. Non-commutative Central Limits. *Prob. Th. Rel. Fields*, 82:527, 1989.

[25] D. Goderis and P. Vets. Central Limit Theorem for Mixing Quantum Systems and the CCR-Algebra of Fluctuations. *Comm. Math. Phys.*, 122:249, 1989.

[26] Goldstein M. Sh. Distribution of the Eigenvalues of the Energy Operator of a Continuous System of Quantum Statistical Mechanics. *Theoret. and Math. Phys.*, 1:412, 1985.

[27] Goldstein M. Sh. Limit Theorem for the Distribution of Eigenvalues of the Operator of Energy. *J. Stat. Phys.*, 40:329, 1985.

[28] F. Haake. *Quantum Signatures of Chaos.* Springer, Berlin, 2nd edition, 2001.

[29] M. Hartmann. *Quantum Thermodynamics*, volume 657 of *Lecture Notes in Physics*, chapter On the Existence of Local Temperatures. Springer, Berlin, 2004.

[30] M. Hartmann, J. Gemmer, G. Mahler, and O. Hess. Scaling behavior of interactions in a modular quantum system and the existence of local temperature. *Euro. Phys. Lett.*, 65:613–619, 2004.

[31] M. Hartmann, G. Mahler, and O. Hess. Existence of Temperature on the Nanoscale. *Phys. Rev. Lett.*, 93:080402, 2004.

[32] M. Hartmann, G. Mahler, and O. Hess. Gaussian Quantum Fluctuations in Interacting Many Particle Systems. *Lett. Math. Phys.*, 68:103, 2004.

[33] M. Hartmann, G. Mahler, and O. Hess. *Handbook of Theoretical and Computational Nanotechnology*, chapter Fundamentals of Nano-Thermodynamics. American Scientific Publishers, Stevenson Ranch, CA, USA, 2004.

[34] M. Hartmann, G. Mahler, and O. Hess. Local Versus Global Thermal States: Correlations and the Existence of Local Temperatures. *Phys. Rev. E*, 70:066148, 2004.

[35] M. Hartmann, G. Mahler, and O. Hess. Spectral densities and partition functions of modular quantum systems as derived from a central limit theorem. *cond-mat/0406100*, 2004.

[36] T.L. Hill. A Different Approach to Nanothermodynamics. *Nano Lett.*, 1(5):273, 2001.

[37] J. Hone, M.C. Llaguno, M.J. Biercuk, A.T. Johnson, B. Batlogg, Z. Benes, and J.E. Fischer. Thermal properties of carbon nanotubes and nanotube-based materials. *Appl. Phys. A*, 74:339, 2002.

[38] I.A. Ibargimov and Y.V. Linnik. *Independent and Stationary Sequences of Random Variables*. Wolters-Noordhoff, Groningen/Netherlands, 1971.

[39] A. N. Jordan and M. Büttiker. Entanglement Energetics at Zero Temperature. *Phys. Rev. Lett.*, 92:247901, 2004. cond-mat/0311647.

[40] G. Jüttner, A. Klümper, and J. Suzuki. The Hubbard chain at finite temperatures: ab initio calculations of Tomonaga-Luttinger liquid properties. *Nucl. Phys. B*, 522:471, 1998.

[41] S. Katsura. Statistical Mechanics of the Anisotropic Linear Heisenberg Model. *Phys. Rev.*, 127:1508, 1962.

[42] M. Kenzelmann, R.A. Cowles, W.J.L. Buyers, R. Coldea, J.S. Gardner, M. Enderle, D.F. McMorrow, and S.M. Bennington. Multiparticle States in the S = 1 Chain System CsNiCl3. *Phys. Rev. Lett.*, 87:017201, 2001.

[43] M. Kenzelmann and P. Santini. Temperature dependence of single particle excitations in a S = 1 chain: Exact diagonalization calculations compared to neutron scattering experiments. *Phys. Pev. B*, 66:184429, 2002.

[44] P. Kim, L. Shi, A. Majumdar, and P.L. McEuen. Thermal Transport Measurements of Individual Multiwalled Nanotubes. *Phys. Rev. Lett.*, 87:215502, 2001.

[45] Ch. Kittel. *Quantum Theory of Solids*. Wiley, New York, 1963.

[46] V. Korepin, N. Bogoliubov, and A. Izergin. *Quantum Inverse Scattering Method and Correlation Functions*. Cambridge Univ. Press, Cambridge, 1993.

[47] H. J. Kreuzer. *Nonequilibrium Thermodynamics and its statistical foundation*. Clarandon Press, Oxford, 1981.

[48] R. Kubo, M. Toda, and N. Hashitsume. *Statistical Physics II: Nonequilibrium Statistical Mechanics*. Number 31 in Solid-State Sciences. Springer, Berlin, Heidelberg, New-York, 2. edition, 1991.

[49] Kuperberg G. A Tracial Quantum Central Limit Theorem. *math-ph/0202035*, 2002.

[50] J.L. Lebowitz and E.H. Lieb. Existence of Thermodynamics for Real Matter with Coulomb Forces. *Phys. Rev. Lett.*, 22:631, 1969.

[51] E. Lieb. *The Stability of Matter: From Atoms to Stars*. Springer, Berlin, 3. edition, 2001.

[52] E. Lieb and D. Mattis. *Mathematical Physics in One Dimension*. Academic Press, New York, 1966.

[53] E. Lieb, T. Schultz, and D. Mattis. Two Soluble Models of an Antiferromagnetic Chain. *Ann. Phys.*, 16:407, 1961.

[54] A.J. Lipa, B.C. Leslie, and T.C. Wallstrom. A Very High Resolution Thermometer for Use Below 7 K. *Physica*, 107B:331, 1981.

[55] S. Ma, D.H. Reich, C. Broholm, B.J. Sternlieb, and R.W. Erwin. Spin correlations at finite temperature in an S=1 one-dimensional antiferromagnet. *Phys. Rev. B*, 51:3289, 1995.

[56] G. Mahler and V.A. Weberruß. *Quantum Networks*. Springer, Berlin, Heidelberg, 2. edition, 1998.

[57] J. Meixner. Zur Thermodynamik der Thermodiffusion. *Ann. Phys.*, 39:333, 1941.

[58] T. Michoel and B. Nachtergaele. Central Limit Theorems for the Large Spin Asymptotics of Quantum Spins. *math-ph/0310027*, 2003.

[59] Th. M. Nieuwenhuizen and A. E. Allahverdyan. Statistical Thermodynamics of Quantum Brownian Motion: Construction of Perpetuum Mobile of the Second Kind. *Phys. Rev. E*, 66:036102, 2002.

[60] H. Pothier, S. Gueron, N.O. Brige, D. Esteve, and M.H. Devoret. Energy Distribution Function of Quasiparticles in Mesoscopic Wires. *Phys. Rev. Lett.*, 79:3490, 1997.

[61] A.K. Rajagopal, C.S. Pande, and Sumiyoshi Abe. Nanothermodynamics - A generic approach to material properties at the nanoscale. *cond-mat/0403738*, 2004.

[62] M. Reed and B. Simon. *Functional Analysis*, volume 1. Academic Press, San Diego, 1980.

[63] D. Ruelle. *Statistical Mechanics*. W.A. Benjamin Inc., New York, 1969.

[64] S. Sachdev. *Quantum Phase Transitions*. Cambridge Univ. Press, Cambridge, 1999.

[65] J.J. Sakurai. *Modern Quantum Mechanics*. Addison-Wesley, Reading, Massachusetts, 1994.

[66] M. Schmidt, R. Kusche, B. von Issendorf, and H. Haberland. Irregular variations in the melting point of size-selected atomic clusters. *Nature*, 393:238, 1998.

[67] K. Schwab, E.A. Henriksen, J.M. Worlock, and M.L. Roukes. Measurement of the quantum of thermal conductance. *Nature*, 404:974–976, 2000.

[68] W. Thirring. *Quantum Mathematical Physics*. Springer, Berlin, New York, 2. edition, 2002.

[69] M. Toda, R. Kubo, and N. Saito. *Statistical Physics I: Equilibrium Statistical Mechanics*. Number 30 in Solid-State Sciences. Springer, Berlin, Heidelberg, New York, 2. edition, 1992.

[70] R.C. Tolman. *The Principles of Statistical Mechanics*. Oxford Univ. Press, London, 1967.

[71] J.H. van Vleck. A Survey of the Theory of Ferromagnetism. *Rev. Mod. Phys.*, 17:27, 1945.

[72] J. Varesi and A. Majumdar. Scanning Joule expansion microscopy at nanometer scales. *Appl. Phys. Lett.*, 72:37, 1998.

[73] X. Wang. Threshold temperature for pairwise and many-particle thermal entanglement in the isotropic heisenberg model. *Phys. Rev. A*, 66:044305, 2002.

[74] U. Weiss. *Quantum Dissipative Systems.* World Scientific, Singapore, 1999.

[75] C.C. Williams and H.K. Wickramasinghe. Scanning thermal profiler. *Appl. Phys. Lett.*, 49:1587, 1986.

List of Figures

Index

Danksagung

Meine Doktorarbeit ist nun doch fertig. Deshalb möchte ich mich hier bei all denen bedanken, die mich schon länger kennen oder denen ich in diesen dreieinhalb Jahren über den Weg gelaufen bin. Insbesondere sind das:

Herr Prof. Mahler, der mich hervorragend betreut hat und dabei sogar für Themen Interesse gezeigt hat, die ich vorgeschlagen habe. Außer der vielen Physik habe ich dabei auch von ihm gelernt, dass man, auch wenn man sich gerade ärgert, mit Freundlichkeit doch am weitesten kommt (Zumindest hoffe ich, dass ich es gelernt habe.).

Herr Prof. Hess, der mich als mein Vorgesetzter ein Thema meiner Wahl bearbeiten lies (Mir ist bewusst, dass das eine Seltenheit ist.) und mir in den ersten eineinhalb Jahren, als es noch nicht absehbar war, dass das Ganze ein gutes Ende haben würde, stets das Gefühl gab Vertrauen in mich zu haben.

Herr Prof. Dürr, der mich mit interessanten Diskussionen und Anregungen unterstützte, mir dabei bestätigt hat, dass der mathematische Teil dieser Arbeit richtig ist und mich ermuntert hat, diesen separat zu veröffentlichen.

Die Kollegen am Institut in der Uni, Christos, Friedemann, Harry, Jochen, Mathias, Marcus und Markus, mit denen ich jederzeit sowohl über Physik als auch Nicht-Physik diskutieren konnte und eine Menge Spaß hatte. Bei zweitem sei hier kurz an eine Nacht in Prag erinnert. (Die Debatte über den richtigen Fussballclub möchte ich hier nicht weiter vertiefen. Dazu sei auf die Dinge verwiesen, die ich von Herrn Mahler gelernt zu haben glaube.)

Die Arbeitsgruppe am DLR, also Achim, Andi, Christian, Didi und Klaus, die mich, den Immigranten aus Bayern, von Anfang an mit offenen Armen aufgenommen haben.

Meine Freundin Mick, die immer dafür gesorgt hat, dass ich mich mit interdisziplinären Ansichten beschäftigt habe. Die mir außerdem nicht böse war, wenn ich mit den Gedanken mal woanders war oder frustriert war, weil ich nicht weiter gekommen bin. Ihr bin ich für noch viel mehr dankbar, aber das sag ich ihr lieber selber.

Meine Eltern, die beide seit dem Schlaganfall meines Vaters im Frühjahr 2002 (Das war kurz nachdem ich mit meiner Promotion begonnen habe.) eine Leistung vollbringen, gegen die eine Doktorarbeit gar nichts ist.